Spectrum Aggregation for Dynamic Spectrum Access based Cognitive Networks

Soheil Rostami

A thesis submitted in partial fulfilment of the
requirements of the University of Greenwich
for the degree of Doctor of Philosophy

August 2016

DECLARATION

I certify that this work has not been accepted in substance for any degree, and is not concurrently being submitted for any degree other than that of Doctor of Philosophy being studied at the University of Greenwich. I also declare that this work is the result of my own investigations except where otherwise identified by references and that I have not plagiarised the work of others.

Signed (student): _____

Signed (supervisor): _____

Date: _____

ABSTRACT

Telecommunication standards bodies and vendors all over the world are seeking ways of continuing the evolution of mobile communication technology on to its next generation. Providing ubiquitous broadband access to all mobile users distributed in a given area with a fragmented spectrum remains a challenging task. This thesis contributes to the global efforts by extending bandwidth by means of Spectrum Aggregation (SA) in Next Generation Mobile Networks (NGMN).

First of all, the motivation behind SA for NGMN is investigated. SA is introduced to create large virtual carrier bandwidths for data hungry users by aggregating fragmented segments of spectrum. By using SA, multiple carriers with different bandwidths, dispersed within intra or inter-bands, can be simultaneously utilised to provide higher data rates, better coverage and simplified multi-band traffic management, resulting in an enhanced user quality of experience. However, SA functionality introduces new challenges for transceiver architecture and Radio Resource Management (RRM) functionality of the network.

Secondly, spectrum assignment for cognitive radio networks with SA is investigated. For this purpose, an aggregation-based spectrum assignment is formulated as an integer optimisation problem. The problem is solved using a genetic algorithm to exploit the discontinuity of the available spectrum and to achieve higher capacity gains. The formulation not only considers interference to primary users but also takes into account co-channel interference among secondary users and maximum aggregation span. Simulation results clearly show that the proposed algorithm outperforms state-of-the-art solutions in terms of spectrum utilisation and higher convergence rate.

Thirdly, RRM in Long-Term Evolution (LTE) networks with SA is considered. It is shown that the optimal solution of RRM in different scenarios can be achieved by solving the relaxed optimisation problem. The optimum RRM algorithm with reduced complexity is proposed and compared with the current solutions in literature. The proposed algorithm optimally assigns component carriers, resource

blocks, modulation and coding scheme values based on users' channel state information and SA capabilities. Simulation results clearly show that the proposed algorithm outperforms current solutions in terms of cell throughput and user throughput fairness.

Last but not least, resource allocation with SA for orthogonal frequency-division multiplexing based networks is studied. A joint resource allocation problem with SA functionality is formulated and sub-optimal solutions with low computational complexity are proposed. Simulation results verify that the proposed algorithms achieve near optimum throughput and exploit the multi-carrier diversity of wireless systems.

ACKNOWLEDGEMENTS

I would like to dedicate my dissertation work to my supervisors and family for their unconditional support. I would like to express my deep gratitude to my first supervisor, Dr Kamran Arshad, for his patient guidance and encouragement, and for the advice he has provided. I have been extremely lucky to have a supervisor who cared so much about my work, and who always impressed me with his wealth of knowledge and his high ethical, academic and personal standards; without him none of my success would be possible.

I am heartily thankful to my second supervisor, Professor Predrag Rapajic, for helping me to develop my research skills and effective means of communication, and for his independent and encouraging comments on my work. Professor Rapajic's feedback and guidance have been incredibly empowering for me, on this important journey of my life.

A special feeling of gratitude to my loving parents, Ashraf and Mahmod whose words of encouragement and push for tenacity ring in my ears. I am indebted to my beloved sister, Sahar who has never left my side and is very special.

I also dedicate this dissertation to my dear uncles, Ebrahim and Saeed, who have supported me throughout the process. I will always appreciate all they have done; they have always been standing by my side.

Contents

List of Figures

List of Tables

Abbreviations

1G	**1**st **G**eneration mobile networks
2G	**2**nd **G**eneration mobile networks
3G	**3**rd **G**eneration mobile networks
3GPP	**3**rd **G**eneration **P**artnership **P**roject
4G	**4**th **G**eneration mobile networks
5G	**5**th **G**eneration mobile networks
AMC	**A**daptive **M**odulation and **C**oding
AP	**A**ccess **P**oint
AWS	**A**dvanced **W**ireless **S**ervices
BCQI	**B**est **C**hannel **Q**uality **I**ndicator
BLER	**BL**ock **E**rror **R**ate
CC	**C**omponent **C**arrier
CCI	**C**o-**C**hannel **I**nterference
CDF	**C**umulative **D**istribution **F**unction
CDMA	**C**ode-**D**ivision **M**ultiple **A**ccess
COA	**CO**mbinatorial **A**lgorithm
CQI	**C**hannel **Q**uality **I**ndicator
CR	**C**ognitive **R**adio
CRN	**C**ognitive **R**adio **N**etwork
CSI	**C**hannel **S**tate **I**nformation
DL	**D**own **L**ink
DSA	**D**ynamic **S**pectrum **A**ccess
eNB	**e**volved **N**ode-**B**
Eq	**Eq**uation

ERAA	**E**fficient **R**esource **A**llocation **A**lgorithm
ETSI	**E**uropean **T**elecommunications **S**tandards **I**nstitute
FBMC	**F**ilter **B**ank **M**ulti **C**arrier
FCC	**F**ederal **C**ommunications **C**ommission
FDD	**F**requency-**D**ivision **D**uplex
FDMA	**F**requency **D**ivision **M**ultiple **A**ccess
FFT	**F**ast **F**ourier **T**ransform
GA	**G**reedy **A**lgorithm
GSM	**G**lobal **S**ystem for **C**ommunications
HB	**H**igher **B**and
HWN	**H**eterogeneous **W**ireless **N**etwork
ILP	**I**nteger **L**inear **P**rogramming
IMT	**I**nternational **M**obile **T**elecommunications
IMT-A	**I**nternational **M**obile **T**elecommunications-**A**dvanced
IP	**I**nternet **P**rotocol
ITU	**I**nternational **T**elecommunication **U**nion
KPI	**K**ey **P**erformance **I**ndicator
LB	**L**ower **B**and
LP	**L**inear **P**rogramming
LTE	**L**ong-**T**erm **E**volution
LTE-A	**L**ong-**T**erm **E**volution-**A**dvanced
LTE-U	**L**ong-**T**erm **E**volution in **U**nlicensed spectrum
M2M	**M**achine to **M**achine
MAC	**M**edia **A**ccess **C**ontrol
MAS	**M**aximum **A**ggregation **S**pan
MB	**M**ulti-frequency **B**and
MCS	**M**odulation and **C**oding **S**cheme
MIMO	**M**ultiple-**I**nput and **M**ultiple-**O**utput
MNO	**M**obile **N**etwork **O**perator
MSA	**M**aximum **S**atisfaction **A**lgorithm
MSR	**M**aximising **S**um of **R**eward

MSRA	**M**aximising **S**um of **R**eward **A**lgorithm
MSUL	**M**inimising **S**ystem **U**tility **L**oss
NGMN	**N**ext **G**eneration **M**obile **N**etworks
NP	**N**on-deterministic **P**olynomial time
Ofcom	**Of**ice of **com**munications
OFDM	**O**rthogonal **F**requency-**D**ivision **M**ultiplexing
OFDMA	**O**rthogonal **F**requency-**D**ivision **M**ultiple **A**ccess
ORAA	**O**ptimal **R**esource block **A**llocation **A**lgorithm
PCC	**P**rimary **C**omponent **C**arrier
PF	**P**roportional **F**airness
PN	**P**rimary **N**etwork
PU	**P**rimary **U**ser
QoE	**Q**uality **o**f **E**xperience
QoS	**Q**uality **o**f **S**ervice
RA	**R**esource **A**llocation
RAT	**R**adio **A**ccess **T**echnology
RB	**R**esource **B**lock
RCA	**R**andom **C**hannel assignment **A**lgorithm
Rel	**Rel**ease
RF	**R**adio **F**requency
ROI	**R**eturn **O**n **I**nvestment
RRC	**R**adio **R**esource **C**ontrol
RRH	**R**emote **R**adio **H**ead
RRM	**R**adio **R**esource **M**anagement
RRS	**R**ound-**R**obin **S**cheduling
RSRP	**R**eference **S**ignal **R**eceived **P**ower
SA	**S**pectrum **A**ggregation
SB	**S**ingle-frequency **B**and
SC	**S**ub-**C**arrier
SCC	**S**econdary **C**omponent **C**arrier
SC-FDMA	**S**ingle **C**arrier-**F**requency **D**ivision **M**ultiple **A**ccess

SISO	**S**ingle **I**nput **S**ingle **O**utput
SNR	**S**ignal-to-**N**oise **R**atio
SOTA	**S**tate-**O**f-**T**he-**A**rt
SU	**S**econdary **U**ser
TDD	**T**ime-**D**ivision **D**uplex
TDMA	**T**ime **D**ivision **M**ultiple **A**ccess
TSRAA	**T**wo-**S**tep **R**esource **A**llocation **A**lgorithm
TTI	**T**ransmission **T**ime **I**nterval
TUM	**T**otal **U**nimodular **M**atrix
UE	**U**ser **E**quipment
UK	**U**nited **K**ingdom
UL	**U**p **L**ink
UMTS	**U**niversal **M**obile **T**elecommunications **S**ystem
UTRA	**U**niversal **T**errestrial **R**adio **A**ccess
Wi-Fi	**W**ireless-**F**idelity
WLAN	**W**ireless **L**ocal **A**rea **N**etwork
WRC	**W**orld **R**adio **C**onferences

Symbols

$\mathbf{0}_n$	n-component all-zero vector
$\mathbf{1}_n$	n-component all-one vector
$\boldsymbol{\alpha}$	Set of users/SUs in the cell
α_n	n^{th} user/SU in the cell
$\overline{\boldsymbol{\alpha}}_m$	Set of SUs in the vicinity that can reuse β_m
$\mathbf{A}$	Sub-channel/SC allocation matrix
$\mathbf{A}^*$	Optimal conflict free sub-channel assignment matrix
$a^k_{m,p,n}$	RB allocation variable
$\boldsymbol{\beta}$	Set of non-overlapping orthogonal CCs/channels
$\overline{\boldsymbol{\beta_n}}$	Set of available channels at α_n's location
$\mathcal{B}$	Reward vector
β_m	m^{th} CC/channel in the cell
$\widetilde{\beta}_{i,m}$	i^{th} sub-channel located in β_m
BW	Channel Bandwidth
$\mathcal{BW}_m$	Bandwidth of channel β_m
$blkd(B, b)$	Block diagonal matrix
C	Constraint matrix
$\mathbf{C}$	Interference constraint matrix
$\mathcal{C}$	Total number of sub-channels in the available spectrum
$c_{m,p,n}$	CQI-index of α_n in p^{th} RB of β_m
$\mathcal{C}_{\text{COA}}$	The required number of waterfilling algorithm for COA
$\mathbf{E}$	CC allocation matrix
E_b	Received energy per bit

$e^k_{m,n}$	CC allocation variable
F	Jain's fairness index
$\mathcal{F}^L_{i,m}$	Lowest frequency of $\widetilde{\beta}_{i,m}$
$\mathcal{F}^H_{i,m}$	Highest frequency of $\widetilde{\beta}_{i,m}$
$f^{(t)}_n$	Achievable throughput over t^{th} TTI for α_n
$\mathbf{G}$	Channel gain matrix
$\mathbf{H}$	Channel quality matrix
I_n	$n \times n$ identity matrix
$\mathcal{K}$	Number of available CQI-indexes
$\mathbf{L}$	Channel availability matrix
$\mathcal{M}$	Number of non-overlapping orthogonal CCs/channels
$\mathcal{N}$	Number of users/SUs in the cell
N	Noise power
N_0	Noise power spectral density
N_{pop}	Population size
$\mathbb{N}$	Set of natural numbers
$\mathbf{P}$	Power allocation matrix
$\mathcal{P}$	Maximum of γ_m
P_T	Power budget of the AP
Q	Markov Chain transition matrix
$Q_{i,j}$	Conditional probability that population j is generated from population i
$\mathcal{R}$	User requested bandwidth vector
R	Channel data rate/aggregated sum-rate of network
$r_{m,n}$	Data rate of α_n over β_m
S	Signal power
t_c	Number of TTIs for average throughput $T^{(t)}_n$
$T^{(t)}_n$	Average throughput of α_n over last t_c TTIs
T	Fraction of time which use of the bandwidth is denied to other users
U	Network/spectrum utilisation function
$\mathcal{U}(a,b)$	Discrete uniform random integer numbers between a and b
$V^{(t)}_n$	Utility function of PF scheduling for α_n up to t^{th} TTI

V_n	Aggregated data-rate of α_n
V	Volume within which use of the bandwidth is denied to other users
$\mathbf{x}_n$	Vectors of dimension n
$y_{m,n}$	Indicator variable, represents whether β_m is assigned to α_n as PCC or not
ϕ	Network load
ν	Spectrum efficiency
κ_m	Number of sub-channels in channel β_m
μ_n	SA capability of α_n
γ_m	Number of RBs/SCs in a given β_m
ω_n	Number of requested sub-channels by SU α_n
ω	Length of binary string
Λ_{L^*,C^*}	Set of sub-channel assignments for given $\mathbf{L}^*$ and $\mathbf{C}^*$
Δf	Bandwidth of sub-channel/SC
Θ	Polyhedron
χ	Total number of possible populations
ϑ	Channel capacity
$(.)^T$	Transpose operation
$\|.\|$	Cardinality of a set
$(x)^+$	$\max(x, 0)$

To my beloved grandparents and parents

Chapter 1

Introduction

Existing wireless networks are regulated by a traditional static spectrum allocation policy, whereby the telecommunication standards bodies allocate spectrum bands to licence holders on a long-term basis over vast geographical regions. This policy generates many unwanted small spectrum fragments that cannot be fully utilised, leading to low spectrum utilisation. In recent times, because of the explosive growth in spectrum demand, this policy is facing spectrum discontinuity and the so-called spectrum scarcity problem in the popular spectrum bands. Next Generation Mobile Networks (NGMN) will provide the capability to utilise fragmented spectrum with Spectrum Aggregation (SA) in an opportunistic manner. SA is a prominent mechanism in the NGMN for improving transmission bandwidth, which is one of the prime factors that enhances both network and users' performance.

1.1 Global Mobile Data Traffic

Global mobile data traffic is estimated to reach 24.3 exabytes (billion gigabytes) per month in 2019 - a nearly six-fold increase over 2015 - according to Cisco Systems [1] as shown in Figure 1.1. Emerging new services continues to increase

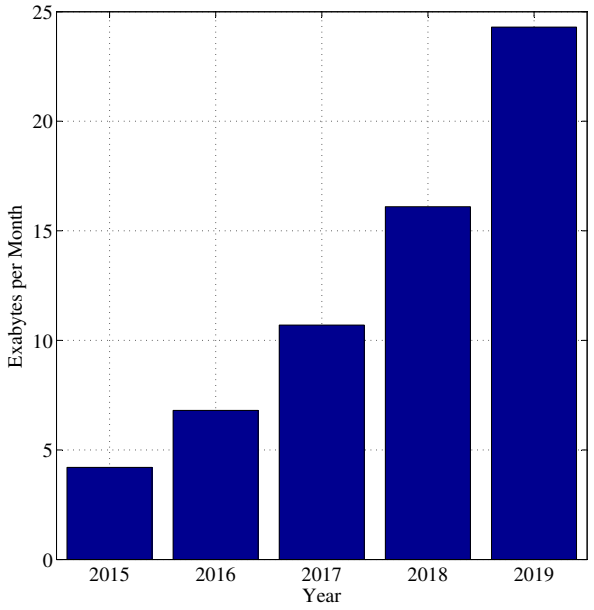

FIGURE 1.1: Global mobile data traffic analysis between 2015 and 2019 [1].

demand for mobile data by introducing new applications that consume a considerable volume of traffic [1]. Video itself contributes to more than 40% of mobile data traffic today, and shows no sign of slowing in the future [1]. According to Cisco Systems, since video streaming has a higher bit rate requirement than other services, mobile video will contribute much of the mobile traffic growth through 2019 [1]. Figure 1.2 illustrates the expected traffic that each service will generate in four years' time.

The growing number of Machine to Machine (M2M) devices, wearable devices, smartphones, tablets, and laptops is a major traffic generator, because these devices provide the data hungry users with a growing range of new services and applications not previously supported. Figure 1.3 compares the typical generated data traffic of modern wireless devices to basic-feature phones [1].

Furthermore, mobile Internet penetration worldwide has been growing fast; it is estimated that by 2017 mobile access will exceed fixed-line access globally [2]. The explosive usage of wireless devices and new services for mobile communications are

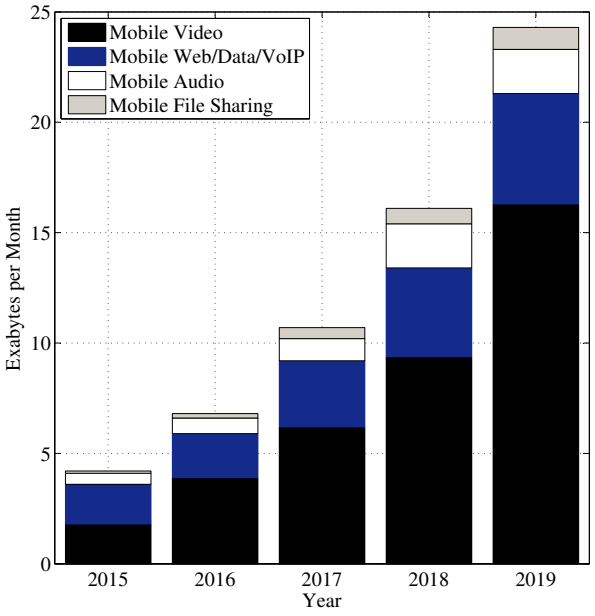

FIGURE 1.2: Analysing mobile applications: mobile video will generate more than 69% of mobile data traffic by 2019 [1].

FIGURE 1.3: High-end devices equivalent traffic usage [1].

converting the digital revolution into an increasingly mobile phenomenon, indicating how much modern society is dependent on a spectrum which is becoming a scarce and precious resource. Demand for high-speed multimedia data communications, such as real-time video streaming, is markedly increasing [2]. Hence, providing high-data rate access is one of the main goals of NGMN.

1.2 Evolution of Mobile Communication Systems

Since the late 1970s and early 1980s, mobile communications have evolved from being expensive technology for a few people to today's ubiquitous systems used by 75% of the world's population [3]. The task of developing mobile technologies is a formidable job, carried out by global telecommunication standards bodies such as the International Telecommunication Union (ITU), the European Telecommunications Standards Institute (ETSI), and the Third Generation Partnership Project (3GPP).

Mobile communication technologies have often been categorised into generations, with 1G using analog transmission for voice services in the 1980s, 2G introducing the first digital mobile systems, 3G the first mobile systems handling broadband data, and 4G the first all-Internet Protocol (IP) based mobile communication [4]. Both 1G and 2G are considered as narrowband, because both offered only low-bandwidth services such as voice and text messaging. Compared to 1G, 2G systems used digital multiple access technology to deliver low-data rate services (at a peak data rate of 9.6 kbps) including text messaging and circuit-switched data services [4].

With the advent of 3G and the higher-bandwidth radio interface of UTRA (Universal Terrestrial Radio Access), a range of new services over the mobile-communication networks was offered. The evolution of 3G systems into 4G (also known as Long-Term Evolution (LTE)) was driven by the creation and development of new services for mobile devices by creating mobile broadband. Supporting the same IP-based services in a mobile device as people use at home with a fixed broadband connection is one of the prime drivers for the evolution of LTE [4].

Recently, LTE has been developed as 4G wireless technology that can support the next generation of multimedia applications with high capacity and high mobility

needs. However, the peak data rate from 3G Universal Mobile Telecommunications System (UMTS) to 4G LTE-Advanced (LTE-A) is increasing by only 55% annually, while global mobile traffic showed an annual growth rate of 131% between 2008 and 2015 [5]. Thus, there is a huge gap between the growth rate of the new air interface and the growth rate of customers' needs. A promising way to alleviate the contention between traffic demand and actual system capacity is to exploit more available spectrum resources.

1.3 Fundamental Constraints of High Data Rates

The maximum data rate at which information can be transferred over a given communication channel is known as channel capacity. In information theory, channel capacity (ϑ) for the channel of a specified bandwidth in the presence of additive white Gaussian noise can be calculated using Shannon–Hartley's theorem [6] as follows:

$$\vartheta = BW \cdot \log_2 \left(1 + \frac{S}{N}\right) \tag{1.1}$$

where BW is the channel bandwidth, S is the average received signal power, and N denotes the average power of the white noise impairing the received signal.

Shannon–Hartley's channel capacity implies that the channel bandwidth and received signal power - or, more precisely, Signal-to-Noise Ratio (SNR) - are two factors limiting the achievable data rate. The average received signal power can be modelled as $S = E_b \cdot R$ where E_b and R are the received energy per bit and channel data rate, respectively. Moreover, because white noise is a random signal with a constant power spectral density, its power can be calculated as $N = N_0 \cdot BW$ where N_0 is the constant noise power spectral density.

Based on the fact that the channel data rate is always less than the theoretical channel capacity, the following inequality can be concluded:

$$R \leq \vartheta = BW \cdot \log_2\left(1 + \frac{S}{N}\right) = BW \cdot \log_2\left(1 + \frac{E_b \cdot R}{N_0 \cdot BW}\right) \tag{1.2}$$

By defining spectrum efficiency $\nu = R/BW$, Eq. (1.2) can be converted to its equivalent as follows:

$$\nu \leq \log_2\left(1 + \frac{E_b}{N_0} \cdot \nu\right) \tag{1.3}$$

Again, by reformulating Eq. (1.3), a lower bound on the required received energy per bit, normalised to the noise power density, can be obtained:

$$\frac{E_b}{N_0} \geq min\{\frac{E_b}{N_0}\} = \frac{2^\nu - 1}{\nu} \tag{1.4}$$

The minimum required $\frac{E_b}{N_0}$ as a function of the spectrum efficiency is shown in Figure 1.4. For spectrum efficiencies less than 1, the $min\{\frac{E_b}{N_0}\}$ is relatively constant, regardless of ν. In other words, increasing data rate requires a proportional increase in the minimum received signal power $S = E_b \cdot R$ (assuming noise power density is constant). Additionally, for spectrum efficiencies larger than 1, $min\{\frac{E_b}{N_0}\}$ increases quickly with ν. Thus, for data rates larger than the channel bandwidth, increasing the data rate requires a larger relative increase in the minimum received signal power.

It is concluded that transmission with a high-spectrum efficiency is power inefficient in the sense that it demands disproportionately high SNR. Provisioning very high data rates within a limited bandwidth is only possible in the high SNR scenarios, for instance when users are close to the cell centre. Instead, in order to provide high data rates as efficiently as possible in terms of required SNR, as well as providing high data rates not only for cell-centre users but also for cell-edge users, the channel bandwidth should be at least of the same order as the data

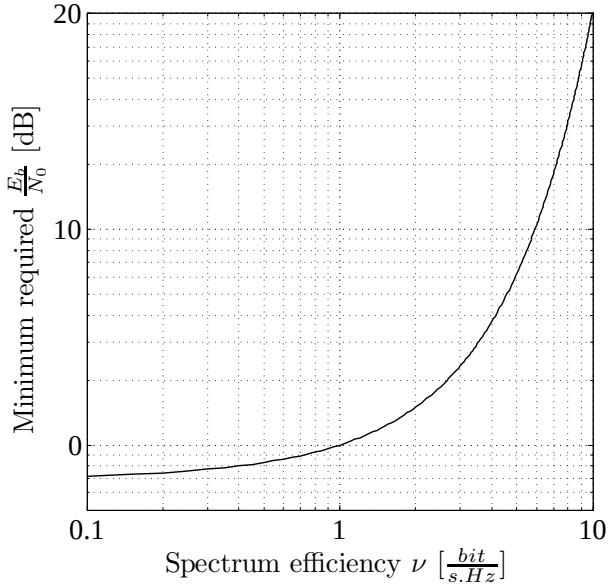

FIGURE 1.4: Minimum required $\frac{E_b}{N_0}$ at the receiver as a function of spectrum efficiency ν.

rates.

1.4 Broadband Mobile Communications

To achieve high-bandwidth transmission, the Federal Communications Commission (FCC) has been investigating the introduction of innovative Radio Resource Management (RRM) techniques to optimally manage the spectrum in such a way as to improve spectrum utilisation [7]. Therefore, telecommunication standards bodies for the NGMN have introduced the exploitation of novel features to enhance spectral utilisation, such as SA, Multiple-Input and Multiple-Output (MIMO) techniques, and the deployment of small cells.

SA is applied to enhance data rate of users by increasing bandwidth, by means of modified RRM functionality of the network. MIMO is employed to improve users' data rate by transmitting multiple data streams from different antennas to users. Small cells are practical and cost-efficient approaches for increasing

spectrum utilisation by allowing users served directly by the low-powered radio access to reuse spectrum [8].

Amongst these mentioned features, SA has attracted much attention recently. SA is a key feature of NGMN that enables Mobile Network Operators (MNOs) to create large virtual spectrum bandwidths for novel data hungry applications by exploiting discontinuous spectrum bands [4]. In this way, the multiple discontinuous spectrum bands can sustain information flow transmission service in the same way as the continuous spectrum bands.

1.5 Motivation

In order to satisfy the exponential growth of wireless data services and the growing number of wireless users, an overall transmission bandwidth of up to 100 MHz and correspondingly higher data rates of up to 1 Gbps is essential [9]. However, nowadays it is hard to find an available continuous spectrum large enough to satisfy the high bandwidth requirements of users of mobile communication systems [10]. SA is an effective tool for providing the high bandwidth requirements for the services and gains to be had in the case of spectrum fragmentation in NGMN.

The Office of Communications (Ofcom) is responsible for the management, regulation, assignment and licensing of the electromagnetic spectrum in the United Kingdom (UK). Ofcom recently investigated spectrum fragmentation in the UK. The adoption of old spectrum management policies and spectrally inefficient techniques are considered to be the main reasons for spectrum fragmentation [10]. In other words, spectrum fragmentation is considered the product of the regulatory environment.

Traditionally, wireless networks can only utilise continuous spectrum resources, but due to static (fixed) spectrum allocation policy, the wide continuous spectrum bands are hardly available under the current situation of spectrum resources. The majority of MNOs have fragmented spectrum dispersed in different frequency bands and bandwidths [11]. Making effective use of multiple and simultaneously available spectral fragments for new services enhances spectrum utilisation of MNO's spectrum resources, leading to an evolutionary development in the use and management of the radio spectrum.

Quality of Experience (QoE) of users is largely coupled to unpredictable transmission wireless environments, leading to intermittent connectivity and therefore low throughput. Because the qualities of channels vary randomly, SA can be used to improve communication reliability in wireless networks. Thus, in addition to enabling higher transmission bandwidth, simultaneous utilisation of multiple spectrum segments offers an extra frequency diversity due to the fact that assigned channels may experience different propagation losses and interference [8].

SA techniques can be applied for supporting simultaneous multi-site transmission in Heterogeneous Wireless Networks (HWNs) using licensed or even unlicensed spectrum, thus generating new spectrum resources for MNOs. Additionally, SA in HWNs, especially ultra-dense ones, can be applied as a promising solution for interference management. For instance, authors in [12] proposed autonomous carrier selection as a fully distributed and scalable method for the interference management problem in local areas, based on LTE networks.

SA supports intra or inter-band aggregation of carriers with different bandwidths, providing considerable flexibility gains for efficient spectrum utilisation. Furthermore, SA provides gradual re-farming (the clearing of frequencies from low-capacity systems and reassignment to high-capacity systems) of frequencies previously used by other systems. Re-farming offers MNOs a cost efficient method

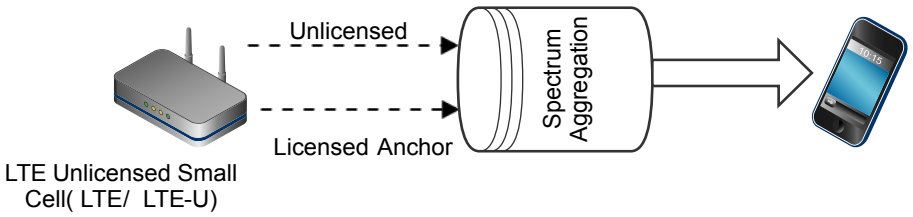

FIGURE 1.5: Through spectrum aggregation, LTE in unlicensed spectrum is combined with LTE in the licensed band, which becomes the anchor carrying all of the control and signalling information.

of increasing a network's capacity and coverage. For instance, as Global System for Mobile communications (GSM) and Code-Division Multiple Access (CDMA) traffic is decreasing, the spectrum can be reallocated to LTE, ensuring improved Return On Investment (ROI) and mobile broadband performance of LTE network.

Recently, Qualcomm introduced LTE in Unlicensed spectrum (LTE-U) for the use of the LTE radio communications technology in unlicensed spectrum, which will be used in conjunction with small cells [13]. The basic functionality of LTE-U is shown in Figure 1.5. LTE-U leverages the performance characteristics of LTE to take advantage of the 500 MHz unlicensed spectrum in the 5 GHz frequency band, through SA, addressing the spectrum scarcity problem. LTE-U could improve coverage and capacity by a factor of 2x to 4x compared to that reachable solely based on Wireless-Fidelity (Wi-Fi) [13]. LTE-U by means of SA enables MNOs to maximise their ROI.

Last but not least, SA increases bandwidth, but also improves trunking gains by dynamically scheduling traffic across the entire spectrum and traffic management. Consequently, this improves cell capacity and network efficiency and so improves the QoE for all users on the network. A user who for any reason encounters congestion on one segment of the spectrum can be seamlessly scheduled onto another segment of spectrum with more capacity, so maintaining a consistent QoE.

1.6 Challenges

As mentioned in Section 1.4 and Section 1.5, SA offers adequate spectrum flexibility to tackle spectrum fragmentation. However, spectrum flexibility comes with cost of complexity in Radio Frequency (RF) design for mobile devices. From a digital perspective, there is not much difference between different SA types (intra or inter-band SA), however from the RF point of view, the implementation and design complexity of SA is highly dependent on the type of SA [14],[15]. For instance, inter-band SA offers full utilisation of fragmented spectrum in comparison to intra-band SA, nevertheless it requires a most complicated RF chain.

To limit unwanted transmission emissions due to adjacent channel interference, transmitters for mobile users and base stations should be designed in such a way as to comply with regulatory requirements. These requirements set limits on all transmission emissions outside of the carrier bandwidth. The unwanted emissions from transmitters can be categorised into out-of-band emissions and spurious emissions [15]. Spectrum emission mask and an adjacent channel leakage power ratio are introduced by regulatory bodies to limit out-of-band emissions [16]. The spurious emissions not only consider frequency bands covered by spectrum emission masks but also in-band frequency. In intra-band non-continuous SA, similar to a single carrier system, aggregating carriers should satisfy the maximum emission level for single-carrier operation [14].

To fully utilise SA, RF architecture of both transmitter and receiver needs to be re-designed. Based on a type of supported SA, the RF chain demands different complexity levels. In [15], authors comprehensively investigated SA from the RF point of view. The authors proposed different RF architectures for SA enabled transmitters and receivers. Simulation results show that support of SA poses a remarkable increase in power amplifier back-off in order to minimise the unwanted emission. Furthermore, the authors concluded that the receiver side performance

FIGURE 1.6: Nexus 6, iPhone 6 Plus and Galaxy Note 4 (from left to right). Nexus 6 supports down link spectrum aggregation with bands 2+13, 2+17, 4+5, 4+13, and 4+17. iPhone 6 Plus supports T-Mobile's 700 MHz band 12, Sprint's 2.5 GHz spectrum aggregation. Galaxy Note 4 supports tri-band spectrum aggregation and Category 6 network service with speeds of up to 300 Mbps [18].

is mainly affected by transmitter emission and phase noise for a large inter-carrier gap, whereas it is dominated by receiver non-linearity for a small inter-carrier gap [15].

Supporting SA of multiple carriers, residing in higher/medium/lower spectrum bands, imposes major challenges for the RF design in handsets [17]. Therefore, handset manufacturers design low and high-end handsets with different transmission capabilities (e.g. supported bands, maximum number of carriers and maximum aggregation bandwidth) [4]. For instance, Nexus 6, iPhone 6/6s/6 Plus and Galaxy Note 4 - as shown in Figure 1.6 - support SA in UMTS frequency bands [18]. To allow the base station to communicate effectively with all connected users, it is necessary for mobile users to report their supported transmission capabilities as part of the connection set up.

In addition, SA adds complexity in both radio planning and RRM framework because different carriers (especially inter-band carriers) exhibit different radio propagation characteristics including path losses and Doppler shifts. Furthermore, because of the RF hardware complexity, each user can aggregate a certain number

of Component Carriers (CCs); therefore, RRM functionality needs to consider SA limitations of users.

RRM with SA for NGMN is the main topic of this thesis. In this study, new methods are proposed to tackle the introduced constraints of SA. The proposed methods not only improve the performance but also reduce the computational complexity.

1.7 Aims and Objectives

In this thesis, RRM for NGMN with SA is addressed in detail. For this purpose, Cognitive Radio Networks (CRNs), LTE networks, and Orthogonal Frequency-Division Multiplexing (OFDM)-based networks are considered. The main aims and objectives of this thesis are listed as follows:

RRM formulation and solution for NGMN with SA: To formulate the RRM function of NGMN with SA capability as a constrained optimisation problem in terms of some parameters and restrictions. The optimisation problem would be a mixed integer optimisation where some of the variables are integer and the rest are continuous. The formulation is required to take into account the practical constraints and requirements of current RF hardware design.

Standard compliant solution: To enable implementation of the proposed solution, a standard-compliant formulation and solution are necessary. The optimisation problem needs to consider all aspects and restrictions of the corresponding standard.

High performance solution: RRM functionality plays a pivotal role in the overall performance of the network and QoE of users. It distributes a finite

number of resources among users at each scheduling time slot under given Quality of Service (QoS) constraints for individual users, such as fairness and priority. Therefore, introducing a solution which improves the network performance, including cell throughput and user throughput as well as fairness amongst users, is imperative. The performance and efficiency of the proposed algorithms are evaluated and presented using extensive simulations.

Computationally-efficient solution: As explained in Section 1.6, SA adds complexity in both radio planning and RRM framework of the network. Due to the fact that RRM is highly dynamic and new decisions have to be made in each scheduling time slot, designing low computationally complex solutions is vital.

1.8 Contribution to Knowledge

The main contribution of this thesis can be listed as follows:

1. An aggregation-enabled spectrum assignment for CRNs is formulated as a mixed integer optimisation problem. The practical constraints of Co-Channel Interference (CCI) and Maximum Aggregation Span (MAS) in aggregation aware CRNs are taken into account. A genetic algorithm is used to resolve the aggregation aware spectrum assignment because of the simplicity, robustness and fast convergence of the algorithm.

2. A joint optimisation problem to maximise a Proportional Fairness (PF) objective function in LTE-A networks is formulated, considering RRM functionality with SA, Resource Block (RB) allocation, Modulation and Coding Scheme (MCS) assignment. The formulation considers MCS constraint as specified in 3GPP TR 36.912 [19], which requires that only one MCS can be selected for each assigned CCs across all its assigned RBs for the user

at any Transmission Time Interval (TTI) in the absence of MIMO spatial multiplexing. Furthermore, the formulated optimisation problem considers the difference between Primary Component Carrier (PCC) and Secondary Component Carrier (SCC).

3. It is shown that the resultant optimisation problem belongs to a class of intractable Integer Linear Programming (ILP) problems. The theory of total unimodular matrices is applied and this proves that solving the equivalent Linear Programming (LP) problem gives the same result as solving the ILP, which leads to an optimal and efficient approach for RRM.

4. Resource Allocation (RA) with SA functionality for OFDM-based networks is formulated as an optimisation problem under the practical constraints of transmission power and the limited number of aggregating CCs available for each user. A sub-optimal low-complexity solution is proposed to solve the optimisation problem. Further, an efficient solution is introduced to approximate the first solution.

The core RRM strategy for NGMN presented in this thesis is to take advantage of multi-user diversity in both time and frequency dimensions across different carriers (multi-carrier diversity) and schedule transmissions to mobile users on resources with better channel conditions.

1.9 Progress beyond State of the Art

This thesis treats the area of RRM in NGMN, with focus on Down Link (DL) direction; Up Link (UL) direction is not discussed. However, most of presented techniques and insights can be adapted to the UL. This study investigates the problem of single-cell RRM with centralised RA without cooperation among users.

In Chapter 3, an aggregation-enabled spectrum assignment algorithm for CRNs is proposed. The additional constraints of CCI and MAS in an aggregation aware CRN are taken into account. Numerical results show that the introduced method significantly increases the spectrum utilisation compared with the State-Of-The-Art (SOTA) solutions including Maximum Satisfaction Algorithm (MSA) [20] and Random Channel assignment Algorithm (RCA). For this purpose, two different scenarios are considered - Scenario-I: without CCI and Scenario-II: with CCI. In Scenario-I, for network load equals 1, the proposed solution improves the rewarded bandwidth to users in network by a factor of 4 compared to RCA and MAS, while in Scenario-II the proposed solution improves the allocated bandwidth to users by a factor of 2 when network load is 1.

The solution proposed in Chapter 4 is the first attempt for an optimal allocation of RBs, CCs, and MCS in LTE networks. Most of the existing research solves the allocation problem in a non-SA based LTE systems [21–23] by using Greedy Algorithms (GAs) or an approximation based approach which guarantees only half of the optimum PF objective [24–26]. Moreover, the majority of the research work in literature neglects concept of PCCs and SCCs. However, the proposed solution not only takes PCCs and SCCs into consideration, but is also an optimal and low-computationally complex solution.

Extensive simulations are performed to validate the performance of the proposed solution, and this is compared with the modified version of GA [24] using a MATLAB based system level simulator [27]. Simulation results show that the proposed solution improves cell throughput by 13% compared to GA when there are 15 users in the cell. Furthermore, numerical results show that the cell-edge users throughput can be improved by the proposed solution by about 10%, while the throughput of cell-centre users remains similar to GA.

Finally, in Chapter 5, RA with SA functionality is formulated for OFDM-based

networks as an optimisation problem under the practical constraints of transmission power and the limited number of CCs available for each user. Two efficient methods - referred to as Two-Step RA Algorithm (TSRAA) and Efficient RA Algorithm (ERAA) - are proposed, both based on a two-step solution with reasonably low complexity. The performance of TSRAA and ERAA are compared with the highly complex COmbinatorial Algorithm (COA) - introduced as an optimal solution. Both are computationally efficient methods, but ERAA is even more efficient than TSRAA. A simulation based study is provided to evaluate the performance of the proposed methods and compare them with the optimum solution. Cell throughput in the case of ERAA and TSRAA is 10% and 2% lower than COA respectively.

1.10 List of Published Works

1. S. Rostami, K. Arshad and P. Rapajic, "Aggregation-based spectrum assignment in cognitive radio networks," Advanced Computing and Communication Systems (ICACCS), 2013 International Conference on, Coimbatore, 2013, pp. 1-6

2. S. Rostami, K. Arshad and P. Rapajic, "A joint resource allocation and link adaptation algorithm with carrier aggregation for 5G LTE-Advanced network," Telecommunications (ICT), 2015 22nd International Conference on, Sydney, NSW, 2015, pp. 102-106

3. S. Rostami, K. Arshad and P. Rapajic, "Resource allocation algorithms for OFDM based wireless systems," Personal, Indoor, and Mobile Radio Communications (PIMRC), 2015 IEEE 26th Annual International Symposium on, Hong Kong, 2015, pp. 1105-1110

4. S. Rostami, S. Alabadi, K. Arshad and P. Rapajic, "Efficient Sub-Carrier Allocation Algorithm for OFDM based Wireless Systems," Universal Technology Management Conference (UTMC), USA, 2016, pp. 56-61

5. S. Rostami, K. Arshad and P. Rapajic, "Resource Allocation in LTE-based MIMO Systems with Carrier Aggregation," accepted by Vehicular Technology Conference (VTC Fall), 2016 IEEE 84th, Montréal, 2016

6. K. Arshad, M. Imran, S. Rostami and P. Rapajic, "Resource Allocation Algorithm in Multi-Carrier Cellular Networks with Carrier Aggregation," under review by International Conference on Recent Advances on Signal Processing, Telecommunications & Computing (SigTelCom), 2017 Da Nang, Vietnam

7. S. Rostami, K. Arshad and P. Rapajic, "Energy-Efficient Resource Allocation for LTE-A Networks," in IEEE Communications Letters, vol. 20, no. 7, pp. 1429-1432, July 2016

8. S. Rostami, S. Alabadi, S. Noori, H. Shihab, K. Arshad and P. Rapajic, "Spectrum Assignment Algorithm for Cognitive Machine-to-Machine Networks," under press in special issue for Smart Spectrum Technologies for Mobile Information Systems

9. S. Alabadi, P. Rapajic, K. Arshad and S. Rostami, "Energy Efficient Cognitive M2M Communications," in International Journal of Interdisciplinary Telecommunications and Networking, vol. 8, Issue 3, July - September 2016

10. S. Rostami, K. Arshad and P. Rapajic, "Optimum Radio Resource Management in Carrier Aggregation based LTE-Advanced systems," under review by IEEE Transactions on Vehicular Technology

1.11 Notation

In this thesis, vectors of dimension n are denoted by small bold letters (e.g. $\mathbf{x}_n$) and matrices are denoted by capital letters (e.g. C). Hence, $\mathbf{0}_n$ denotes the n-component all-zero vector and $\mathbf{1}_n$ denotes the n-component all-one vector. Occasionally the vector subscripts can be removed to save space and in that case the exact vector size can be realised from the context. Further, I_n represents the $n \times n$ identity matrix and $(.)^T$ denotes the transpose operations. A block diagonal matrix, $A = blkd(B, b)$ represents a matrix of the form:

$$A = \begin{bmatrix} B & 0 & \dots & 0 \\ 0 & B & \dots & 0 \\ \vdots & \vdots & \ddots & \vdots \\ 0 & 0 & \dots & B \end{bmatrix}$$

where 0 is an all-zero matrix with the same size as B and B is repeated b times.

1.12 Structure and Organisation of the Thesis

The thesis is organised as follows:

1. In Chapter 2, the system architecture of CRNs and LTE networks is reviewed briefly and the SA for both networks is then studied in detail. A qualitative overview of the SA emerged in recent literature, and the aim of emphasising their approach in NGMN is presented. 3GPP status for Release 10-12 (Rel 10-12) SA is explained.

2. In Chapter 3, an aggregation-based spectrum assignment algorithm using a genetic algorithm for CRNs is proposed. The proposed algorithm takes

into consideration interference to the Primary Users (PUs), CCI among Secondary Users (SUs), and MAS to aggregate whitespaces. Furthermore, simulation results and analysis of the convergence of the proposed algorithm are provided.

3. In Chapter 4, an optimum RRM algorithm for LTE-A with reduced complexity is proposed and compared with the SOTA solutions. The proposed algorithm optimally assigns CCs, RBs, and MCS values to the users based on their Channel State Information (CSI) and SA capabilities. Finally, performance of the proposed solution has been evaluated using extensive simulations and results are provided.

4. In Chapter 5, the RA problem with SA in OFDM-based networks is formulated as a complex mixed integer optimisation problem under the practical constraints of transmission power and the limited number of CCs available for each user. Simulation results are provided for comparison purposes.

5. The conclusion and proposals for future work are given in Chapter 6.

Chapter 2

Background and Literature Review

With growing demand for broadband mobile access, MNOs need to allow their networks to operate in a number of different frequency bands, in spectrum allocations of different sizes, and in fragmented spectrum. Therefore high spectrum flexibility is vital for NGMN, and this can be provided by SA. SA enables a flexible radio resource allocation among mobile users. It also improves frequency diversity by introducing multi-carrier diversity. But although SA offers these advantages, it also poses a number of new challenges such as 1) Complexity in RF design, 2) Radio planning, and 3) Complexity in Radio resource management. In this thesis, novel techniques are proposed to address the resource management for NGMN.

In Section 2.1, CRN architecture and spectrum management functions in CRNs are reviewed briefly. Afterwards, in Section 2.2, SA and RRM in LTE-A network are discussed in detail. In Section 2.3, OFDM-based networks are reviewed briefly, followed by a review of recent works on SA in Section 2.4.

2.1 Cognitive Radio Networks

The increasing demand for the spectrum is a consequence of an almost incalculable rise in penetration and usage of Internet enabled wireless devices such as M2M devices, wearable devices, smartphones, tablets, and laptops [28]. Data usage of these devices is being spurred on by the growing availability of numerous applications, high quality video streaming and cloud computing. Nowadays, lack of spectrum has become the retardant of the development of the wireless networks.

Ofcom, as the communications regulator, is responsible for all spectrum management in the UK. Ofcom uses an auction-based policy to allocate spectrum for MNOs [29]. To enable wireless communication signals to penetrate through walls, trees and other obstacles, lower frequency bands are the best candidates for wireless communication purposes. Historically, frequency ranges between 700 MHz and 2.6 GHz are granted for mobile communication systems, but most of the spectrum in this range has already been allocated. Therefore, wireless companies cannot enhance their capacity by introducing new spectrum.

In brief, the spectrum utilisation, U can be expressed by the measure:

$$U = \frac{R}{V \times BW \times T} \tag{2.1}$$

where R is the quantity of information rate, BW is the occupied bandwidth, V and T are the volume and fraction of the time within which use of that bandwidth is denied to other users. The space factor, V can usually be regarded as a geographical area. The spectrum under-utilisation over both geographical locations and time is evidenced by multiple spectrum measurement surveys [30]. The result is in direct contradiction to the spectrum shortage problem. In other words, the problem is not one of physical spectrum scarcity but of poor spectrum utilisation, an inevitable result of the current spectrum management policy which allocates

spectrum exclusively to licensed users, also known as PUs. In this perspective, an enormous amount of work has been carried out to improve spectrum utilisation over the last several decades [31–33]. This includes the use of different multiple access technologies, e.g. Frequency Division Multiple Access (FDMA), Time Division Multiple Access (TDMA), CDMA, and Orthogonal Frequency Division Multiple Access (OFDMA).

From the network configuration point of view, the radio spectrum is reused geographically to overcome spectrum scarcity. For instance, in LTE, the radio spectrum is geographically re-utilised through small cells. However, experiments from the FCC reveal that spectrum utilisation still varies from 15%-85% with frequency, time and geographical location. Consequently, Cognitive Radio (CR) has been introduced as an intelligent radio able to utilise the unused segments of spectrum opportunistically.

The idea of CRNs is to share the spectrum between PUs and unlicensed users, also known as SUs. CR is based on Dynamic Spectrum Access (DSA) as a new spectrum sharing method that allows SUs to access the idle spectrum in the licensed spectrum bands. CR is a promising technology to alleviate the spectrum scarcity problem and increase spectrum utilisation. The network of SUs creates the CRN.

The seminal paper of J. Mitola at KTH (the Royal Institute of Technology in Stockholm) in 1998, introduced the concept of CR for the first time and was published in an article in 1999 [34]. Akyildiz et al. defines CR as [35]:

"A Cognitive Radio is a radio that can change its transmitter parameters based on interaction with the environment in which it operates."

The motivation behind CRNs is twofold:

1. To change the traditional static spectrum allocation policy.

2. To improve under-utilisation of spectrum usage and overcome the problem of spectrum scarcity.

CRNs aim to detect and opportunistically exploit the under-utilised spectrum. In the CRNs, SUs are permitted to operate only on those idle channels which are not utilised by the PUs. Moreover, SUs must avoid causing harmful interference to PUs during their communication. PUs are the legacy users and they have higher priority to use the licensed spectrum than SUs [36].

2.1.1 Cognitive Radio Network Architecture

According to the concept of DSA-based networks, wireless networks can be classified as Primary Network (PN) and the CRN [37]. The PN is composed of PUs and generally has an existing infrastructure, which has an exclusive right to access certain spectrum bands. Examples of PNs are cellular networks and TV broadcast networks. Figure 2.1 shows the architectural diagram of PNs and CRNs in DSA-based networks [37].

Infrastructure-less and infrastructure-based networks are two different classification of CRNs. Infrastructure-less CRNs may also be classified as CR ad-hoc networks. The infrastructure-based CRN generally has a central entity managing the overall network, such as an Access Point (AP) in Wireless Local Area Networks (WLANs) or a base station in cellular networks. On the other hand, CR ad-hoc networks can be deployed without any infrastructure support (i.e. no central entity is present).

In CRNs, idle channels can be managed by different entities. For example, in the CR ad-hoc networks, SUs themselves are responsible for spectrum sensing, assignment and management, while in infrastructure based architectures, a spectrum broker is responsible for spectrum sensing, assignment and management. The

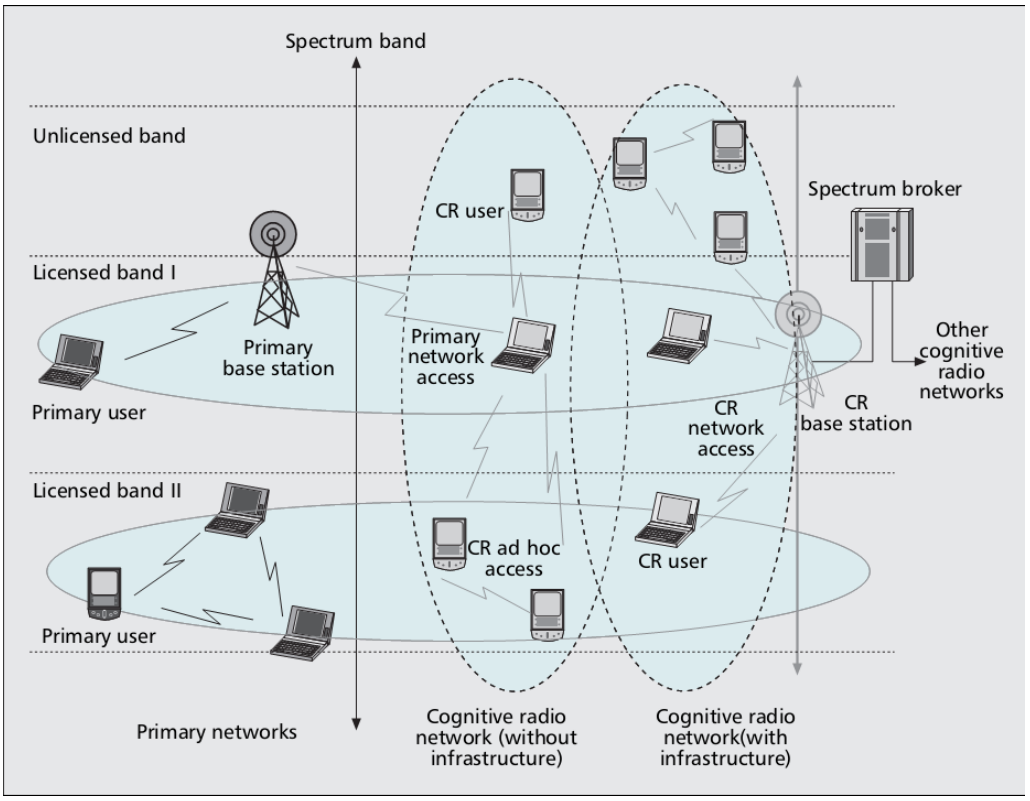

FIGURE 2.1: Architecture diagrams of PNs and CRNs [37].

latter needs a dedicated control channel and may be exposed to different threats like denial of service attack [37], while in the CR ad-hoc networks, the use of a dedicated control channel is optional.

2.1.2 Spectrum Management Functions in Cognitive Radio Networks

In order to enable DSA, CR should adapt its transmission parameters to the spectrum environments [35]. The process of accessing spectrum in CRNs consists of four spectrum management functions: spectrum sensing, spectrum decision, spectrum sharing and spectrum mobility [35].

Spectrum sensing is one of the main functionalities of CRNs. SUs can only transmit if they detect that licensed band is free, and rely on the spectrum sensing to

detect the idle channels. In this case, a SU monitors a licensed frequency band and opportunistically transmits when PUs are not present. Based on the amount of knowledge that SUs have from the PU's signal structure, a number of spectrum sensing techniques are available in literature [36],[38–40]. For instance, if the structure of the PU's signal is fully-known, the optimal detector is a matched filter [36]. A simpler alternative for the identification of the PU's signal is to employ an energy detector. The energy detector does not need to know any information about the PU's signal structure, but simply measures the energy received on a licensed band during the observation interval and declares it as idle if the measured energy is less than a properly set threshold [39]. Waveform-based or coherent spectrum sensing is another robust method for identifying the presence of PU. This method exploits the known patterns of preambles that are regularly transmitted from particular PU. For this purpose, a SU calculates the correlation of the received signal with a known copy of itself and then compares the correlation metric with a defined threshold [40],[41]. In [40], it is shown that waveform-based sensing outperforms the energy detector.

Once the SUs detect the idle spectrum by performing spectrum sensing, it is vital that the SUs select the most appropriate band according to channel condition and their QoS requirements without causing any harmful interference to PUs. Spectrum decision involves spectrum characterisation and spectrum assignment [42]. It is important to characterise the spectrum band not only in terms of spectrum environment but also on the statistical behaviours of the PUs' traffic. In order to design a spectrum assignment algorithm that incorporates dynamic spectrum characteristics, CRN needs to select the most appropriate spectrum band to satisfy the SUs' QoS requirements [43],[44].

To share the idle spectrum among SUs in CRN, it is necessary that SUs' transmissions are coordinated with each other. Moreover, spectrum sharing in CRN is more complex than typical wireless networks due to the presence of heterogeneous

PUs and the wide range of spectrum available for SUs. The architecture, spectrum allocation and spectrum access techniques are different aspects of spectrum sharing [35]. The architecture of spectrum sharing can be classified as centralised and distributed spectrum sharing. In the former, all spectrum assignment and access procedures occur in central entity where all measurements of distributed SUs are forwarded [37]. The central entity, which is known as a spectrum broker, can grant unused spectrum to SUs for a specific space (geographical location) during the time when no PUs are using the spectrum. Because of the large number of SUs and limited available spectrum, there is not only competition for spectrum but also competition for SUs in the central entity. Conversely, in distributed spectrum sharing, each SU, based on local policies, performs spectrum assignment and access procedures distributively [35]. Typically, the performance of centralised spectrum sharing is superior to the distributed one, but at the cost of the inevitable signalling load between SUs [45]. Furthermore, distributed spectrum sharing require more radio resources as the physical network layout will change as devices move around, while an AP in infrastructure mode generally remains stationary. If many devices are connected to the ad-hoc network, there will be more wireless interference. Therefore, in this thesis, the centralised spectrum sharing is considered.

Spectrum access can be cooperative or non-cooperative. In cooperative spectrum sharing, each SU has access to the interference measurements of other SUs in the CRN. In other words, each SU knows the interference level of the transmission of another SU in a particular channel. To share spectrum cooperatively, a group of neighbouring SUs form a cluster, and each SU in their corresponding cluster shares the interference measurements [30], in contrast to non-cooperative spectrum sharing, where only a single SU is considered. The SU's lack of knowledge of the interference situation of neighbouring SUs may cause low spectrum utilisation. Nevertheless, non-cooperative spectrum sharing schemes do not need message exchanges between neighbours, as in cooperative solutions [35].

Cooperative approaches generally give better performance than non-cooperative approaches [30],[37]. Cooperative spectrum access improves throughput as well as fairness among SUs, because of its collaborative nature. Nevertheless, the performance degradation of non-cooperative approaches is generally offset by the significantly lower signalling load and hence, energy consumption.

There are two types of spectrum access techniques: overlay spectrum sharing and underlay spectrum sharing. In the former, SUs use spectrum only if it is not being used by PUs [46]. Therefore, overlay spectrum sharing offers minimum interference to PUs. However, in the underlay approach, SUs employ spread spectrum techniques in such a way that the interference level to PUs is less than a predefined threshold i.e. PUs see the data transmissions of SUs as noise. In this thesis, because of the reasons mentioned above, the overlay spectrum sharing is considered.

The fourth function in the spectrum management framework of CRNs is spectrum mobility management [35]. The primary goal of spectrum mobility is guaranteeing continuous SU transmission while PU's presence is detected. Spectrum mobility can be separated into two different techniques: spectrum handoff and connection management [47]. Spectrum handoff is the process of switching the operating spectrum of SU to another free spectrum. This switching to another channel generates an additional latency to SU. Therefore, to tackle the inevitable handoff delay, the connection management process manages and adjusts protocol stack parameters, depending on network conditions [48].

2.2 LTE Networks

Since the introduction of the first generation of mobile communication systems (1G) in the 1980s, there has been a tremendous paradigm shift in the design

methodology, implementation, development and considerable enhancement in the QoS of mobile communication systems. In addition, the past decade has witnessed an explosive growth in data traffic which is driven by expanding Internet usage and the growing demand of data-rich multimedia applications. Therefore, increasing the wireless capacity of the network and offering better QoE for users have become vital goals for different standardisation bodies and companies.

In order to satisfy the exponential growth of wireless data services and the growing number of wireless users, the ITU initiated a global standard, referred to as International Mobile Telecommunications-Advanced (IMT-A) or 4G, to identify an all-IP cellular network whose capabilities go beyond those of IMT-2000 [9],[49]. Specific requirements for IMT-A have been set to a minimum support of 40 MHz bandwidth as well as 1 Gbps and 500 Mbps peak data rates for DL and UL respectively [9],[19],[49–51].

Since 2004, 3GPP has been developing LTE and the first complete set of specifications (i.e. Rel-8) was published in 2008, providing DL and UL peak data rates up to 300 Mbps and 75 Mbps respectively. In response to an ITU invitation for the submission of potential technologies for IMT-A, 3GPP started LTE-A specifications in 2008 and published Rel-10 in 2010. In 2010, ITU approved LTE Rel-10 (LTE-A) as one of two IMT-A technologies. LTE-A not only fulfils IMT-A requirements, but in many cases even surpasses them (for instance, UE Category 8 exceeds the requirements of IMT-A by a remarkable margin) [52]. LTE-A provides a suitable base for enhanced services because of the provision of higher data rates, improved coverage, and low latency services [53]. To achieve many of the aggressive performance targets, four important features that are included in LTE-A are:

Spectrum Aggregation: Improving spectrum flexibility to allow for the deployment of LTE radio access in difference frequency bands with varying channel

bandwidth. Furthermore, to support peak data rates of up to 1 Gbps, the use of high channel bandwidth is imperative. Unfortunately, worldwide MNOs do not have access to a continuous portion of wider bandwidth (e.g. 100 MHz) due to spectrum fragmentation and an inefficient command and control spectrum management approach [54]. To achieve this, 3GPP introduced SA as one of the most important features in LTE-A specifications to allow efficient and flexible usage of fragmented spectrum by aggregating multiple CCs dispersed in fragmented spectrum bands (intra-band SA and inter-band SA) [8],[14].

Extended Multi-Antenna Transmission: Enhancing MIMO technology by supporting up to eight transmission layers in DL and four transmission layers in UL. MIMO improves overall system performance including spectrum efficiency and system capacity without requiring additional bandwidth [4]. Transmit diversity, beamforming, and spatial multiplexing are the main MIMO configurations used in LTE-A systems. Transmit diversity increases the received SNR and the robustness of communication in fading channels by transmitting the same version of the transmitted signal from different antennas. Beamforming is applied to shape the transmit beam to maximise the antenna gain in the direction of the target user, or to suppress interference at the target user location. Furthermore, spatial multiplexing increases throughput by transmitting different streams of data simultaneously in parallel from different antennas [55].

Relaying: Data rate between User Equipments (UEs) and the radio access network is mainly dependent on the path loss between UEs and evolved Node-B (eNB). According to LTE specifications, the gap between the link performance of LTE and Shannon's capacity limit is very close. Therefore to achieve the maximum possible data rate by LTE, high SNR is vital. SNR can be enhanced, for instance with MIMO techniques, or by using ultra-dense

cellular networks. A denser infrastructure is mainly a deployment aspect, however in LTE-A and subsequent releases, the possibility of relaying is supported. Relaying can reduce the effective distance between UEs and eNB, leading to an improved SNR level and higher data rates, especially for cell-edge UEs. The type of relays used in LTE are transparent to UEs. Relays in LTE, instead of fibre optics, are connected to the radio access network using LTE air interface [17].

Heterogeneous Deployments: The exponential growth of data traffic caused by the proliferation of Internet-connected mobile devices, forcing MNOs to considerably increase the capacity of their networks [17]. It is not cost-effective for the conventional homogeneous wireless networks to provide the required network capacity. To this end, LTE supports a new network architecture of low-power nodes such as femtocell and picocell to achieve a more cost-effective way to remove coverage holes and improve the capacity of the network. Using HWNs is a promising solution to achieve the requirements defined by IMT-A [56],[57].

2.2.1 Spectrum Aggregation in LTE-A Networks

LTE offers flexible spectrum allocation ranging from 1.4 MHz to 20 MHz by means of OFDM in DL and Single-Carrier FDMA (SC-FDMA) in UL [58]. In order to improve peak data rate to achieve the requirements of IMT-A, 3GPP introduced SA as one of the main features of LTE-A, which not only increases bandwidth but also enhances spectrum flexibility remarkably by allowing it to exploit different CCs dispersed in the same or different frequency bands. The frequency bands which are specified for IMT for different years are depicted in Figure 2.2 [8]. As shown, the continuous available spectrum is limited. Thus to achieve the wide bandwidth requirement, LTE-A has to support SA.

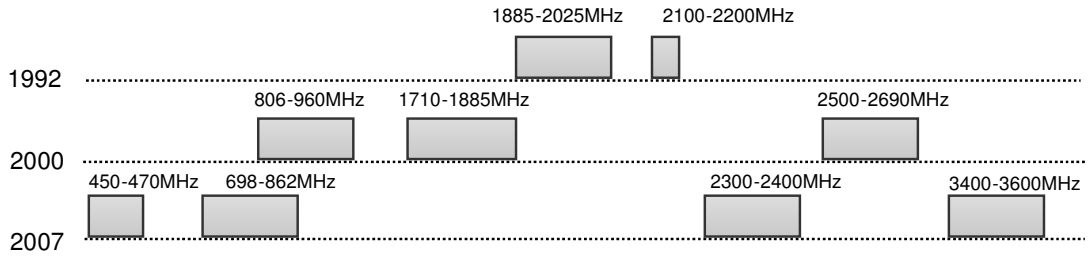

FIGURE 2.2: Frequency bands for IMT, identified at World Radio Conferences (WRC) are non-continuous, and some of them are less than 100 MHz [8].

To ensure the coexistence of legacy Rel-8 and Rel-9 users in LTE-A network, SA is designed to be backward compatible. Therefore, each CC from the physical and Media Access Control (MAC) layer view is inherently an LTE carrier. However, the introduction of SA demands the introduction of new functionalities and modification of the RRM functionality of the network.

2.2.1.1 Spectrum Aggregation Configuration Scenarios

LTE-A (Rel-10) supports SA of a maximum of 5 CCs of 20 MHz with a maximum supported bandwidth of 100 MHz, as shown in Figure 2.3 [59]. SA can be used in both DL and UL in both frame structures of Frequency-Division Duplex (FDD) and Time-Division Duplex (TDD). Additionally, SA can be continuous, as shown in Figure 2.3(a), or non-continuous, as illustrated in Figure 2.3(b). Aggregated CCs may have different bandwidths. Three different configurations for SA can be defined as follows [15]:

1. **Intra-band continuous SA:** Multiple adjacent CCs within the same frequency band are utilised to form wider bandwidth.

2. **Intra-band non-continuous SA:** Multiple CCs are separated along the same frequency band.

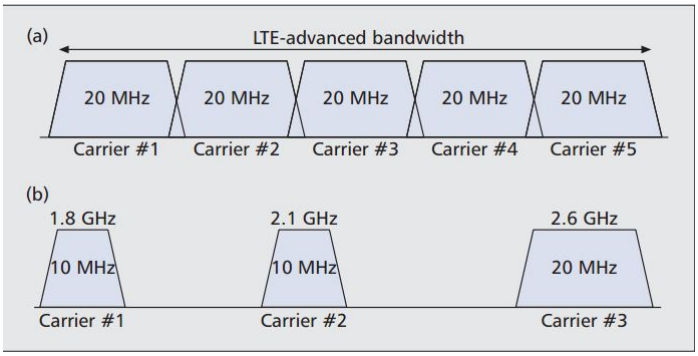

FIGURE 2.3: SA configuration scenarios: a) continuous aggregation of five CCs with equal bandwidth; b) non-continuous aggregation of CCs with different bandwidths [59].

3. **Inter-band SA:** Multiple CCs belonging to different frequency bands are aggregated to serve UE.

Because the continuous SA can be implemented by means of a single Fast Fourier Transform (FFT) and a single RF unit, its implementation is easier and cheaper than non-continuous SA, which demands multiple RF chains and FFTs. In addition, compared to intra-band non-continuous and inter-band SA, it is easier to design RRM for intra-band continuous SA [14]. Moreover, the non-continuous SA adds complexity in both radio planning and RRM framework because different CCs (especially inter-band CCs) exhibit different radio propagation characteristics including path losses and Doppler shifts. In LTE with FDD, UL and DL CCs are separated with frequency duplex distance determined by the MNO. For mobile users with SA capability (LTE-A), only one CC is considered as an anchor CC, which is referred to as the PCC. The PCC is responsible for all primary functionalities such as radio link failure monitoring. The rest of the CCs for LTE-A devices are denoted as SCCs.

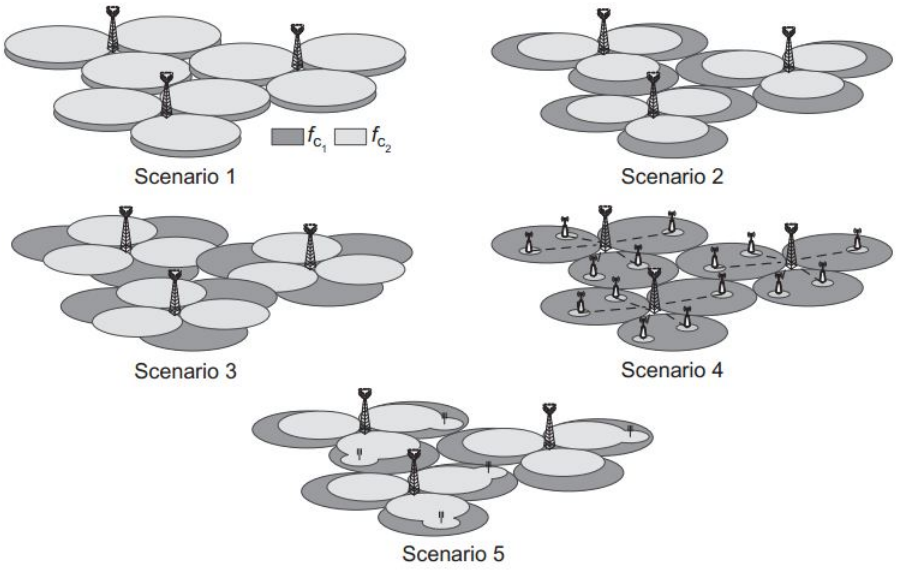

FIGURE 2.4: Spectrum aggregation deployment scenarios [60].

2.2.1.2 Spectrum Aggregation Deployment Scenarios

SA has proceeded rapidly in network deployments because of its promising performance benefits and because it allows MNOs to turn their investment in additional LTE carriers into marketable higher data rates. SA-enabled network can be deployed in such a way as to enhance data rates for UEs in cell edges or to mitigate inter-cell interference. For the purpose of simplicity, it is assumed that there are only two different CCs in the network, f_{C_1} and f_{C_2} (as shown in Figure 2.4). The following deployment scenarios can be considered [60]:

Scenario 1: In this case, both f_{C_1} and f_{C_2} are in the same frequency band (same path loss characteristics) and collocated; therefore their coverage is virtually the same and overlaps each other. This SA scenario is used to achieve higher data rates for UEs where both layers provide sufficient coverage and mobility.

Scenario 2: In this case, f_{C_1} and f_{C_2} are in different frequency bands but both are collocated and overlaid. Due to different path loss characteristics of f_{C_1} and f_{C_2}, this scenario provides different coverage. Sufficient coverage

and mobility are supported on the CC in the lower frequency band (f_{C_1}), however the CC in the higher frequency band (f_{C_2}) is used to further extend bandwidth and consequently data rates.

Scenario 3: Similar to deployment Scenario 2, f_{C_1} and f_{C_2} are on different frequency bands. Antennas for cells with f_{C_2} are directed to the cell boundaries of the cells with f_{C_1}, to enhance data rate of cell-edge UEs and reduce coverage holes.

Scenario 4: Cells for f_{C_1} provide macro coverage and Remote Radio Heads (RRHs) are used to increase data rate. Generally, f_{C_1} and f_{C_2} are in different frequency bands. UEs within coverage of RRHs and macrocells are the only UEs that can aggregate both f_{C_1} and f_{C_2}. The mobility is performed based on the coverage area of f_{C_1}.

Scenario 5: This case is similar to deployment Scenario 2 where there are distributed antennas to improve coverage of only the higher frequency band CC, f_{C_2}.

2.2.1.3 3GPP Status for Release 10-12 Spectrum Aggregation

As mentioned, SA configurations can be classified as intra band (continuous and non-continuous) and inter band. In Rel-10, only intra-band continuous and inter-band SA of two CCs are specified. Because 3GPP for the first time defined SA in Rel-10, it only specifies two basic SA combinations, including continuous intra-band SA for bands 1 (FDD) and band 40 (TDD) - named CA_C-1 and CA_C-40 respectively (Table 2.1) - and an inter-band SA between bands 1 and 5, named CA_1-5 (Table 2.2) [4],[61].

TABLE 2.1: Intra-band continuous spectrum aggregation(2DL/2UL) in 3GPP Rel-10 [62].

SA band	LTE operating bands
CA_C-1	1
CA_C-40	40

TABLE 2.2: Inter-band spectrum aggregation (2DL/1UL) in 3GPP Rel-10 [62].

SA band	LTE operating bands
CA_1-5	1
	5

TABLE 2.3: Intra-band continuous and non-continuous spectrum aggregation in 3GPP Rel-11 [62].

SA band	LTE operating bands	Requested by
CA_C-41	41(2DL/2UL)	Clearwire,CMCC
CA_C-38	38(2DL/2UL)	CMCC
CA_C-7	7(2DL/2UL)	CUC, CT, Telenor
CA_NC-B25	25(2DL/1UL)	Sprint
CA_NC-B41	41(2DL/1UL)	CMCC

Rel-11 offers new SA configurations which not only support continuous intra-band SA but also non-continuous intra-band SA (Table 2.3), as well as band 29 for inter-band SA (Table 2.4). Band 29, also known as supplemental DL, is a special band which has only a single DL CC without UL CC. Band 29 is defined as bandwidth expansion only and can be used as an additional DL SCC [61],[63],[64].

In Rel-12, SA of both FDD and TDD frequency bands are specified. In addition, aggregating three DL CCs and two UL CCs are considered. In UL, it supports new SA configurations, including inter-band and intra-band non-continuous SA, as well as supporting band 32 (1500 MHz), which has only one DL CC [4]. Additionally, in Rel-12 dual connectivity, known as multi-site SA, is introduced for the first time to support the aggregation of CCs between different sites. This feature can be an useful method for HWNs with incompatible core networks. In this solution, a macrocell is responsible for mobility management of UEs, however small cell provisions extra capacity to UEs with dual connectivity. In other words, UEs take advantage of both macrocells coverage and small cells capacity. Because of

TABLE 2.4: Inter-band spectrum aggregation (2DL/1UL) in 3GPP Rel-11 [62].

SA band	LTE operating bands	Requested by
CA_1-19	1+19	NTT DOCOMO
CA_3-7	3+7	TeliaSonera
CA_4-13	4+13	Verizon Wireless
CA_4-17	4+17	AT&T
CA_7-20	7+20	Orange et al
CA_5-12	5+12	US Cellular
CA_4-12	2+12	Cox Communication
CA_2-17	2+17	AT&T
CA_4-5	4+5	AT&T
CA_5-17	5+17	AT&T
CA_3-5	3+5	SKTelecom
CA_4-7	4+7	Rogers Wireless
CA_3-20	3+20	Vodafone
CA_8-20	8+20	Vodafone
CA_1-18	1+18	KDDI
CA_1-21	1+21	NTT DOCOMO
CA_11-18	11+18	KDDI
CA_3-8	3+8	KT
CA_2-29	2+29	AT&T
CA_4-29	4+29	AT&T

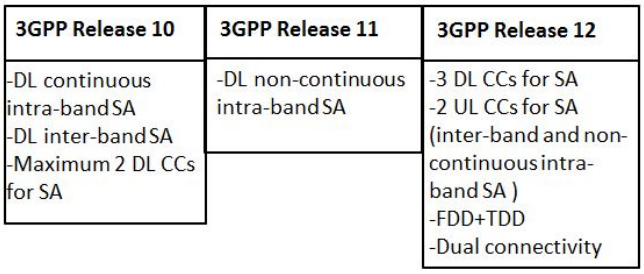

FIGURE 2.5: 3GPP release status for spectrum aggregation [16].

providing higher bandwidth through SA, multi-site SA can enhance cell-edge gain by 50% even in highly loaded networks [16]. Figure 2.5 briefs 3GPP release status for SA.

TABLE 2.5: Spectrum aggregation capability associated with each UE category [64].

UE Category	Possible number of aggregated DL-CCs	Typical number of aggregated DL-CCs	Possible number of aggregated UL-CCs	Typical number of aggregated UL-CCs
Category 1	1...5	1	1...5	1
Category 2	1...5	1	1...5	1
Category 3	1...5	1,2	1...5	1
Category 4	1...5	1,2	1...5	1
Category 5	1...5	1	1...5	1
Category 6	1...5	2	1...5	1
Category 7	1...5	2	1...5	2
Category 8	5	5	5	5
Category 9	1...5	3	1...5	1
Category 10	1...5	3	1...5	2

2.2.1.4 UE Categories for Spectrum Aggregation

3GPP specification defines a number of UE categories in order to enable eNB to communicate with UEs based on their transmission capabilities and to create device segmentation [61]. Supported transmission parameters and performance vary according to UE's category. There are five categories (Category 1-5) defined in LTE Rel-8 and Rel-9. For instance, Category 1 does not support MIMO, but Category 5 supports 4×4 MIMO. In LTE Rel-10, with the introduction of SA and enhanced MIMO capability (up to 8×8 DL MIMO and up to 4×4 UL MIMO), new categories of 6-8 are defined. Recently, in Rel-11, new categories of 9 and 10 have been added.

Although UE categories are closely linked to the SA capability of UEs, this does not dictate the number of supported aggregating CCs. In other words, there is no direct mapping between UE's category and SA capability of UEs. The possible and typical numbers of aggregating CCs for both DL and UL, based on UE category, are summarised in Table 2.5 [64]. It is anticipated that in newer releases of LTE (Rel-12 and Rel-13), new UE categories will be added to achieve a 600 Mbps data rate.

As shown in Table 2.5, the number of CCs in DL is always equal to or greater than

the number of CCs in UL. This difference is also known as asymmetric configuration. For instance, it is possible to have multiple DL CCs and a single UL CC for a mobile user, informed to UE through system information signalling. Bandwidth of DL CCs in Rel 10-12 are the same as UL CCs bandwidth.

Furthermore, in DL, to support soft decoding, UE needs to have adequate memory for saving soft channel bits. Interestingly, the size of memory is not dependent on the number of aggregating CCs but on UE category. There is no need to increase memory size by the number of aggregated SA capability; the reason is that the same memory can be shared equally between different CCs [16].

CCs in LTE, regardless of UE's release, have LTE Rel-8 structure to ensure backward compatibility. In other words, LTE Rel-10 (Category 6-8) must also support LTE Rel-8 and Rel-9 (Category 1-5), or Rel-11 UE Category 9 and 10 must be compatible with both Rel-10 and Rel-8 UE categories. Furthermore, if UEs with SA capability accommodate the guard band between CCs such as specified in the Rel-8, there would not be any issue for the legacy LTE users (which comply with the UE's indicated capabilities). As part of signalling between UEs and eNB, UEs indicate their transmission capabilities regarding operation on different frequency bands and supported SA configurations for both DL and UL.

2.2.1.5 Impact of Spectrum Aggregation on Battery Life

Utilising multiple CCs simultaneously increases energy consumption of UEs in both DL and UL due to the need for additional signal processing, RF front end activity, and potentially more UL activity (feedback reporting). The energy consumption can be as high as multiplying the non-SA energy consumption by the number of aggregated CCs [16]. The amount of consumed energy is mainly linked to RF architecture in the receiver or transmitter, SA type, and the channel quality on CCs. To limit energy consumption, the number of aggregating CCs and the

SA type for delivering data can be configured, based on the amount of data to be transmitted or received. CC selection can be done in MAC level by activating or deactivating CCs. Activating CCs increases the UE activity and consequently increases energy consumption of UE, and vice versa.

When the UE is not transmitting on certain CCs, it still needs to measure and report CSI on the deactivated CCs. This means that UE would periodically turn off its RF chain for active CCs and turn it on for deactivated CCs. If in the RF architecture of UE, a single RF chain is applied (corresponding to lower UE categories), switching the chain on and off impacts the data transmission on different CCs and may degrade the performance by interruption. To reduce the interruption in one RF chain architecture, it is possible to entirely turnoff the measuring and reporting of the deactivated CCs by MAC command, but this would result in higher energy consumption [16]. UE which is using multiple RF chains may not encounter the same problems of transmission interruptions and would be able to take advantage of SA fully.

2.2.1.6 Spectrum Aggregation Enhancement beyond Five Component Carriers

3GPP introduced basic SA functionality for the first time in Rel-10 of LTE. SA of Rel-10 supports a maximum of 5 CCs with the same frame structure. Later in Rel-11, work on SA is extended to support inter-band TDD SA with different UL-DL configurations and SA with multiple UL timing advance.

To further expand bandwidth in LTE and supporting the operation of the LTE in the 5 GHz band, more recently LTE-U has attracted remarkable attention. The 5 GHz band, which is mainly used for WLAN, consists of 80 MHz in the field with additional 160 MHz in Wave 2 deployments of IEEE 802.11ac [13],[16]. In addition

to the bands already widely in use for LTE, in some regions there are also other frequency bands, such as 3.5 GHz, where intra-band SA is possible.

To enable operation of LTE-U, modifying SA functionality of LTE in such a way as to aggregate more than 5 CCs is necessary. The LTE-U would enhance spectrum utilisation of MNOs and increase ROI. Increasing the number of aggregating CCs can be translated to new challenges such as DL and UL signalling and CC configuration.

2.2.1.7 Spectrum Aggregation for NGMN

Key wireless industry players anticipate NGMN will be standardised and finalised by 2019, ahead of commercial deployments of standardised NGMN in 2020 and beyond [65]. It is expected that SA will play a pivotal role in NGMN similar to 4G. However, SA in NGMN covers very wide bandwidths and very high frequency bands. Therefore to adapt different characteristics of frequency bands, it is possible that for CCs located in different bands, different transmission technologies are used. Aggregating different CCs with different transmission technologies makes operating in wide bandwidth and very high frequency bands feasible.

NGMN will rely on small cells connected to existing superfast fibre networks to meet the growing demand of mobile data traffic [66]. It can be expected that NGMN, similar to LTE Rel-12, will use dual connectivity to further improve system capacity. As mentioned in Section 2.2.1.3, multi-site SA offers SA between CCs belonging to different sites independently. In multi-site SA, in contrast to regular SA, physical and MAC layer signalling are not shared between different sites. Moreover, in regular SA, CSI of different CCs can be sent on PCC but in multi-site SA, CSI of a particular CC should be sent on that CC. Thus there is no need for tight inter-operability among different sites. Furthermore, in regular SA, there is a need for a minimum of one UL CC per UE, however in multi-site

SA, there is a need for one UL CC per site per UE. It is possible that a similar approach would be taken for aggregation of wider bandwidths, higher frequency bands and a wider frequency gap between CCs for NGMN.

Furthermore, it is anticipated that in NGMN, in addition to improving capacity through aggregating CCs, SA could be used to improve the reliability of the network. This could be achieved by transmission of the same data with different coding from different CCs simultaneously. This approach could be applied in cases where there are CCs with an adverse propagation condition or in the case of less reliable unlicensed spectrum, as well as for any application with higher QoS requirements.

One of the main concerns of SA in LTE-A is high power consumption, however for NGMN, it could be one of the main enhancements for SA. This could be solved by both improvement of RF circuit design, and RRM in respect of selecting the best CCs and RBs, as well as in physical and MAC layer procedures. The RRM should support faster turning on and off of given CCs, to reduce interruption time on the active CCs.

2.2.1.8 Global Market Trends in LTE-A with Spectrum Aggregation

As mentioned previously, MNOs are interested in SA because of improving spectrum utilisation by using fragmented spectrum. Spectrum is a scarce and very precious resource. The majority of MNOs worldwide have a national spectrum allocation of less than 100 MHz continuous spectrum, mostly they have multiple non-continuous spectrum segments in different bands. SA as a promising solution, enables MNOs with LTE-A as their network, to achieve peak data rates of 1 Gbps DL and 500 Mbps UL. Although SA is a new feature, because of its enormous benefits for MNOs and UEs, there is growing number of commercialised networks that deploy it, for example:

- For the first time, commercial LTE-A with SA was launched in 2013 in South Korea by SK Telecom. To reach peak DL data rates of 150 Mbps, SK telecom aggregated 10 MHz of 800 MHz and 10 MHz of 1800 MHz frequency bands. The MNO claimed that their customers with LTE-A devices could download an 800 MB movie in 43 seconds. LG Plus, another South Korean MNO, used SA a month later [67].

- UK based operator EE deployed 40 MHz of inter-band SA with 300 Mbps data rate in November 2013, in London [68]. EE's SA technology is provided by Huawei to bring together 20 MHz of 1800 MHz and 20 MHz of 2.6 GHz frequency bands. EE is planning to expand the high-speed network across the UK, in preparation for ultra high-definition 4K TV, which is required to stream at least 20 Mbps [68],[67].

- Huawei and Australian MNO, Optus, launched the world-first LTE-TDD SA network in December 2013 [69]. Afterwards, several other MNOs launched SA on LTE-TDD such as A1 Telekom in Austria, Softbank Japan, CSL Limited Hong Kong and Telstra Australia [70].

- In North America, AT&T announced SA capability in Chicago and plans for other markets to boost its LTE capacity. AT&T combines the two bands of 700 MHz and 2.1 GHz to deliver 15 MHz of DL spectrum, increasing theoretical download speeds to around 110 Mbps [71]. Sprint plans to use SA as part of the Sprint Spark service to combine LTE frequency bands of 800 MHz, 1900 MHz and 2.5 GHz. T-Mobile and Verizon plan to use SA to further enhance their Advanced Wireless Services (AWS) spectrum holdings.

- Apple, Samsung, LG and HTC have launched SA-capable devices such as the Samsung Galaxy S4, Note 3, Edge, LG Pro2, HTC One M8 and Apple iPhone 6/6s and 6 Plus (Figure 1.6) [67],[72–74].

The majority of initial SA enabled devices and networks are limited to a maximum of two CCs. However, work on SA with three CCs was tested by multiple MNOs (SK Telecom, LG UPlus and Telestra) in 2014. Recently, Qualcomm has completed a commercial verification of inter-band SA on LTE-TDD over three CCs for both Huawei and China Mobile [75].

2.2.2 Radio Resource Management in LTE-A Networks

To achieve higher spectral efficiency and peak data rates, OFDM with a shared channel concept for DL data transmission is adopted in LTE [76],[77]. Assuming the default LTE configuration with normal cyclic prefix, in the time domain, every 7 OFDM symbols make one time slot equals 0.5 ms; double time slots make one TTI. In the frequency domain, 12 OFDM Sub-Carriers (SCs) corresponding to 180 KHz make one sub-channel [77]. A RB corresponds to one time slot (i.e. 0.5 ms in the time domain) and one sub-channel (i.e. 180 KHz in the frequency domain) is the smallest radio resource that LTE applies for allocating spectrum. All available RBs in the cell are distributed in the time and frequency domain. Because of the fixed size of sub-channels, the number of RBs in each carrier depends on the bandwidth of carrier. According to 3GPP TR 36.912 [19], LTE supports only carrier configuration with bandwidth equals $\{1.4, 3, 5, 10, 15, 20\}$MHz and its corresponding number of RBs is $\{6, 15, 25, 50, 75, 100\}$.

In LTE, to compensate for the instantaneous radio-link conditions and to make efficient use of the channel capacity, link adaptation by means of Adaptive Modulation and Coding (AMC) is employed. In AMC, the radio-link data rate is controlled by adjusting MCS-index value, referred to as k [78]; for instance if the radio-link conditions are favourable (i.e. sufficiently high SNR), higher order modulation with higher code rate can be used to increase capacity. Furthermore, let R_k be the code rate associated with the k, M_k is the constellation size of the k,

and t_s is the time-slot duration. Thus, the bit rate $d(k)$ achieved by k for a single RB is given by [79]:

$$d(k) = \frac{1}{t_s} R_k \log_2 (M_k) N_{sc} N_s \tag{2.2}$$

To select an appropriate MCS for DL transmission, UE provides CSI to eNB, indicating the instantaneous DL channel quality in both time and frequency domains. The contents of CSI in the absence of MIMO consists of only Channel Quality Indicator (CQI) and can be obtained by measuring SNR on the reference signals transmitted in the DL [77]. The value of CQI-index value per RB, implicitly indicates the maximum data rate that the UE can achieve with Block Error Rate (BLER) of 10% or below on the RB [27].

According to 3GPP TS 36.213 [80], there are 16 different CQI index values (4 bits) ranging from 0 to 15; where 0 and 15 indicate the out of range and best channel quality respectively. Corresponding modulation scheme, code rate, and data rate per RB can be obtained from the TABLE 2.6 [80]. In this study, the method mentioned in [27] is adopted to map CQI index values to their corresponding SNR values (and vice versa) as shown in Figure 2.6. Based on CQI values, the highest-rate k per CC per UE in a given TTI is assigned; furthermore an important constraint in LTE DL (in absence of spatial multiplexing mode of MIMO) is that all RBs in the CC, allocated to a given UE must use an identical MCS (also known as MCS constraint) [80].

SA functionality was introduced in LTE Rel-10 and subsequently enhanced in Rel-11 and Rel-12. For Rel 10-12 UEs, up to 5 carriers (depending on UE category) each with a bandwidth of up to 20 MHz can be aggregated. This allows an overall transmission bandwidth of up to 100 MHz and correspondingly higher data rates of up to 1 Gbps [8]. To ensure backward compatibility, each carrier can also be accessed by Rel-8 UEs (i.e. UEs without SA capability). Therefore,

TABLE 2.6: CQI-index values (Table 7.2.3-1 [80]) and corresponding RB data rate (assuming $N_s = 7$ and $N_{sc} = 12$). A Resource Element (RE) is the smallest defined unit which consists of one OFDM subcarrier during one OFDM symbol interval.

CQI Index	Modulation	Code Rate×1024	Information bits per RE	Data rate per RB
1	QPSK	78	0.1523	25.58 kbps
2	QPSK	120	0.2344	39.37 kbps
3	QPSK	193	0.3770	63.33 kbps
4	QPSK	308	0.6016	101.06 kbps
5	QPSK	449	0.8770	147.33 kbps
6	QPSK	602	1.1758	197.53 kbps
7	16 QAM	378	1.4766	248.06 kbps
8	16 QAM	490	1.9141	321.56 kbps
9	16 QAM	616	2.4063	404.25 kbps
10	64 QAM	466	2.7305	458.72 kbps
11	64 QAM	567	3.3223	558.14 kbps
12	64 QAM	666	3.9023	655.58 kbps
13	64 QAM	772	4.5234	759.93 kbps
14	64 QAM	873	5.1152	859.32 kbps
15	64 QAM	948	5.5547	933.20 kbps

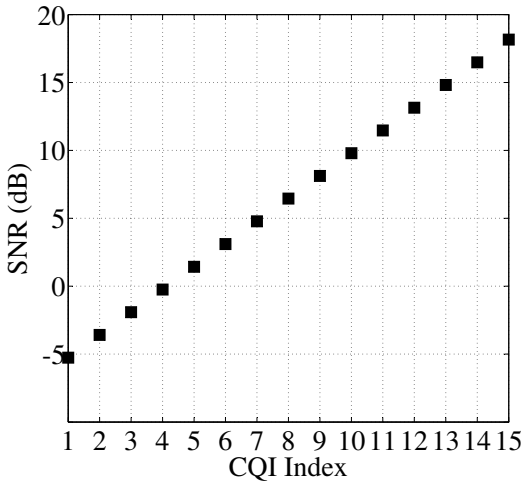

FIGURE 2.6: CQI-to-SNR mapping function, ensuring BLER $\leq 10\%$.

in most respects physical and MAC layer functionalities apply to each carrier independently, while SA is invisible to the upper layers of protocol stack [59].

LTE-A UE (Rel-10 and above) has one DL-PCC and an associated UL-PCC. In addition, it may have one or several SCCs in either DL or UL direction in licensed or unlicensed spectrum [5],[12]. Similar to LTE UE (Rel-8), the configuration of PCC is UE specific [4],[81]. When UE with SA capability starts establishing or re-establishing Radio Resource Control (RRC) connection with eNB (using cell search and random access procedures), following the same steps as in the absence of SA, only PCC is configured. Once the communication between eNB and UE is established, additional SCCs can be configured by RRM functionality located at

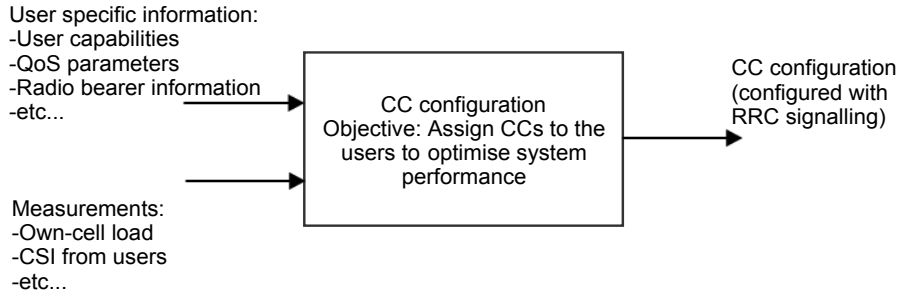

FIGURE 2.7: Overview of spectrum aggregation configuration of LTE network.

eNB. In other words SCC assignment is cell-specific and signalled as part of the system information [4],[81]. Therefore to support SA, RRM functionality needs to be modified in such a way that backwards compatibility with LTE is always catered for.

The RRM framework for LTE exploits various functionalities, including QoS management, admission control, hybrid automatic retransmission request, link adaptation, and resource scheduling [82],[83]. The RRM for LTE-A has many similarities with that of LTE except modification of resource scheduling and inclusion of a new functionality referred to as CC configuration. This functionality configures SCC sets for each UE with SA capability in both UL and DL direction. The overall CC configuration functionality of the network is illustrated in Figure 2.7. As input, user's SA capability, QoS parameters, and radio bearer configuration are used to assign CCs. To enhance system performance, traffic load among different CCs should be roughly even [84]. The selected CCs are reported to UE via RRC signalling. Similar to RB allocation, CC configuration plays an important role in network performance, as well as the power consumption of network. The latter is much more important especially in UL, as matter of fact, the power consumption of UEs increases with transmission bandwidth.

The resource scheduler assigns RBs within cell-selected SCCs and UE-selected PCCs to UEs. In other words, LTE UEs benefit from dynamic scheduling of RRM only within PCCs, while LTE-A UEs not only take advantage of PCCs but also

SCCs. There are a number of methods available for PCC selection [84]; in this thesis, UEs select PCC based on the Reference Signal Received Power (RSRP) of candidate CCs; i.e. CC with the highest RSRP is selected as PCC by each UE.

RB allocation is one of the most important functionalities of RRM, and may impact on the overall performance of the network. It distributes a finite number of RBs among UEs at each TTI under given QoS constraints of individual UEs, such as fairness and priority [8]. RB allocation strategy is not specified by the 3GPP and is MNO specific [4],[61], closely coupled to link adaptation and SCC allocation. Herein, the proposed RRM framework models RB allocation, link adaptation and SCC configuration as a joint functionality located at eNB.

The Best CQI (BCQI) is one of the basic strategies that can be applied to assign RBs to UE with the best channel conditions. From a system capacity perspective BCQI is the best, but gives the worst fairness among UEs and may end UE starvation [4]. Round-Robin Scheduling (RRS) strategy is an alternative to BCQI. This strategy neglects CSI and ensures that all UEs are allocated the same number of RBs for the same amount of time [4]. It assigns RBs more fairly among UEs, but presents inferior throughput performance compared to BCQI. Proportional fair (is incorporated in this thesis) is another common scheduling strategy, a compromise between RRS and BCQI. This maintains a balance between two competing interests, i.e. maximising the overall system throughput while at the same time providing all UEs with a minimum throughput [4].

2.3 OFDM-based Networks

In order to meet the growing demand of user data rates, NGMN's radio access is anticipated to be built on evolving existing technologies (LTE-A, CRN and WLAN), as well as new Radio Access Technologies (RATs). In other words, NGMN (also

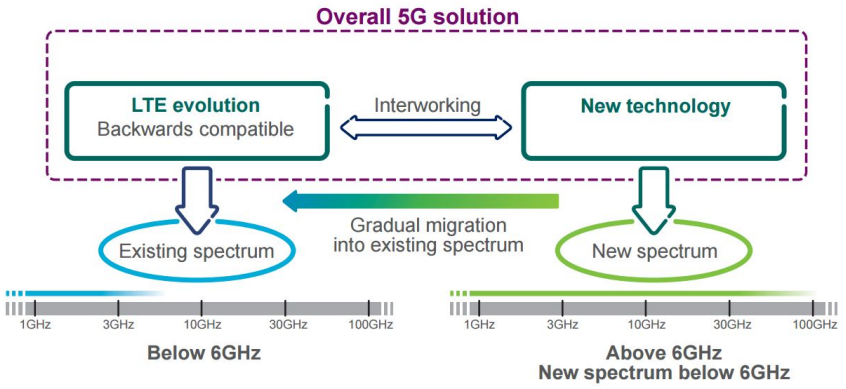

FIGURE 2.8: The overall 5G wireless-access solution consisting of LTE evolution and new RAT[85].

known as 5G) wireless access can be seen as an overall wireless-access solution (LTE-A as backwards-compatible for low-frequency bands, $\leq$ 6 GHz, and new RAT without backwards-compatibility requirements for higher-frequency bands, $\geq$ 6 GHz) providing the QoS requirements of mobile communication beyond 2020 (Figure 2.8). Similar to 4G, radio access of NGMN will be schedule-based system to guarantee the QoS demands of users [58],[85].

The selection of the radio waveform has a significant impact on the NGMN's RAT, because it plays an important role on the link performance and transceiver's complexity (a very important factor to enable M2M communication). The radio waveform for NGMN should support wide bandwidth (several 100 MHz to GHz order) at higher frequency bands. As shown in Figure 2.8, to provide interworking between the evolution of LTE-A and the new RAT for NGMN, multi-site SA is necessary. Therefore, radio waveform should support SA also.

OFDM and Filter Bank Multi Carrier (FBMC) are two powerful candidates for a NGMN waveform. Several research works (e.g. [86],[87]) compare both technologies from different aspects. It is concluded that FBMC outperforms OFDM in terms of spectral containment and time/frequency overhead, however, OFDM's

transceiver has least complexity. Because the limited complexity is imperative for NGMN, OFDM is still the strongest candidate for a NGMN waveform [88].

Furthermore, the cognitive capability of NGMN to access the whitespace in the licensed spectrum bands is necessary to improve spectrum utilisation and solve the spectrum scarcity problem. For this purpose, NGMN waveform should be highly flexible and adaptable. OFDM has the potential to achieve the required spectrum flexibility by means of SA. SA-enabled OFDM can be considered as a very strong candidate for NGMN waveform in realising the concept of NGMN by providing a proven, scalable, and adaptive technology for air interface.

Moreover, OFDM has been adopted in several of the latest wireless standards, such as LTE, DVB-T, IEEE 802.11x, 802.16e, 802.15.3, etc. OFDM provides outstanding capabilities to combat multi-path fading with high spectral efficiency as well as providing frequency, time and user diversity due to its flexible and precisely per-SC RA capability with finer granularity [76]. It is one of the best techniques for overcoming the adverse effects of multipath spread, and permits many users to transmit simultaneously on the different SCs per OFDM symbol. Although, OFDM has been extensively studied from the spectrum efficiency perspective, the aggregation capability of users is much less studied. To keep pace with the requirements of NGMN, it is necessary to modify resource (power and SC) allocation for OFDM-based networks to support SA.

2.4 Related Works

As explained in Section 1.1 and Section 1.2, wireless traffic volume generated by the new generation of devices (M2M devices, wearable devices, smartphones, tablets, and laptops) is quickly becoming too overwhelming for the existing networks to handle [1],[5]. The exploitation of more available spectrum resources with wider

transmission bandwidths is a promising solution for traffic explosion and capacity demands.

Traditionally, wireless networks can only utilise a continuous spectrum resource, but due to a fixed spectrum allocation policy, the wide continuous spectrum bands are hardly available under the current situation of spectrum resource. Recently, researchers both in academia and industry have been motivated by the so-called spectrum fragmentation problem to work towards flexible spectrum usage. To solve the problem, SA is introduced to increase system capacity by providing additional bandwidth to mobile users. The SA exploits fragmented spectrum segments to provide high bandwidth transmission. After CR identifies all white spaces sensed by intelligently inspecting the radio environment, the combination of multiple spectrum bands becomes feasible using SA. Many different standard organisations and companies have started to study SA. One of the best-known companies is QinetiQ, which has designed new solutions for SA to sustain broadband services [10].

One of the most challenging problems in CRNs is the spectrum assignment problem [35]. The spectrum assignment problem is well-studied in traditional wireless networks. When considering spectrum assignation, the objective is to satisfy the interference constraints and maximise the system throughput for a given spectrum. Nevertheless, CRNs impose challenges due to the fluctuating and discontinuous nature of the available spectrum, as well as the diverse QoS requirements of various applications.

Despite standardisation of SA in LTE-A networks, little effort has been made to optimise SA by exploiting CR technology. There is limited literature available on spectrum assignment among users having SA capabilities. In [89], an aggregation aware spectrum assignment algorithm is proposed to aggregate discrete spectrum fragments in a greedy manner. The algorithm in [89] utilises the first available

aggregation range from the low frequency side and assumes all users have the same bandwidth requirement.

In [20], a prediction based SA scheme is introduced to increase the capacity and decrease the re-allocation overhead. The proposed scheme is referred to as MSA for spectrum assignment. The main idea is to assign spectrum for the user with larger bandwidth requirement first, leaving better spectrum bands for remaining SUs, while taking into consideration the different bandwidth requirements of SUs and the state statistics of each channel.

Recently, Fang, et al. [90] introduced a genetic algorithm based spectrum assignment in CRNs. In [90], the population of a genetic algorithm is composed of sets of feasible assignment and infeasible assignment. The penalty function is added to the fitness function, and the fitness of chromosomes that dissatisfied within the constraints are reduced; thus the feasible assignment is achieved with the objective of maximising the system utility. However, [90] neglects SA capability of SUs.

Authors in [91] introduced a spectrum assignment method with SA based on graph colouring. The introduced method in [91] maximises throughput and fairness as a criterion to realise spectrum assignment. Compared to the assignment of continuous spectrum, [91] improves the spectrum utilisation of tiny spectrum fragments, increases the throughput of CRN, and improves the fairness of spectrum assignment among SUs.

Furthermore, authors in [92] proposed a utility-based SA algorithm to enhance the performance of a CRN considering multiple objectives: 1) maximisation of overall throughput, 2) reduction of channel switching, 3) reducing the number of sub-channels comprising the aggregate channel, aimed at opportunistic spectrum use by SUs. These three objectives are integrated into a weighed sum utility function. The proposed algorithm allows for the automated adaptable setting of objective-function weights depending on environment changes.

Finally, authors in [93] analytically formulated the channel access problem as a joint power control and channel assignment optimisation problem, with the objective of minimising the required spectrum resources for a given CR transmission. [93] shows that the optimisation problem is a binary linear program, which is, in general, a Non-deterministic Polynomial-time (NP)-hard problem. Accordingly, [93] presents a near-optimal solution based on sequential fixing, where the binary variables are determined iteratively by solving a sequence of linear programs.

For CRNs, existing spectrum assignment and SA solutions are not applicable directly as practical constraints, such as MAS, must be taken into account. Further, in an aggregation-based spectrum assignment a major challenge is to manage CCI among SUs, which is not taken into account in the existing literature.

The RRM functionality plays an important role in optimising network performance from the MNO perspective, as well as improving QoS of UEs and consequently improving churn rate and increasing revenue for MNOs [94]. Since LTE-A, the concept of RRM for SA-enabled LTE networks has gained significant attention [8],[24],[25]. Most of the previous studies related to RRM in LTE-A assume CC selection, RB allocation and link adaptation as completely separate problems. For instance, authors in [95] developed a RRM algorithm that assigns CC to each newly-arrived UE on the basis of the average channel quality, independent of RB allocation.

In [96], CC selection and RB allocation are considered jointly, but link adaptation (MCS assignment) is neglected. The authors in [96] proposed an algorithm referred to as Minimising System Utility Loss (MSUL) algorithm, in which UEs can be categorised as either narrow-band or broadband UEs, where the former can support only one CC while the latter can support all CCs in a given cell [96]. The MSUL algorithm also assumes that different CCs have the same number of RBs. It is used to assign each CC independently and then removes all but one

of the assigned CCs from narrow-band UEs, provided that they have minimum contribution to the utility function.

More recently, authors in [24] proposed a radio resource allocation scheme which is known as the GA. The GA considers MCS assignment jointly with the CC selection and RB allocation. However, the authors assumed that all CCs have same number of RBs and that all LTE-A UEs have the same SA capability, both of which are unrealistic assumptions. Further, the GA is an iterative process which calculates the utility function for all possible combinations of UEs, CCs, and MCSs at each iteration. An assignment with the highest value of the utility function is selected at each iteration until the algorithm converges [24].

Most of the current research neglects LTE-A constraints in respect to PCC and SCC selection. Further, none of the mentioned SOTA solutions optimise RRM functionally, but are based on approximate algorithms that only achieve half of the PF objective function of the optimal solution.

Recently, OFDM systems have become one of the most intensively studied paradigms in wireless communications. The vast majority of previous contributions in literature focus on RA for cases where the users employ the non-SA OFDM technologies [21],[22] or solve RA for LTE-A networks [25],[24].

For instance, authors in [21] considered scheduling and RA for the DL of OFDM-based networks. During each scheduling time slot, the RA problem involves selecting a subset of users for transmission, determining the assignment of available SCs to selected users, and for each SC determining the transmission power, the coding and modulation scheme used. [21] provides optimal and sub-optimal algorithms for the formulated RA problem which is convex.

Authors in [22] proposed an efficient solution to minimise the total transmit power

subject to each user's data rate requirement by using convex optimisation techniques. Due to the non-convexity of the optimisation problem, the proposed solution is not guaranteed to be optimal. However, for a realistic number of SCs, the duality gap is practically zero, and optimal RA can be evaluated efficiently. Simulation results show large performance gains over a fixed SC allocation.

In addition, capacity and coverage gains can be improved dramatically if users employ SA to increase the transmission bandwidth and provide an additional frequency diversity [12]. In this thesis, RA for OFDM-based networks with the practical constraints of users' SA capabilities and finite transmission power is considered. Table 2.7 briefly explains some of the SOTA solutions available in literature and compare them with the proposed algorithm in this study - Optimum RB Allocation Algorithm (ORAA).

2.5 Summary

In this chapter, fundamental concepts of NGMN including CRN, LTE-A and OFDM-based networks are reviewed briefly. The concept of SA in corresponding architectures is explained. Furthermore, all challenges that SA poses in the network, are investigated in details. Finally, the SOTA solutions are presented and will be used in next chapters to compare with performance of introduced methods.

TABLE 2.7: Summary of RRM methods for SA-enabled LTE-A networks available in SOTA (including the proposed algorithm in this thesis-ORAA)

References	Characteristics	Advantages	Disadvantages	MCS Constraint	SCC Assignment	Power Allocation	QoS	MIMO
[95]	A novel CC selection method is proposed.	An improvement on the performance of network for non-continuous CA with low complexity	RB allocation and CC allocation are considered independently.	✗	✗	✗	✗	✗
[96]	CC selection and RB allocation are considered jointly.	Improving the system performance compared with the algorithms optimising CCs and RBs allocation independently	Based on iterative process	✗	✗	✗	✗	✗
[24],[26]	MCS assignment is considered jointly with the CC selection and RB allocation.	Guaranteeing at least half of the performance of the optimal solution	Based on iterative process	✓	✗	✗	✗	✗
[81]	Energy efficient CA algorithms are proposed.	Guaranteeing performance under various models of continuous and non-continuous CA as well as backlogged and finite user buffers	Based on approximation approach (also easy-to-implement)	✓	✓	✓	✗	✗
[97]	Joint CA and packet scheduling considering packets delay is introduced.	Achieving load balancing across CCs, better throughput and delay performance for users compared with the existing schemes	A two-tier resource allocation framework which incorporates dynamic CC assignment and backlog based scheduling schemes.	✓	✗	✗	✓	✗
[98]	Joint CA and packet scheduling for LTE MIMO systems are investigated.	Considering MIMO mode selection based on users' mobility	Based on greedy algorithm	✓	✗	✗	✗	✓
ORAA	Joint CA and RB allocation for LTE systems is studied.	An optimal and efficient solution	Did not consider MIMO mode selection and QoS requirements of users.	✓	✓	✗	✗	✗

Chapter 3

Aggregation based Spectrum Assignment for Cognitive Radio Networks

As explained in Chapter 1 and Chapter 2, NGMN is preparing for an explosive increase in data traffic. NGMN technology will deliver fast and cost-effective data connectivity anywhere and anytime for anyone and anything, whilst minimising the deployment cost. Despite the success of HWNs and MIMO in 4G systems, there is no single technological advance that can meet this traffic demand. In fact, NGMN's technology demands wide bandwidth and high spectrum efficiency towards meeting this ambitious target. This chapter targets both bandwidth and spectrum efficiency through flexible use of spectrum in order to optimise spectrum utilisation in CRNs. It is expected that NGMN will integrate the conventional licensed mobile communication systems and CRN into a holistic system.

In CRNs, SUs exploit CR technology to opportunistically access licensed spectrum as long as interference to licensed users is kept at an acceptable level [36]. Owing to cognitive functionalities of CRNs, SUs can interact with the radio environment

either by performing spectrum sensing and/or accessing spectrum databases to detect spectrum opportunities [99]. After sensing, the characteristics of available spectrum bands are analysed and spectrum is assigned according to user requirements. In CRN, there are multiple SUs trying to access the opportunistic spectrum and, hence, spectrum access must be coordinated to prevent multiple SUs colliding in the overlapping portions of the spectrum which can degrade the overall performance of the CRN.

As SUs can sense and be aware of their radio environment, the aggregation of narrow spectrum opportunities becomes possible using SA, which provides higher throughput for the SUs. To enable SUs to transmit in the discontinuous spectrum due to the presence of incumbent PUs, a flexible modulation technique based on multi-carrier modulation that turns off SCs which would otherwise interfere with incumbent transmissions is required. Fortunately, with the advancement of modulation techniques and RATs, a single radio can access discontinuous portions of the spectrum simultaneously and aggregate them, e.g. by using OFDM [100],[101].

In this chapter, an aggregation-based spectrum assignment algorithm using a genetic algorithm for CRNs is proposed. It is assumed that a CRN exploits discontinuity of available spectrum, i.e. whitespaces, opportunistically in order to achieve higher spectrum utilisation. The proposed algorithm takes into consideration interference to the PUs, CCI among SUs, and MAS to aggregate whitespaces. As the spectrum assignment problem is inherently seen as a NP-hard optimisation problem, evolutionary approaches can be applied to solve this challenging problem. In this thesis, a genetic algorithm is used to solve aggregation aware spectrum assignment because of its simplicity, robustness and the high convergence rate of the algorithm [102].

Spectrum efficiency of the algorithm is compared with the MSA [20] and the RCA. In Section 2.4, SOTA solutions regarding SA in CRNs are reviewed. Simulation

results clearly show that the proposed algorithm outperforms SOTA algorithms. Furthermore, analysis of the convergence of the proposed algorithm is provided and numerical results verify its fast convergence.

This chapter is organised as follows: in Section 3.1, spectrum assignment and an aggregation model are presented. The proposed algorithm is explained in Section 3.2. Simulation results are discussed in Section 3.3, followed by conclusions in Section 3.4.

3.1 Spectrum Aggregation Model

A CRN consisting of $\mathcal{N}$ SUs as $\boldsymbol{\alpha} = \{\alpha_1, \alpha_2, \cdots, \alpha_{\mathcal{N}}\}$ competing for $\mathcal{M}$ non-overlapping orthogonal channels $\boldsymbol{\beta} = \{\beta_1, \beta_2, \cdots, \beta_{\mathcal{M}}\}$ is assumed. All spectrum assignment and access procedures are controlled by a central entity known as the spectrum broker. It is assumed that a distributed sensing mechanism and measurement conducted by each user is forwarded to the spectrum broker [99]. A spectrum occupancy map is constructed by the spectrum broker and CCI among SUs is determined. Furthermore, the spectrum broker can lease single or multiple channels for user $\alpha_n \in \boldsymbol{\alpha}$ in a limited geographical region for a certain amount of time. Finally, a secondary base station can transmit data to the SU α_n in the assigned channels.

Channel availability matrix $\mathbf{L} = \{l_{n,m} | l_{n,m} \in \{0,1\}\}_{\mathcal{N}\times\mathcal{M}}$ is defined as an $\mathcal{N} \times \mathcal{M}$ binary matrix, representing channel availability where $l_{n,m} = 1$ if and only if channel β_m is available to SU α_n and $l_{n,m} = 0$ otherwise. Each SU α_n is associated with a set of available channels at its location, defined as $\overline{\boldsymbol{\beta_n}} \subset \boldsymbol{\beta}$; i.e. $\overline{\boldsymbol{\beta_n}} = \{\beta_m | l_{n,m} \neq 0\}$. Due to the different interference range of each PU (which depends on PU's transmission power and the physical distance between PU and SU) at the location of each SU, $\overline{\boldsymbol{\beta_n}}$ of different SUs may be different [103]. According

to the sharing agreement, any channel $\beta_m \in \boldsymbol{\beta}$ can be reused by a group of SUs in the vicinity defined by $\overline{\boldsymbol{\alpha}}_m$ such that $\overline{\boldsymbol{\alpha}}_m \subset \boldsymbol{\alpha}$, if SUs are located outside the interference range of PUs; i.e. $\overline{\boldsymbol{\alpha}}_m = \{\alpha_n | l_{n,m} \neq 0\}$.

The interference constraint matrix $\mathbf{C} = \{c_{n,k,m} | c_{n,k,m} \in \{0,1\}\}_{\mathcal{N}\times\mathcal{N}\times\mathcal{M}}$ is defined as an $\mathcal{N} \times \mathcal{N} \times \mathcal{M}$ binary matrix, representing the interference constraint among SUs where $c_{n,k,m} = 1$ if SUs α_n and α_k would interfere with each other on channel β_m, and $c_{n,k,m} = 0$ otherwise. It should be noted that for $n = k$, $c_{n,n,m} = 1 - l_{n,m}$. The value of $c_{n,k,m}$ depends on the distance between SU α_n and α_k. Interference constraint also depends on the channel β_m as power loss varies greatly in different frequency bands. The bandwidth requirements of all SUs are diverse because of different QoS requirements for each user. $\mathcal{R} = \{r_n\}_{1\times\mathcal{N}}$ is defined as user requested bandwidth vector, where r_n represents the bandwidth demand of SU α_n.

In dynamic environments, channel availability and the interference constraint matrix both vary continually. For simplicity, it is assumed that spectrum availability is static or varies slowly in each scheduling time slot. In other words, all mentioned matrices remain constant during the scheduling period. In the proposed solution, a subset of SUs is scheduled during each time slot and the available spectrum is allocated among them without causing interference to PUs.

In the traditional spectrum assignment, available spectrum is composed of continuous channels and users are able to transmit on one continuous channel. Therefore, it is not feasible for a user to utilise spectrum fragments which are smaller than the user's bandwidth demand. SA is the key technology to solve this problem. SA-enabled CR terminals are capable of exploiting fragmented portions of the spectrum and provide high data rates by using specialised air interface techniques, such as OFDM. If the user's bandwidth demand is larger than the bandwidth of each available channel, CRN based on continuous spectrum assignment blocks the user request, even if there is an adequate non-continuous free bandwidth available.

Nevertheless, by aggregating fragmented spectrum in one virtual channel, the aggregated bandwidth will be larger than the demand. In this way, small fragments are fully utilised to improve spectrum utilisation.

For instance, assume a CRN where every CR requires 4 MHz channel bandwidth, and the available spectrum consists of two spectrum fragments of 4 MHz, and four spectrum fragments of 2 MHz (Figure 3.1). For continuous spectrum allocation, the 2 MHz spectrum fragments cannot be utilised by CR. Therefore, a continuous spectrum assignment mode can only support two CR terminals for communication (2×4 MHz). If a number of small spectrum fragments are aggregated into a wider channel, then 16 MHz of unused spectrum is available to support four CR users (4×4 MHz).

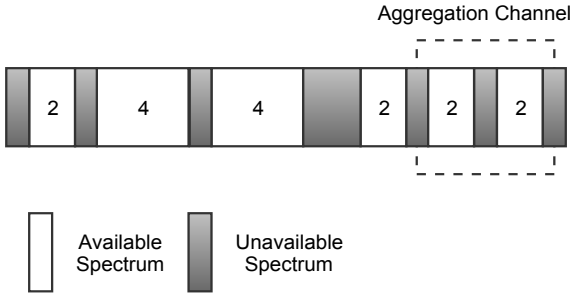

FIGURE 3.1: Aggregation of disjointed spectrum fragments.

Although SA in CR terminals is possible from the baseband processing point of view, RF-implementation complexity is still high [10]. Due to the limited aggregation capabilities of the RF front-end, only those channels that reside within a range of MAS may be aggregated. With this constraint, some spectrum fragments may not be aggregated because their span is larger than the MAS. According to the study commissioned by Ofcom [10] on new methods of spectrum management, current hardware technology allows for the aggregation of a maximum 50 MHz bandwidth spectrum fragments at different frequency bands, provided that the difference between the maximum and minimum frequency of multiple fragments

which are aggregated do not exceed 1.5 GHz [10]. The value of MAS depends on the RF architecture of CR's transmitter and receiver.

For example, in Figure 3.2, it is assumed that the CR's transceiver can operate with a MAS of 10 MHz, therefore if a CR user needs 8 MHz bandwidth, the channel aggregated by B and C may not be utilised. And if the CR's transceiver can aggregate the minimum 0.5 MHz bandwidth spectrum fragment, then the spectrum fragments of E and F can be aggregated.

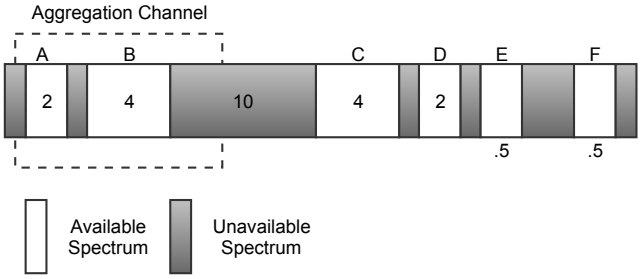

FIGURE 3.2: CR's receiver and transmitter can operate with MAS of 10 MHz.

Without loss of generality, the following assumptions have been made:

1. All SUs have the same aggregation capability (i.e. MAS for all SUs is same).
2. The guard band between adjacent channels is neglected.
3. All users' bandwidth requirements and the bandwidth of each channel is a multiple of sub-channel bandwidth Δf; which is the smallest unit of bandwidth (in fact, the smaller fragments would demand excessive filtering to limit adjacent channel interference) i.e.

$$r_n = \omega_n \cdot \Delta f, \quad \omega_n \in \mathbb{N},\ 1 \leq n \leq \mathcal{N} \tag{3.1}$$

$$\mathcal{BW}_m = \kappa_m \cdot \Delta f, \quad \kappa_m \in \mathbb{N},\ 1 \leq m \leq \mathcal{M} \tag{3.2}$$

where $\mathbb{N}$ is a set of natural numbers, ω_n is the number of requested sub-channels by SU α_n, κ_m is the number of sub-channels in channel β_m, and $\mathcal{BW}_m$ is the bandwidth of channel β_m.

The total available spectrum (i.e. $\mathcal{M}$ channels) is subdivided into multiple numbers of sub-channels. If the available spectrum band consists of $\mathcal{C}$ sub-channels, (i.e. total available bandwidth is $\mathcal{C} \cdot \Delta f$), then:

$$\beta_m = \bigcup_{i=1}^{\kappa_m} \widetilde{\beta}_{i,m}, \quad \kappa_m = \frac{\mathcal{BW}_m}{\Delta f}, \quad \text{where} \quad 1 \leq m \leq \mathcal{M} \tag{3.3}$$

$$\mathcal{C} = \sum_{m=1}^{\mathcal{M}} \kappa_m \tag{3.4}$$

where the m^{th} channel β_m has κ_m sub-channels and $\widetilde{\beta}_{i,m}$ represents the i^{th} sub-channel of β_m. Each sub-channel $\widetilde{\beta}_{i,m}$ can be represented in an interval defined as $[\mathcal{F}^L_{i,m}, \mathcal{F}^H_{i,m}]$; where $\mathcal{F}^L_{i,m}$ and $\mathcal{F}^H_{i,m}$ are the lowest and highest frequency of i^{th} sub-channel located in m^{th} channel, respectively ($\mathcal{F}^H_{i,m} - \mathcal{F}^L_{i,m} = \Delta f$). Based on this new sub-channel indexing, matrices $\mathbf{L}$ and $\mathbf{C}$ can be rewritten as follows:

$$\mathbf{L}^* = \left\{ l^*_{n,\mathsf{c}} | l^*_{n,\mathsf{c}} = l_{n,m} \right\}_{\mathcal{N} \times \mathcal{C}} \tag{3.5}$$

$$\mathbf{C}^* = \left\{ c^*_{n,k,\mathsf{c}} | c^*_{n,k,\mathsf{c}} = c_{n,k,m} \right\}_{\mathcal{N} \times \mathcal{N} \times \mathcal{C}} \tag{3.6}$$

if

$$1 \leq \mathsf{c} \leq \kappa_1 \quad \text{for} \quad m = 1$$

and

$$\sum_{j=1}^{m-1} \kappa_j < \mathsf{c} \leq \sum_{j=1}^{m} \kappa_j \quad \text{for} \quad 1 < m \leq \mathcal{M}$$

where c represents the index of each sub-channel within the available spectrum. The sub-channel assignment matrix $\mathbf{A} = \{a_{n,\mathsf{c}} | a_{n,\mathsf{c}} \in \{0,1\}\}_{\mathcal{N} \times \mathcal{C}}$ is an $\mathcal{N} \times \mathcal{C}$ binary matrix, representing sub-channels assigned to SUs for aggregation such that

$a_{n,\mathsf{c}} = 1$ if and only if sub-channel c is available to SU α_n and 0 otherwise. The reward vector $\mathcal{B} = \{b_n = \Delta f \cdot \sum_{\mathsf{c}=1}^{\mathcal{C}} a_{n,\mathsf{c}}\}_{\mathcal{N}\times 1}$ is defined to represent the total bandwidth allocated to each SU during the time period scheduled for given sub-channel assignment.

3.2 Problem Formulation and Solution

3.2.1 Optimisation Problem

One of the key objectives of the deployment of CRNs is to enhance spectrum utilisation. To consider this crucial goal, network utilisation $U(\mathcal{B})$ is defined as maximising the total bandwidth assigned to SUs $\boldsymbol{\alpha}$ in the CRN and is referred to as the Maximising Sum of Reward (MSR):

$$U(\mathcal{B}) = \sum_{n=1}^{\mathcal{N}} b_n \tag{3.7}$$

To maximise $U(\mathcal{B})$ the SA problem can be formed as a constrained optimisation problem to maximise $U(\mathcal{B})$ as follows:

$$\max_{a} \quad \sum_{n=1}^{\mathcal{N}} b_n \tag{3.8}$$

subject to,

$$b_n = \Delta f \cdot \sum_{\mathsf{c}=1}^{\mathcal{C}} a_{n,\mathsf{c}} = \begin{cases} 0 & \text{if } \alpha_n \text{ is rejected,} \\ r_n & \text{if } \alpha_n \text{ is accepted.} \end{cases} \quad \text{for} \quad 1 \le n \le \mathcal{N} \tag{3.9}$$

$$\mathcal{F}_{d,t}^{H} - \mathcal{F}_{e,f}^{L} \le \text{MAS} \tag{3.10}$$

$$a_{n,\mathsf{c}} = 0 \text{ if } l_{n,\mathsf{c}}^{*} = 0 \text{ for } 1 \le n \le \mathcal{N} \text{ and } 1 \le \mathsf{c} \le \mathcal{C} \tag{3.11}$$

$$a_{n,\mathsf{c}} \cdot a_{k,\mathsf{c}} = 0 \text{ if } c^*_{n,k,\mathsf{c}} = 1 \text{ for } 1 \leq n, k \leq \mathcal{N} \text{ and } 1 \leq \mathsf{c} \leq \mathcal{C} \tag{3.12}$$

Eq. (3.9) ensures that rewarded bandwidth b_n to each accepted SU must be equal to the SU's bandwidth demand r_n. If CRN cannot satisfy α_n's bandwidth request, α_n is rejected and $b_n = 0$. If $\mathcal{F}^L_{e,f}$ ($1 \leq e \leq \kappa_f$ and $1 \leq f \leq \mathcal{M}$) is the lowest frequency of an initial aggregated sub-channel and $\mathcal{F}^H_{d,t}$ ($1 \leq d \leq \kappa_t$ and $1 \leq t \leq \mathcal{M}$) is the highest frequency of a terminative sub-channel, Eq. (3.10) guarantees that the range of allocated spectrum is equal or less than MAS. The sub-channel assignment matrix, **A**, must satisfy the interference constraints (3.11) and (3.12); Eq. (3.11) and Eq. (3.12) guarantee that there is no harmful interference to PUs and other SUs respectively.

3.2.2 Spectrum Aggregation Algorithm Based on Genetic Algorithm

Traditionally, the spectrum assignment problem has been classified as an NP-hard problem [102]. In this thesis, a genetic algorithm is employed to solve the aggregation-based spectrum assignment problem in order to obtain fast convergence. A genetic algorithm is a stochastic search method that mimics the process of natural evolution. In addition, it is easy to encode solutions of the spectrum assignment problem to chromosomes in a genetic algorithm, and compare the fitness value of each solution. The specific operations of the proposed algorithm, referred to as the MSR Algorithm (MSRA), can be described as follows:

Step1 (Encoding): In MSRA, a chromosome represents a possible conflict free sub-channel assignment as explained in Section 3.2.1. In order to decrease search space (by reducing redundancy in the data) and obtain faster solutions, a similar approach to that described in [102] is adopted in this thesis. A mapping process between **A** and the chromosomes is applied based on the

characteristics of $\mathbf{L}^*$ and $\mathbf{C}^*$. Only those elements of $\mathbf{A}$ are encoded whose corresponding elements in $\mathbf{L}^*$ take the value of 1, i.e. $a_{n,\mathsf{c}} = 0$ where (n, c) satisfies $l^*_{n,\mathsf{c}} = 0$. As a result of this mapping, the chromosome length equals the number of non-zero elements of $\mathbf{L}^*$, and the search space is greatly reduced. Based on a given $\mathbf{L}^*$, the length of the chromosome (ω) can be written as:

$$\omega = \sum_{i=1}^{\mathcal{N}} \sum_{j=1}^{\mathcal{C}} l^*_{i,j} \tag{3.13}$$

Step2 (Initialisation): During the initialisation process, the initial population is randomly generated based on a binary coding mechanism as introduced in [102]. The size of the population depends on $|\boldsymbol{\alpha}|$ and $|\boldsymbol{\beta}|$. For larger $|\boldsymbol{\alpha}|$ and $|\boldsymbol{\beta}|$, the population size should be increased, where $|.|$ indicates cardinality of a set.

Step3 (Selection): The fitness value of each individual of the current population according to the MSRA criteria defined in Eq. (3.7) is computed. According to the individuals' fitness value, excellent chromosomes (parents) are selected and remain in the next generation. The individual with the highest fitness value replaces the chromosome with a lower fitness value by the selection process.

Step4 (Genetic operators): To maintain the high fitness values of all chromosomes in a successive population, crossover and mutation operators are applied. Two randomly selected chromosomes are chosen in each iteration as the parents, and the crossover of the parent chromosomes is carried out at probability of crossover rate. In addition to selection and crossover operations, mutation at a certain mutation rate is performed to maintain genetic diversity.

Step5 (Termination): The stop criteria of genetic algorithm is checked in each iteration. If they are not satisfied, Step3 and Step4 are repeated. The

maximum number of iterations and fitness value difference are used as the criteria to determine the termination of genetic algorithm.

The population of chromosomes generated after initialisation, selection, crossover and mutation may not satisfy the given constraints defined in Eq. (3.9)-(3.12). To find feasible chromosomes that satisfy all constraints, a constraint free process is applied that has the following steps in order:

1. **Bandwidth Requirements:** The vector $\mathcal{B}$ as given in Section 3.1 is calculated. b_n should either equal r_n or zero, otherwise all genomes related to α_n are changed to zero.

2. **MAS:** Eq. (3.10) is examined and should satisfy the hardware limitations of the transceiver, otherwise all of genomes related to α_n are changed to zero.

3. **No interference to PUs:** Eq. (3.11) guarantees that SUs' transmissions do not interfere PUs' transmissions; ensuring that CRN does not harm the PUs performance. If Eq. (3.11) is not satisfied, all genomes related to α_n are changed to zero.

4. **CCI:** Eq. (3.12) guarantees that there is no harmful interference between SUs. If Eq. (3.12) is not satisfied, one of two conflicted users is chosen at random, and then all genomes of the selected user are changed to zero.

To achieve higher spectrum efficiency and faster convergence, after each generation the MSRA whenever possible randomly assigns all unassigned spectrum to remaining SUs, whilst simultaneously ensuring that the constraints defined in Eq. (3.9)-(3.12) are satisfied at all times.

TABLE 3.1: Simulation parameters.

Parameter	**Value**
Δf	1M Hz
MAS	40 MHz
$\mathcal{BW}_j$	$\Delta f \cdot \mathcal{U}(1, 20)$
r_n	$\Delta f \cdot \mathcal{U}(1, 20)$
Population Size	20
Number of Generations	10
Mutation Rate	0.01
Crossover Rate	0.8

3.3 Simulation Results and Discussion

In this section, simulation results are presented to evaluate the performance of the proposed algorithm. Due to the random nature of the channel bandwidth, $\mathcal{BW}_m$, and the users' bandwidth demand r_n, Monte Carlo simulations are performed and each simulation scenario is repeated $100,000$ times. The default parameters used in the simulations are listed in Table 3.1, where $\mathcal{U}(1, 20)$ represents the discrete uniform random integer numbers between 1 and 20. Initially, matrices $\mathbf{C}$ and $\mathbf{L}$ are randomly generated.

3.3.1 Scenario-I: without CCI

In this scenario, the performance of the MSRA is compared with the SOTA algorithms. Specifically, the performance of the MSRA is compared with the MSA (explained in Section 2.4) [20] and the RCA when the CCI among SUs is not considered. Therefore, it is assumed that SUs' transmissions do not overlap with the transmissions of other SUs using the same channel.

Ratio of sum of all SUs' bandwidth requirements to the sum of all available bandwidth is defined as network load (ϕ), i.e.

$$\phi = \frac{\sum_{n=1}^{\mathcal{N}} r_n}{\sum_{m=1}^{\mathcal{M}} \kappa_m} \tag{3.14}$$

For $M = 30$, network load increases by increasing the number of SUs from 5 to 60. Figure 3.3 shows that when the number of SUs increases the sum of rewarded bandwidth also increases in all three methods, but MSRA utilises all available whitespace in various network loading conditions more efficiently than MSA and RCA. For MSRA, when the network load is over 3, CRN becomes saturated due to the lack of available spectrum.

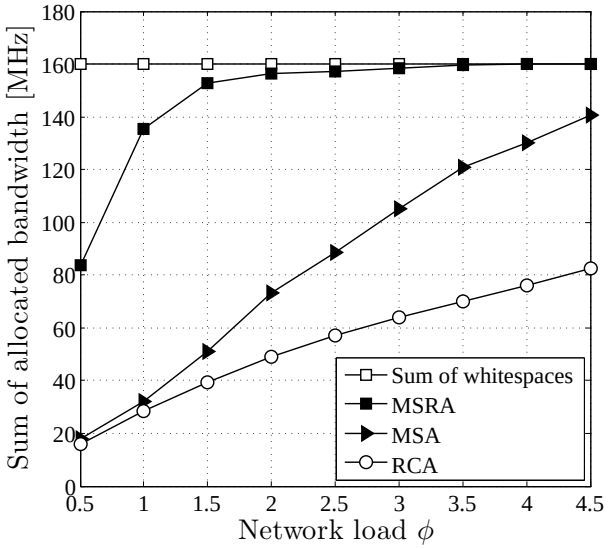

FIGURE 3.3: Sum of bandwidth of SUs admitted to the network under varying network load conditions (scenario-I: without CCI).

3.3.2 Scenario-II: with CCI

In this scenario, CCI exists among SUs $\boldsymbol{\alpha}$ and the proposed algorithm, MSRA is compared with RCA. MSA does not inherently consider CCI, and for that reason MSA is not included for comparison. Figure 3.4 shows the sum of the bandwidth of SUs admitted to the network according to different network loads by increasing the number of SUs from 5 to 55 when there are only seven available channels

(i.e. $\mathcal{M} = 7$). As shown in Figure 3.4, MSRA is a factor of over 2-times better efficiency than RCA for a network load of 5.5. Figure 3.5 represents the number of rejected SUs when the network load increases. As seen in Figure 3.5, the number of rejected users increases with the network load, but MSRA has fewer rejected users of different network loads (or more satisfied users) than RCA of different network loads.

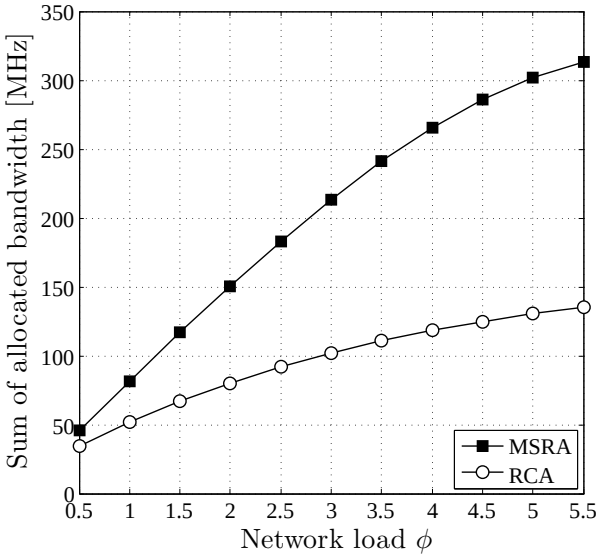

FIGURE 3.4: Sum of bandwidth of SUs admitted to the network under varying network load conditions (scenario-II: with CCI).

3.3.3 Convergence Analysis of MSRA

This section discusses the convergence rates of MSRA by using the minorisation condition in the Markov chain theory. The search space is the collection of binary strings of length ω. Thus, there are 2^{ω} possible chromosomes. Since the search space for a MSRA is nominally over a finite collection of binary strings, the candidate solutions may also be represented by a collection of integers $\psi \in \{0, 1, 2, ..., 2^{\omega} - 1\}$. Each value of ψ represents a unique label for one of the 2^{ω} possible chromosomes. The total number of possible populations is given by:

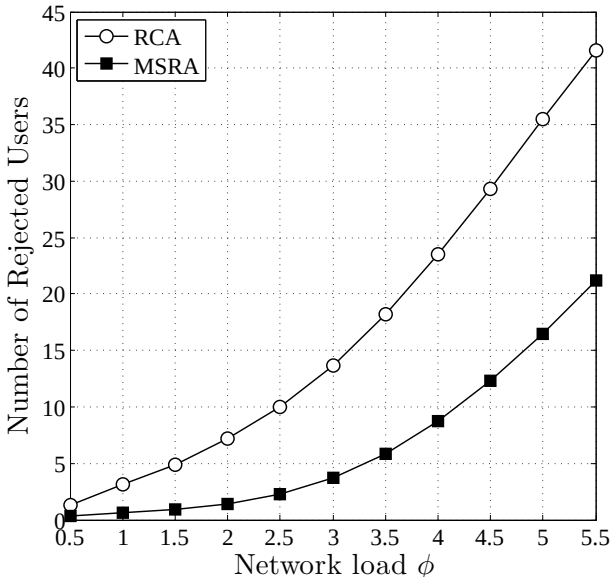

FIGURE 3.5: Number of SUs rejected from the network under varying network load conditions (scenario-II: with CCI).

$$\chi = \frac{N_{pop} + 2^{\omega} - 1}{(2^{\omega} - 1)\,! N_{pop}\,!} \tag{3.15}$$

where N_{pop} denotes the population size. The genetic algorithm may be modeled as a Markov chain so that all of the tools of Markov chain theory may be used to explore the properties of genetic algorithms. Authors in [104] showed that the stochastic transition through these genetic operations can be described completely by the transition matrix for one generation. With this assumption that the genetic algorithm operates on each generation to produce the next, then the $\chi \times \chi$ Markov Chain transition matrix Q has elements $Q_{i,j}$ = conditional probability that population j is generated from population i where each possible individual $\psi \in \{0, 1, 2, ..., 2^{\omega} - 1\}$ is included $s(\psi, i)$ times in population i.

The elements of the transition matrix give the probability of producing population j from population i and may be written as a multinomial distribution given by

[105]:

$$Q_{i,j} = N_{pop}\,! \prod_{\psi=0}^{2^{\omega}-1} \frac{(\phi_{\psi}(i))^{s(\psi,i)}}{s(\psi,i)\,!} \tag{3.16}$$

where $\phi_{\psi}(i)$ is the probability of producing chromosome ψ from population i. Clearly, $\phi_{\psi}(i)$ depends upon the MSRA parameters, namely the mutation rate and convergence rate. Let q_k be a $1 \times \chi$ row vector having j^{th} component, $q_k(j)$ equal to the probability that the k^{th} generation will result in population j. From the definition of the transition matrix, $q_k = q_0 Q^k$ where q_0 is an initial probability distribution.

The stationary distribution of the genetic algorithm is then given by:

$$q = \lim_{k\to\infty} q_k = \lim_{k\to\infty} q_0 Q^k \tag{3.17}$$

It can be seen that q is a solution to $q = qQ$. If one can solve directly for q then the stationary distribution of the genetic algorithm can be obtained in terms of the genetic algorithm parameters, since Q is completely specified in terms of the genetic algorithm parameters through the $\phi_{\psi}(i)$. The method of solving for $q_k(j)$ is well known [105]:

$$q(j) = \frac{D_j}{\sum_{i=0}^{N-1} D_i} \tag{3.18}$$

where D_j is the cofactor of the main diagonal entries of the matrix $I - Q$. The cofactors D_j are found by taking the determinant of the matrix obtained from $I - Q$ by removing the j^{th} row and column.

The rate of convergence, representing probability of achieving a solution θ lying in some "satisfactory set". The convergence rate results for three cases with varying evolutionary parameters are shown in Table 3.2.

In this section, the impact of a number of generations is shown on the performance of MSRA. For the purpose of convergence studies, $\mathcal{N} = 40$ and $\mathcal{M} = 6$ are assumed. Figure 3.6 shows the best fitness value of MSRA for a population in a

TABLE 3.2: Convergence rate (probability that the MSRA has a population that contains the optimal solution) results for three cases.

	Rate convergence of MSRA						
Number of Generations	0	5	10	15	20	30	40
Crossover Rate=0.4, N_{pop}= 10, Mutation Rate= 0.05	0.0	0.1	0.2	0.3	0.4	0.7	1.0
Crossover Rate=0.8, N_{pop}= 15, Mutation Rate= 0.08	0.2	0.5	0.7	0.8	0.9	1.0	1.2
Crossover Rate=1.0, N_{pop}= 20, Mutation Rate= 0.1,	0.1	0.2	0.3	0.4	0.5	0.7	1.0

different number of generations. As shown in Figure 3.6, the performance of the algorithm is enhanced, when the number of generations increases, however this is at the cost of increased processing time. After roughly 34 generations, the fitness value saturates at optimal value, which shows the effectiveness of using a genetic algorithm for spectrum assignment with SA.

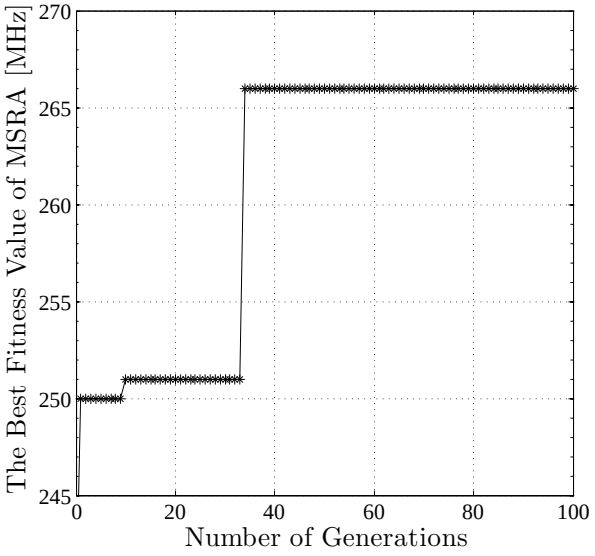

FIGURE 3.6: The impact of a number of generations on the genetic algorithm results under MSRA.

3.4 Conclusions

This chapter introduces aggregation-aware spectrum assignment algorithm using a genetic algorithm referred to as MSRA. The proposed algorithm maximises the rewarded bandwidth to SUs as a criterion to realise spectrum assignment. Further, MSRA takes into account the realistic constraints of CCI and MAS. The performance of MSRA is validated by simulations and the results are compared with SOTA algorithms available in literature, i.e. RCA and MSA. MSRA is a factor of over 2-times better spectrum utilisation than RCA. Moreover, MSRA decreases the number of rejected users. Simulation results verify very fast convergence of MSRA to obtain an optimum solution.

Chapter 4

Radio Resource Management in LTE-A Networks with Spectrum Aggregation

Both CR and LTE-A are anticipated to be the main enabling technologies for NGMN. CR allows different RATs to coexist and share the same spectrum efficiently by utilising unused spectrum. This DSA is achieved in a distributed fashion and relies on software-defined radio. On the other hand, LTE-A offers advanced all-digital packet switched all-IP implementation that offers a variety of multimedia services together with significantly increased capacity. In Chapter 3, an aggregation-based spectrum assignment for CRNs is proposed. However, in this chapter, RRM for SA-enabled LTE-A networks is considered.

SA is one of the most important functionalities in the 3GPP LTE that was introduced in Rel-10. By using SA, multiple CCs with different bandwidths, dispersed within intra or inter-bands, can be simultaneously utilised to provide higher data rates, better coverage and simplified multi-band traffic management, resulting in

enhanced user QoE. However, SA functionality introduces new challenges for RRM function of the network.

In this chapter, an optimum RRM algorithm for LTE-A with reduced complexity is proposed and compared with the SOTA solutions. The proposed algorithm optimally assigns CCs, RBs, and MCS values to the users based on their CSI and SA capabilities. Most of the SOTA solutions are based on approximate approaches which guarantee only half of the PF objective function of the respective optimum solution. Finally, performance of the proposed solution has been evaluated using single-cell multi-user simulations and the results clearly show that the proposed algorithm outperforms the SOTA algorithms in terms of average cell throughput and throughput fairness.

This chapter is organised as follows: a joint RRM problem for SA-enabled LTE-A is formulated as an optimisation problem in Section 4.2. The proposed solution is explained in Section 4.3. Simulation results are discussed in Section 4.5 followed by conclusions in Section 4.6.

4.1 Assumptions and Technical Limitations

1. In LTE for the DL transmission, the eNB distributes its power on the RBs according to the corresponding channel quality. For near-optimal power allocation, the waterfilling power allocation might be used, whereby higher power is allocated to subcarriers whose fading and interference are in favorable conditions [106]. However, Yu *et al.* [107] proved that for the Rayleigh fading channel in adaptive modulation framework - more general than the OFDM based setting - the spectral efficiency loss due to constant-power waterfilling is negligible. Hence, in this thesis for simplicity purposes, it is

assumed that DL power is distributed uniformly over the RBs, i.e. no DL power control is employed.

2. RB, SCC, and MCS on next scheduling time slot are allocated based on UEs measurements in previous CQI reports. Therefore the predictability of the channel conditions has high importance from the overall system point of view; large and uncorrelated interference variation or high mobility of UEs from one time slot to the other makes the network optimisation difficult. In this thesis, it is assumed that CQI feedback varies slowly in each scheduling time slot and is available on a RB size granularity over all CCs.

3. To assess the network performance backlogged traffic model (known as full-buffer model) is used where queue length of every UE is much longer than the amount of data that can be scheduled during each TTI [24].

4. For the sake of simplicity, control DL channels overhead and time-dynamic models of feedback channels are excluded.

5. In this thesis, DL transmission of LTE-FDD without MIMO functionality is considered.

6. The formulation does not consider the buffer size of UEs as well as QoS class identifier of packets - which is a method to ensure bearer traffic is allocated appropriate QoS. Therefore, the formulation treat different types of bearer traffic as one, i.e. neglects different delivery requirements of packets.

7. There are a number of methods available for PCC selection [108]; in this study, UEs select their corresponding PCCs based on the RSRP of the candidate CCs; i.e. CC with highest RSRP is selected as PCC by each UE.

8. In this work, PF scheduler is incorporated to maximise cell throughput while maintaining fairness among UEs.

4.2 System Model and Problem Formulation

4.2.1 System Model

An LTE-A cell, consisting of $\mathcal{N}$ UEs as $\boldsymbol{\alpha} = \{\alpha_1, \alpha_2, \cdots, \alpha_{\mathcal{N}}\}$ is considered. Each $\alpha_n \in \boldsymbol{\alpha}$ may have different SA capability which is modelled as μ_n. Each μ_n represents the maximum number of CCs that $\alpha_n \in \boldsymbol{\alpha}$ can support, for instance, if $\alpha_n \in \boldsymbol{\alpha}$ is a Rel-8 UE, $\mu_n = 1$. According to Rel 10-12 of 3GPP, $\mu_n \in \{1, 2, ..., 5\}$. All UEs in a given TTI compete for $\mathcal{M}$ non-overlapping orthogonal CCs as $\boldsymbol{\beta} = \{\beta_1, \beta_2, \cdots, \beta_{\mathcal{M}}\}$ where each $\beta_m \in \boldsymbol{\beta}$ has a different number of RBs and can be written as γ_m where $\gamma_m \in \{6, 15, 25, 50, 75, 100\}$ is the number of RBs in a given β_m. Each β_m can be chosen as a PCC or SCC for different UEs; i.e. a certain CC for a specific UE may be selected as PCC but for another UE it can be selected as a SCC. In this thesis, without loss of generality, it is assumed that CQI feedback is available on a RB size granularity over all CCs. CQI-index value of α_n in p^{th} RB of β_m is represented by $c_{m,p,n} \in \{0, 1, ..., \mathcal{K}\}$, $\forall m \in \{1, 2, ..., \mathcal{M}\}$, $\forall n \in \{1, 2, ..., \mathcal{N}\}$ and $\forall p \in \{1, 2, ..., \mathcal{P}\}$, where $\mathcal{P}$ and $\mathcal{K}$ are the maximum of γ_m and 15, respectively.

As mentioned in Section 2.2.2, according to 3GPP all RBs allocated to a given UE per CC in a given TTI have an identical MCS. Hence, to guarantee BLER $\leq 10\%$ in all RBs [4],[24] the worst CQI-index value is selected as a representing the CQI of all selected RBs in CC for a particular UE. It is referred to as a worst CQI-index value k and has the same range as $c_{m,p,n}$.

To represent RB allocation, a binary variable $a^k_{m,p,n}$ where $m \in \{1, 2, ..., \mathcal{M}\}$, $n \in \{1, 2, ..., \mathcal{N}\}$, $p \in \{1, 2, ..., \mathcal{P}\}$ and $k \in \{1, 2, ..., \mathcal{K}\}$ is defined. The value of $a^k_{m,p,n} = 1$ if and only if p^{th} RB located in β_m is allocated to α_n with k as a worst CQI-index value and $a^k_{m,p,n} = 0$ otherwise. A binary variable $e^k_{m,n}$, representing carrier (PCC and SCC) allocation is defined, where $e^k_{m,n} = 1$ represents β_m that is assigned to α_n with k as a worst CQI-index value and $e^k_{m,n} = 0$ otherwise.

Finally, to represent PCC for each α_n, a binary variable $y_{m,n}$ is defined where $y_{m,n} = 1$ represents β_m is assigned to α_n as PCC and $y_{m,n} = 0$ otherwise. A schematic diagram of the proposed RRM method is shown in Figure 4.1. Dashed lines indicate signaling between eNB and UEs.

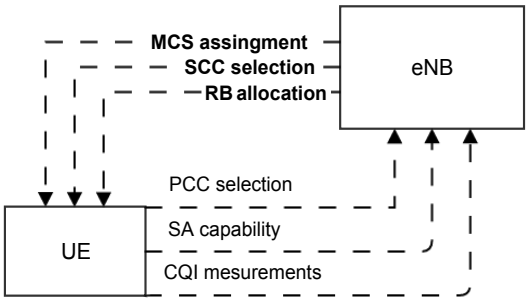

FIGURE 4.1: RRM functionality of network notifies UEs about MCS values, RB allocations and SCC selections of upcoming data stream by means of DL signaling. Moreover, to allow eNB to communicate effectively with all connected UEs, it is necessary that as part of the connection setup, UEs report their transmission capabilities. All measurement reports and new decisions have to make in each TTI.

In each TTI, $a^k_{m,p,n}$ and $e^k_{m,n}$ must satisfy the following conditions:

1. The interference constraint defined in Eq. (4.1) must be satisfied i.e. two or more UEs cannot utilise the same RB simultaneously. In addition, Eq. (4.1) ensures that there is a maximum of one non-zero k per allocated RB.

$$\sum_{n=1}^{\mathcal{N}} \sum_{k=1}^{\mathcal{K}} a^k_{m,p,n} \leq 1 \tag{4.1}$$

2. SA capability of each UE must be taken into account i.e. the number of aggregated CCs for each α_n should be less than its maximum supported CC number μ_n, i.e.

$$\sum_{m=1}^{\mathcal{M}} \sum_{k=1}^{\mathcal{K}} e^k_{m,n} \leq \mu_n \tag{4.2}$$

3. The p^{th} RB located in β_m is allocated to α_n with k as the worst CQI-index value ($a^k_{m,p,n} = 1$) if and only if β_m is allocated to α_n with k as the worst CQI-index value ($e^k_{m,n} = 1$), i.e.

$$a^k_{m,p,n} \leq e^k_{m,n} \tag{4.3}$$

4. All allocated RBs to α_n in β_m must have an identical k (MCS constraint), i.e.

$$\sum_{k=1}^{\mathcal{K}} e^k_{m,n} \leq 1 \tag{4.4}$$

5. Because each α_n has one and only one PCC, in the case where β_m is selected as PCC for α_n, there is one $e^k_{m,n}$ $\forall k \in \{1, 2, ..., \mathcal{K}\}$ equals 1, i.e.

$$y_{m,n} \leq \sum_{k=1}^{\mathcal{K}} e^k_{m,n} \tag{4.5}$$

For α_n, achievable throughput over t^{th} TTI ($f^{(t)}_n$) can be estimated as follows (t is a positive integer number):

$$f^{(t)}_n = \sum_{m=1}^{\mathcal{M}} \sum_{p=1}^{\mathcal{P}} \sum_{k=1}^{\mathcal{K}} r^{k(t)}_{m,p,n} \cdot a^{k(t)}_{m,p,n} \tag{4.6}$$

where

$$r^k_{m,p,n} = \begin{cases} 0 & \text{for } c_{m,n,p} < k, \\ d(k) & \text{for } c_{m,n,p} \geq k. \end{cases} \tag{4.7}$$

$a^{k(t)}_{m,p,n}$ and $r^{k(t)}_{m,p,n}$ are $a^k_{m,p,n}$ and $r^k_{m,p,n}$ in t^{th} TTI respectively. Furthermore, $d(k)$ is defined in Eq. (2.2). In 3GPP LTE standard, all RBs allocated to a given UE per CC must adopt the identical MCS, therefore it is vital that only those RBs that can provide the required QoS (BLER $\leq 10\%$) are selected [4],[24]. For this

reason, Eq. (4.7) ensures that if a RB's CQI is lower than target MCS, then the RB cannot be utilised to transmit data by the MCS.

The utility function of PF scheduling for α_n up to t^{th} TTI is referred to as $V_n^{(t)}$ and can be written as:

$$V_n^{(t)} = \frac{f_n^{(t)}}{T_n^{(t)}} \tag{4.8}$$

where $T_n^{(t)}$ is the average throughput of α_n over last t_c TTIs (average throughput between $(t-t_c)^{\text{th}}$ and $(t-1)^{\text{th}}$ TTI) [109] and can be calculated as follows:

$$T_n^{(t)} = \left(\frac{t_c - 1}{t_c}\right) T_n^{(t-1)} + \frac{1}{t_c} f_n^{(t-1)} \tag{4.9}$$

$T_n^{(t)}$ for all UEs is updated before the next TTI, and the process repeats. To ensure fairness among UEs with different SA capabilities, priority weight for each α_n is inversely proportional to its average throughput $T_n^{(t)}$, which is computed with respect to all RBs located over all CCs available in the cell. For simplicity, time notation is omitted for the rest of this chapter. The overall system utility of the cell, referred to as U can be modelled as the sum of each individual α_n's utility function:

$$U = \sum_{n=1}^{\mathcal{N}} \sum_{m=1}^{\mathcal{M}} \sum_{p=1}^{\mathcal{P}} \sum_{k=1}^{\mathcal{K}} z_{m,p,n}^k \cdot a_{m,p,n}^k \tag{4.10}$$

where $z_{m,p,n}^k = \frac{r_{m,p,n}^k}{T_n}$.

4.2.2 Optimisation problem

In this section, carrier selection, RB allocation and MCS assignment are formulated as a constrained joint optimisation problem with the objective of maximising the system utility function U, defined in Eq. (4.10). The optimisation problem can be written as follows:

$$\max_{a,e} \quad U \tag{4.11}$$

subject to,

$$\sum_{n=1}^{\mathcal{N}} \sum_{k=1}^{\mathcal{K}} a_{m,p,n}^{k} \leq 1 \tag{4.12}$$

$$\sum_{m=1}^{\mathcal{M}} \sum_{k=1}^{\mathcal{K}} e_{m,n}^{k} \leq \mu_n \tag{4.13}$$

$$a_{m,p,n}^{k} \leq e_{m,n}^{k} \tag{4.14}$$

$$\sum_{k=1}^{\mathcal{K}} e_{m,n}^{k} \leq 1 \tag{4.15}$$

$$y_{m,n} \leq \sum_{k=1}^{\mathcal{K}} e_{m,n}^{k} \tag{4.16}$$

$$e_{m,n}^{k}, a_{m,p,n}^{k} \in \{0,1\} \tag{4.17}$$

where $m \in \{1,2,...,\mathcal{M}\}, p \in \{1,2,...,\mathcal{P}\}$, $n \in \{1,2,...,\mathcal{N}\}$, and $k \in \{1,2,...,\mathcal{K}\}$. By solving the optimisation problem (4.11)-(4.17), the RB allocation (across PCCs and SCCs), SCC allocations and MCS-index values can be obtained (and signalled to UEs as shown in Figure 4.1).

4.3 ILP

4.3.1 Objective Function

The optimisation problem (4.11)-(4.17) belongs to an 0-1 ILP class of optimisation problems. The original optimisation problem does not have a canonical form, but

can be converted to an equivalent problem by the transformation of variables, i.e. $a^k_{m,p,n}$, $z^k_{m,p,n}$ and $e^k_{m,n}$ can be ordered to construct vectors $\mathbf{a}$, $\mathbf{z}$ and $\mathbf{e}$ respectively. The relationship between original variables and their corresponding vectors can be expressed as follows:

$$\mathbf{a} = \begin{bmatrix} \overline{a}_1 & \cdots & \overline{a}_i & \cdots & \overline{a}_{\mathcal{MPNK}} \end{bmatrix}^T \tag{4.18}$$

$$\mathbf{z} = \begin{bmatrix} \overline{z}_1 & \cdots & \overline{z}_i & \cdots & \overline{z}_{\mathcal{MPNK}} \end{bmatrix}^T \tag{4.19}$$

$$\mathbf{e} = \begin{bmatrix} \overline{e}_1 & \cdots & \overline{e}_j & \cdots & \overline{e}_{\mathcal{MNK}} \end{bmatrix}^T \tag{4.20}$$

where $\overline{a}_i = a^k_{m,p,n}$, $\overline{z}_i = z^k_{m,p,n}$, $\overline{e}_j = e^k_{m,n}$ and

$$i = p + \mathcal{P}(k-1) + \mathcal{PK}(m-1) + \mathcal{PKM}(n-1) \tag{4.21}$$

$$j = k + \mathcal{K}(m-1) + \mathcal{KM}(n-1) \tag{4.22}$$

The vectors $\mathbf{a}$ and $\mathbf{e}$ can be concatenated and transposed into a new vector referred to as $\mathbf{x}$ with dimensions of $\mathcal{MPNK} + \mathcal{MNK}$ as follows:

$$\mathbf{x} = [\mathbf{a}^T, \mathbf{e}^T]^T \tag{4.23}$$

Similarly, constraint vector $\mathbf{g}$ with a dimension of $\mathcal{MPNK} + \mathcal{MNK}$ can be expressed as:

$$\mathbf{g} = [\mathbf{z}^T, \mathbf{0}^T_{\mathcal{MNK}}]^T \tag{4.24}$$

Accordingly, objective function defined in Eq. (4.11) can be rewritten as:

$$\max_{\mathbf{x}} \ \mathbf{g}^T\mathbf{x} \tag{4.25}$$

4.3.2 Inequality Constraints

In this section, the constraints defined in Eq. (4.12)-(4.17) are converted into an equivalent canonical form. From Eq. (4.12):

$$C_1\mathbf{a} \preceq \mathbf{1} \tag{4.26}$$

where $C_1 = \Big[blkd(L_1, \mathcal{M}) \quad \cdots \quad blkd(L_1, \mathcal{M})\Big]_{\mathcal{MP}\times\mathcal{MPNK}}$ and $L_1 = \Big[I_{\mathcal{P}} \quad \cdots \quad I_{\mathcal{P}}\Big]_{\mathcal{P}\times\mathcal{PK}}$. Similarly, constraint (4.13) can be rewritten as:

$$C_2\mathbf{e} \preceq \boldsymbol{\mu} \tag{4.27}$$

where $\boldsymbol{\mu} = \Big[\mu_1 \quad \cdots \quad \mu_{\mathcal{N}}\Big]^T$ and $C_2 = blkd(\mathbf{1}^T_{\mathcal{KM}}, \mathcal{N})$. Constraint (4.14) can be expressed as:

$$C_3\mathbf{x} \preceq \mathbf{0} \tag{4.28}$$

where $C_3 = \Big[I_{\mathcal{NKMP}}, \quad L_3\Big]_{\mathcal{NKMP}\times(\mathcal{NKMP}+\mathcal{MNK})}$ and $L_3 = -blkd(\mathbf{1}_{\mathcal{P}}, \mathcal{MNK})$. Similarly for constraint (4.15):

$$C_4\mathbf{e} \preceq \mathbf{1} \tag{4.29}$$

where $C_4 = blkd(\mathbf{1}^T_{\mathcal{K}}, \mathcal{MN})$. Finally, constraint (4.16) can be expressed as:

$$-C_4\mathbf{e} \preceq \mathbf{y} \tag{4.30}$$

where $\mathbf{y} = \Big[\overline{y}_1 \quad \cdots \quad \overline{y}_o \quad \cdots \quad \overline{y}_{\mathcal{NM}}\Big]^T$ with $\overline{y}_o = -y_{m,n}$ and suffix $o = m + \mathcal{M}(n-1)$.

Accordingly, constraints (4.26)-(4.30), can be integrated as follows:

$$C\mathbf{x} \preceq \mathbf{q} \tag{4.31}$$

where C is a constraint matrix:

$$C = \begin{bmatrix} C_1^T & 0 & I_{\mathcal{NKMP}} & 0 & 0 \\ 0 & C_2^T & L_3^T & C_4^T & -C_4^T \end{bmatrix}^T \tag{4.32}$$

and

$$\mathbf{q} = \begin{bmatrix} \mathbf{1}_{\mathcal{PM}}^T & \boldsymbol{\mu}^T & \mathbf{0}_{\mathcal{NKMP}}^T & \mathbf{1}_{\mathcal{NM}}^T & \mathbf{y}^T \end{bmatrix}^T \tag{4.33}$$

Equivalently, the optimisation problem (4.11)-(4.17) can be rewritten as:

$$\max_{\mathbf{x}} \ \mathbf{g}^T\mathbf{x} \tag{4.34}$$

subject to:

$$\left\{\mathbf{x} | C\mathbf{x} \preceq \mathbf{q}, \mathbf{x} \subseteq \mathbb{Z}^{(\mathcal{MPNK}+\mathcal{MNK})}\right\} \tag{4.35}$$

Constraints (4.29) and (4.30) assure that the elements of **e** from polyhedron (4.35) contain only integer numbers 0s and 1s. However, constraint (4.28) implies that the elements of **a** from polyhedron (4.35) has any integer number with maximum of 1. Furthermore, it is shown in next section that the optimum values of **a** (or **x**) are binary (0s and 1s) regardless that the polyhedron (4.35) contains negative integers of **a**.

4.3.3 Linear Programming Relaxation

As mentioned in Section 4.3.1, the optimisation problem (4.11)-(4.17), or its equivalent (4.34)-(4.35), belongs to 0-1 ILP. There are variety of algorithms that can be used to solve ILP problems, however, no polynomial-time algorithm has been discovered. One obvious solution is enumeration - systematically checking all feasible solutions and finding one with the maximum objective value - which is difficult, time-consuming and practically unsolvable, especially for the large-scale

ILP-problems such as (4.34)-(4.35). In fact the ILP is regarded as NP-complete (when the problem is both in NP and NP-hard) [110],[111]. However, such problems can be solved efficiently under certain conditions such as total unimodularity and total dual integrality [110].

The solution set of a finite number of inequalities can be defined as a polyhedron [112]:

$$\Theta = \{\mathbf{x} | C\mathbf{x} \preceq \mathbf{q}\} \tag{4.36}$$

where Θ is convex, and there always is an optimum solution which is one of the finitely many extreme points.

Definition 1 (Integral Polyhedron): A polyhedron Θ is called integral if every nonempty face of Θ contains an integral point, i.e. if Θ is the convex hull of the integral vectors contained in it [110].

Total unimodularity and total dual integrality are sufficient conditions in which Θ is integral, in other words if C and $\mathbf{q}$ satisfy certain properties then Θ can be concluded as an integral. Total unimodularity can be applied for any arbitrary integral $\mathbf{q}$ but total dual integrality requires only specific class of integral $\mathbf{q}$ - total dual integrality is a weaker sufficient condition for integrality than total unimodularity. In this work, total unimodularity is used to prove that Θ is integral for any arbitrary integral vector $\mathbf{q}$ (which is dependent on the UEs SA capabilities).

Definition 2 (Total Unimodular Matrix (TUM)): A matrix C is total unimodular if determinant of its every square sub-matrix equals $-1, 0, 1$[110].

Theorem 1 (Hoffman and Kruskal's theorem): Let C be an integral matrix. Then C is TUM if and only if for each integral vector $\mathbf{q}$ the polyhedron $\{\mathbf{x} | C\mathbf{x} \preceq \mathbf{q}, \mathbf{0} \preceq \mathbf{x}\}$ is integral [113],[114].

Lemma 1: The constraint matrix C defined in Eq. (4.32) and used in the optimisation problem (4.34)-(4.35) is TUM (the proof is given in the Appendix A).

Since C is TUM, according to **Theorem 1**, $\{\mathbf{x}|C\mathbf{x} \preceq \mathbf{q}, \mathbf{0} \preceq \mathbf{x}\}$ is integral. Moreover, constraints (4.28), (4.29) and (4.30) - which are already included in $C\mathbf{x} \preceq \mathbf{q}$ - make the following set equalities:

$$\{\mathbf{x}|C\mathbf{x} \preceq \mathbf{q}, \mathbf{0} \preceq \mathbf{x}\} = \{\mathbf{x}|C\mathbf{x} \preceq \mathbf{q}, \mathbf{0} \preceq \mathbf{x} \preceq \mathbf{1}\} \tag{4.37}$$

Thus, as result integral polyhedron $\{\mathbf{x}|C\mathbf{x} \preceq \mathbf{q}, \mathbf{0} \preceq \mathbf{x}\}$ contains only 0s and 1s (implying the negative integers will not be in optimum solution - as mentioned in previous section) which satisfies the binary constraint (4.17). A link between integral polyhedron and LP is given by the following Theorem:

Theorem 2: Consider an LP-problem of the form:

$$\max_{\mathbf{x}} \ \mathbf{g}^T\mathbf{x} \tag{4.38}$$

$$\{\mathbf{x}|C\mathbf{x} \preceq \mathbf{q}, \mathbf{0} \preceq \mathbf{x}\} \tag{4.39}$$

if the problem's polyhedron $\{\mathbf{x}|C\mathbf{x} \preceq \mathbf{q}, \mathbf{0} \preceq \mathbf{x}\}$ is integral, then the LP-problem has an integral optimal solution (the proof is given in [115]).

According to **Theorem 2**, the 0-1 ILP-problem defined in (4.34)-(4.35) can be relaxed to the LP mentioned in (4.38) and (4.39) and then be solved (the optimal basic solution is guaranteed to be binary). Schematically, a visual diagram of the concepts taken for LP relaxation, is shown in Figure 4.2.

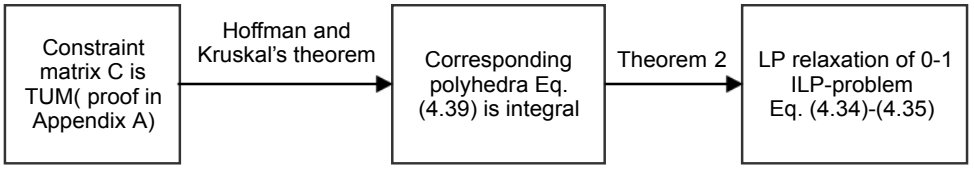

FIGURE 4.2: Schematic proof of the LP relaxation.

4.4 Computational Complexity Analysis

There is no simple analytical formula for the solution of LP problems, but there are a variety of very effective methods for solving them, including the Dantzig's simplex algorithm [116], interior point methods [117], and the Ellipsoid method [118]. In contrast to interior point and Ellipsoid method, no variant of the simplex algorithm is polynomial-time algorithm (in the worst-case it might have to make a very large number of steps which depends exponentially on the problem dimension), but in practice it has proved to be a very efficient and reliable method. The Ellipsoid method - the first polynomial-time algorithm for LP - is too inefficient to be used in practice, because the per-iteration cost of the linear algebra operations to update the ellipsoids is too high [113].

Interior point methods low degree polynomial worst-case complexity and an an almost constant number of iterations which depends very little, if at all, on the problem dimension, make them particularly attractive for very large scale optimisation [119]. Interior point methods are competitive when dealing with small problems of dimensions and are beyond competition when applied to large problems of dimensions going into millions of constraints and variables [120].

The LP-problem of (4.38) and (4.39) is an order $(\mathcal{N}+\mathcal{MP})\times(\mathcal{MPNK}+\mathcal{MNK})$ to maximise $\mathbf{g}^T\mathbf{x}$ over all $\mathbf{x}$ in $\mathbb{R}^{(\mathcal{MPNK}+\mathcal{MNK})}$ such that $C\mathbf{x} \preceq \mathbf{q}$. In this work, since the mentioned problem's dimension is high, a family of interior point method named the primal Newton barrier method [121] is employed in the solution. Barrier

methods for LP generate approximations to both the primal and dual variables at each iteration. The formulation of the barrier requires the specification of a bounded sequence ϵ that determines the accuracy of the solutions of the problem. In this work it is assumed that $\epsilon = 10^{-4}$.

It is not possible to give the exact number of arithmetic operation required to solve a LP problem [112], however, Robere *et al.* [121] established higher bound on the number of operations required to solve the problem, to a given accuracy ϵ, using the primal Newton barrier method. According to [121], the worst-case complexity of the (4.38) and (4.39) equals $\mathcal{O}(\sqrt{\mathcal{N} + \mathcal{MP} + \mathcal{MPNK} + \mathcal{MNK}} \ln \frac{1}{\epsilon})$. Since $\mathcal{P}$, $\mathcal{K}$ and $\mathcal{M}$ are relatively small numbers, the worst-case scenario is investigated as the number of UEs $\mathcal{N}$ approaches infinity:

$$\lim_{\mathcal{N}\to\infty} \mathcal{O}(\sqrt{\mathcal{N} + \mathcal{MP} + \mathcal{MPNK} + \mathcal{MNK}} \ln \frac{1}{\epsilon}) \approx \mathcal{O}(\delta \mathcal{N}^{(\frac{1}{2})}) \tag{4.40}$$

where δ is a constant number. Liao *et al.* [24] analysed the computational complexity of GA and its complexity equals $\mathcal{O}(\mathcal{NPK}(\mathcal{M} + \mathcal{N} \max \mu_n - 1))$. Similarly, for large $\mathcal{N}$, the GA's complexity approaches to:

$$\lim_{\mathcal{N}\to\infty} \mathcal{O}(\mathcal{NPK}(\mathcal{M} + \mathcal{N} \max \mu_n - 1)) \approx \mathcal{O}(\delta^* \mathcal{N}^2) \tag{4.41}$$

where δ^* is a constant number. As it can be seen from Eq. (4.40) and (4.41), the computational complexity of ORAA is much less than the GA.

4.5 Simulation Results and Discussion

In this section, a set of single-cell multi-user simulation results are presented in order to compare and show the efficiency of ORAA over GA [24] (due to ease of accessibility). Network-centric Key Performance Indicators (KPIs) such as overall

system throughput and CC spectral efficiency are demonstrated. Moreover QoS at the UE level, measured by UE throughput and throughput fairness to the benefit of UEs are shown. The simulation results demonstrate the high potential of proposed method in terms of both system-level and UE-level efficiency.

To investigate the network performance, set of dynamic simulations are performed where UEs are distributed independently under three UE deployment scenarios, 1) Random, 2) Cell center, 3) and Cell edge. In random deployment, UEs are distributed with uniform distribution within each cell whereas in cell center and cell edge, UEs are distributed near the cell center and cell edge, respectively. Furthermore, DL performance is assessed in two different SA scenarios: Single-frequency Band (SB) and Multi-frequency Band (MB). In SB scenario, it is assumed that each CC is of 1.4 MHz and each cell has been configured for 6 CCs all located in 2 GHz FDD band. In MB scenario, simulations are conducted for 3 CCs in 2 GHz (Higher Band - HB) and 3 CCs in 800 MHz (Lower Band - LB).

MATLAB based standard compliant system level simulator is employed [27] to simulate the network scenarios and evaluate the performance of the proposed algorithm. The number of UEs per cell (including LTE and LTE-A) is 10 and all UEs are moving with low velocity, unless stated otherwise. Each simulation scenario lasts for $10,000$ TTIs or 10 seconds and repeated 100 times for averaging results. Other simulation parameters are summarised in TABLE 4.1.

4.5.1 Throughput of a Cell

Figure 4.3 shows normalised values of cell throughput as a function of average SA capability of UEs in the cell, defined as $\overline{\mu} = \sum_{n=1}^{\mathcal{N}} \mu_n$, where $\overline{\mu} = 1$ represents the case when all UEs are LTE Rel-8 terminals and $\overline{\mu} = 5$ represents the case when all UEs are LTE-A Rel-10 devices and can aggregate up to 5 CCs. As seen from Figure 4.3, regardless of network deployment, UEs in the cell with higher $\overline{\mu}$ have

TABLE 4.1: Simulation parameters.

Parameter	**Value**
$\mathcal{M}$	6
$\mathcal{N}$	10
$\mathcal{P}$	6
t_c	100
Cyclic prefix length	4.7μ s
Total transmit power	40 dBm (10 W)
Site layout	7 cells wrap-around
Traffic model	Backlogged
Inter-cell distance	500m
Transmission mode	FDD-DL-SISO

higher probability to have higher-rate RBs available in the network. Therefore, for both algorithms (i.e. GA and ORAA) in both scenarios (SB and MB) and all three deployment scenarios cell throughput increases with SA capability of UEs. This can be explained by the fact that in case of higher SA capability, UEs can utilise higher bandwidths and higher frequency diversity. Furthermore, since the achievable throughput of UEs is limited by the available SNR to UEs (especially cell-edge users), increasing the transmission bandwidth provides high data rates to cell-edge UEs and eventually increases cell throughput.

Moreover, in MB scenario, because UEs are allowed to operate on lower frequency band, cell-edge UEs experience better channel quality than SB, leading improved cell throughput of both ORAA and GA. As can be seen in Figure 4.3(a) and Figure 4.3(b), because of the limited number of CCs in the cell (only 6) and better SNR conditions in random and cell-center deployments for $\overline{\mu} \geq 4$, cell throughput does not improve further, however in case of cell-edge deployment (Figure 4.3(c)), cell throughput still increases. Interestingly, there is a sharp increase in cell throughput from $\overline{\mu} = 1$ to 1.5 and the reason is that if $\overline{\mu} = 1$, the only CC (precisely PCC) is selected based on RSRP level. However if $\overline{\mu} > 1$, SCCs are selected by RRM entity based on RBs' CQI values. The cell throughput of ORAA significantly outperforms GA in both SB and MB scenarios in all three different deployments.

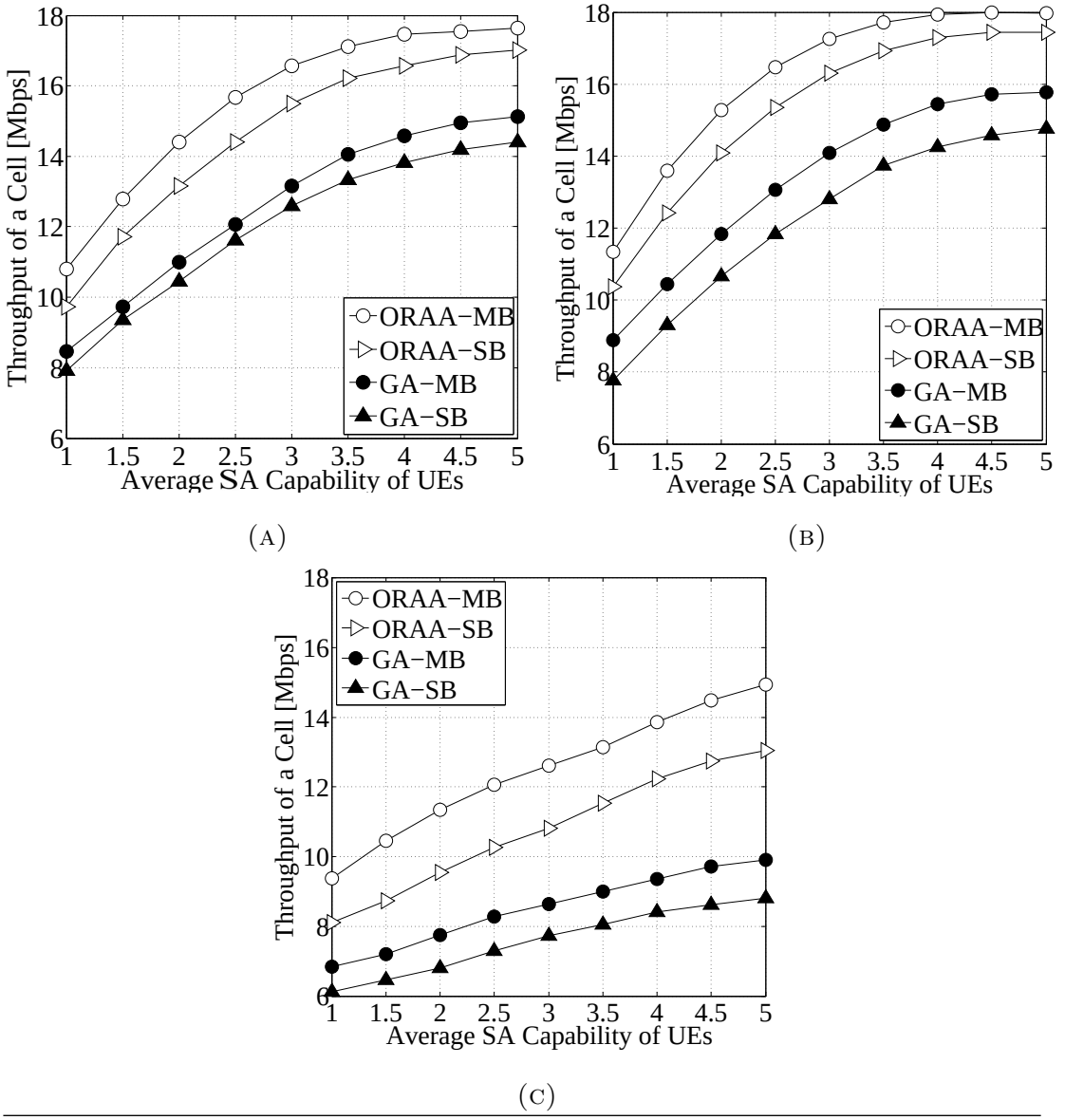

FIGURE 4.3: The impact of SA capability and multi-band accessibility of UEs on cell throughput when $\overline{\mu}$ increases in the network and $\mathcal{N} = 10$, (A) random deployment (B) cell-center deployment (C) cell-edge deployment.

Figure 4.4 shows a comparison of the cell throughput as a function of the number of UEs in both scenarios (SB, MB) and all three deployment scenarios when $\overline{\mu} = 3$. Similar to the case of increasing $\overline{\mu}$ as in Figure 4.3, increasing $\mathcal{N}$ improves cell throughput in all cases. When $\mathcal{N}$ increases in the cell, it enhances the likli-hood that available RBs are assigned to UEs with better channel quality. Hence, by exploiting multi-user diversity, cell throughput improves in all cases. However, when there are too many UEs in the cell, all available RBs in the cell are shared

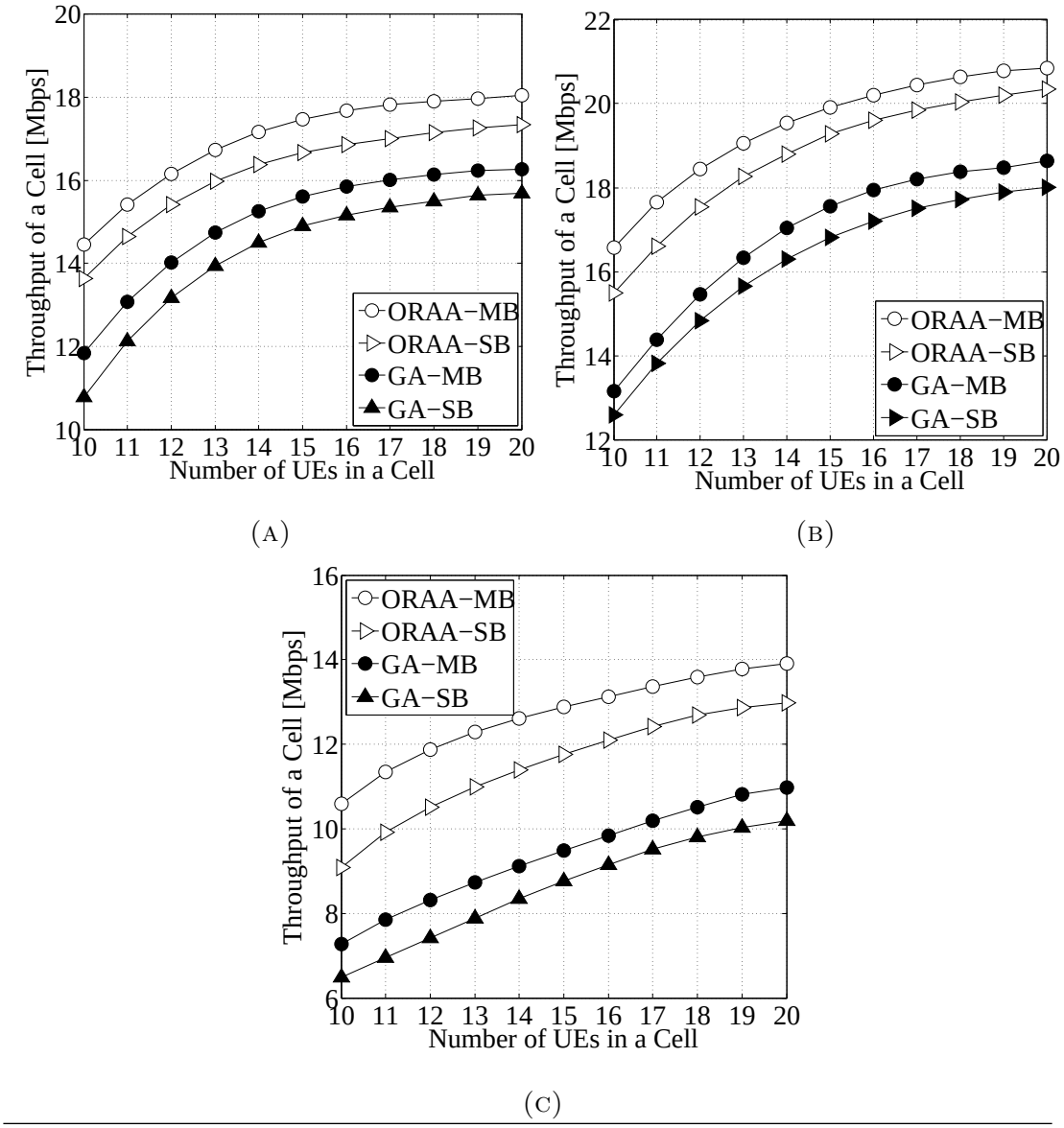

FIGURE 4.4: The impact of SA capability and multi-band accessibility of UEs on cell throughput when $\mathcal{N}$ increases in the network and $\overline{\mu} = 3$, (A) random deployment (B) cell-center deployment (C) cell-edge deployment.

exclusively between them and therefore fewer RBs are assigned to UEs. Therefore, the cell throughput of all cases changes slightly as the ratio of LTE-A UEs increases. The cell throughput of ORAA outperforms GA in both SB and MB scenarios and in all deployment scenarios.

4.5.2 Throughput of UEs

The average throughput of individual UEs in three different deployment scenarios are analysed when $\mathcal{N} = 10$ as shown in Figure 4.5. UE index is ordered based on UE's SA capability, i.e. UE index is formatted as $\alpha_n(\mu_n)$. For instance, in case of A(1) and B(1) UEs A and B can utilise only 1 CC, but I(5) and J(5) mean UEs I and J can aggregate up to 5 different CCs. As shown in Figure 4.5, most of time ORAA in MB scenario provides highest throughput to each UE as expected. UEs with higher SA capability have slightly better throughput than others. If the priority weight of each α_n is computed with respect to all RBs located over its corresponding CC, the gap between throughput of UEs with 1 and 2 CCs aggregation capability, i.e. A(1), B(1) and C(2), D(2) could be bigger and leads to unfair RB distribution for non LTE-A UEs. But as mentioned in Section 4.2, priority weight of each α_n is considered as an inversely proportional to its average throughput $F_n^{(t)}$ which is computed with respect to all RBs located over all CCs available in the cell. Similarly, in cell-centre deployment scenario (Figure 4.5(b)), UEs experiences better throughput than cell-edge deployment (Figure 4.5(c)).

In Figure 4.6, throughput distribution of UEs in random deployment scenario is considered; UE index is ordered based on their average RSRP level, UE J has lowest average RSRP and UE A has the highest. For simplicity and comparison purposes, it is assumed that all UEs can aggregate same number of CCs i.e. 4. In both ORAA and GA, throughput of UEs decreases by decreasing RSRP level, however in case of ORAA, cell-edge UEs experience better throughput than GA. ORAA assigns CC efficiently in such a way that RBs belong to HB CCs are mostly allocated to cell-center UEs and RBs from LB CCs to cell-edge UEs.

Similarly, in Figure 4.7, Cumulative Distribution Function (CDF) of UEs throughput in the random deployment scenario is shown, throughput of UEs are averaged and the CDF curves of the averaged throughput for four cases are shown. In case

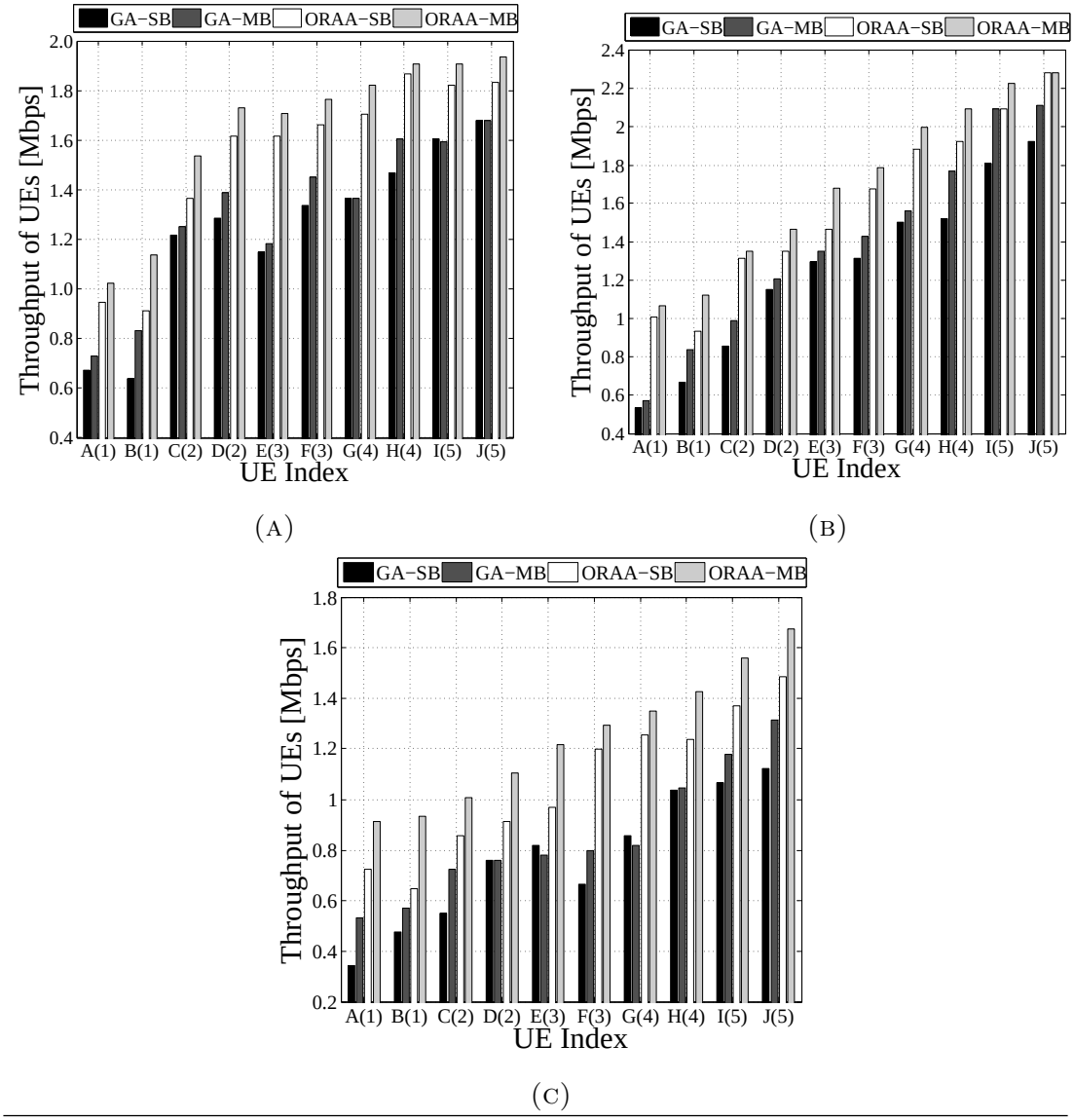

FIGURE 4.5: The impact of SA capability and multi-band accessibility of UEs on each UE throughput ($\mathcal{N} = 10$, $\overline{\mu} = 3$), (A) random deployment (B) cell-center deployment (C) cell-edge deployment.

of ORAA-MB, 55% of UEs have throughput less than 0.6, as for GA-MB, 90% of UEs have throughput less than 0.55. From the Figure 4.6 and Figure 4.7, it can be concluded that the cell-edge UE's throughput can be improved by the ORAA, while the throughput of cell-center UEs remains similar to GA.

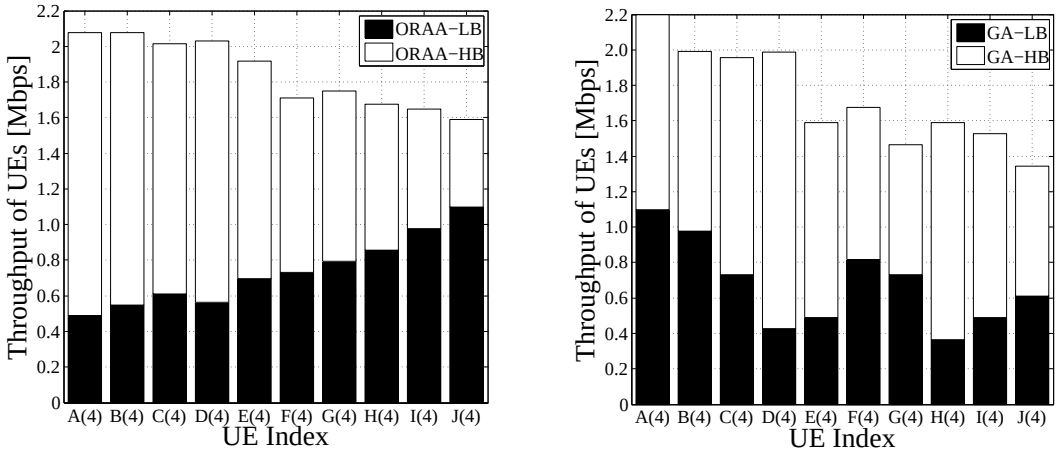

(A) (B)

FIGURE 4.6: Throughput distribution of UEs in MB scenario in random deployment scenario ($\mathcal{N} = 10$, $\overline{\mu} = 4$).

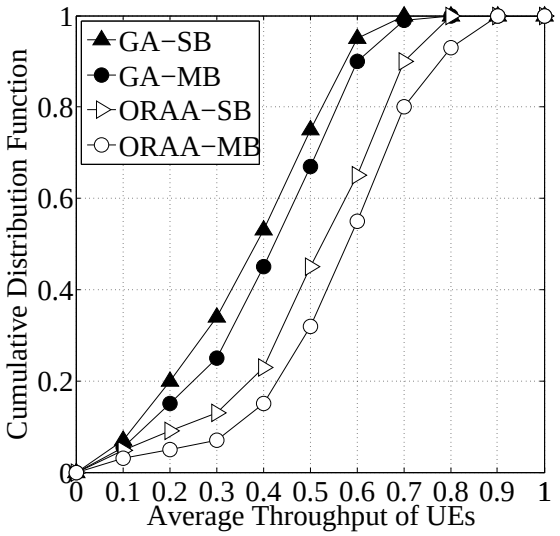

FIGURE 4.7: Cumulative distribution function of UEs throughput in the cell in random deployment scenario ($\mathcal{N} = 10$, $\overline{\mu} = 3$).

4.5.3 Throughput Fairness

In order to compare throughput fairness among UEs in the cell, Jain's fairness index [122] can be applied as follows:

$$T = \frac{(\sum_{n=1}^{\mathcal{N}} f_n)^2}{\mathcal{N} \sum_{n=1}^{\mathcal{N}} f_n^2} = \frac{(\sum_{n=1}^{\mathcal{N}} \sum_{m=1}^{\mathcal{M}} \sum_{p=1}^{\mathcal{P}} \sum_{k=1}^{\mathcal{K}} r_{m,p,n}^k a_{m,p,n}^k)^2}{\mathcal{N} \sum_{n=1}^{\mathcal{N}} \sum_{m=1}^{\mathcal{M}} \sum_{p=1}^{\mathcal{P}} \sum_{k=1}^{\mathcal{K}} (r_{m,p,n}^k a_{m,p,n}^k)^2} \tag{4.42}$$

The value of T ranges form $\frac{1}{\mathcal{N}}$ to 1, and $T = 1$ indicates that all UEs have equal throughput in average. Figure 4.8 depicts the fairness index for different number of UEs and it can be seen the fairness index is almost same for both ORAA and GA. ORAA outperforms slightly better than GA for smaller $\mathcal{N}$, partially because of providing higher throughput for cell-edge UEs. However, for bigger $\mathcal{N}$, GA presents fairer allocation than ORAA.

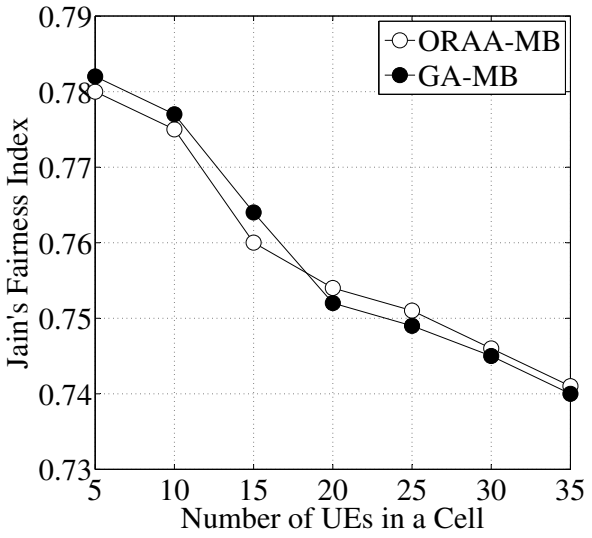

FIGURE 4.8: Jain's fairness index (4.42) as function of $\mathcal{N}$ from 5 to 35 ($\overline{\mu} = 3$).

4.5.4 Component Carrier Spectral Efficiency

In this section, spectral efficiency (bits/s/Hz) per CC, representing overall throughput per bandwidth unit in each CC is investigated. CC spectral efficiency can be interpreted for load balancing which may avoid situations in which multiple UEs compete for the RBs in a single CC while the RBs in other CCs are wasted. For optimal system performance, it is desirable to have approximately equal load on different CCs. As seen in Figure 4.9, introducing LB CCs increases spectral efficiency even in HB CCs because of allocating LB CCs to cell-edge UEs. As it is expected, ORAA provides better CC spectral efficiency than GA and distributes

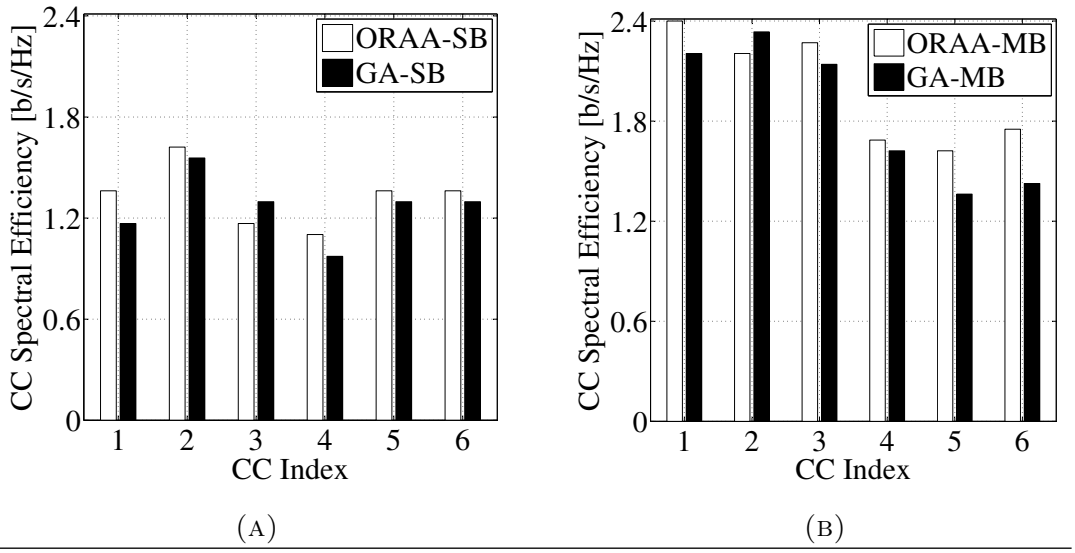

FIGURE 4.9: Component carrier spectral efficiency ($\mathcal{N} = 10$, $\overline{\mu} = 3$).

load in such a way that prevents from overloaded CC in the cell in order to maintain appropriate UE experience and system performance.

4.6 Conclusions

In this chapter, RRM function of LTE-A with SA is formulated as an ILP considering standard-compliant LTE constraints, such as MCS and SA constraints. It is proven that the given ILP can be relaxed to LP and solved by using LP techniques optimally. An optimum-efficient solution based on PF scheduling is proposed. The simulation results demonstrate the high potential of proposed method, in terms of efficiency on the system-level and UE level. The results show that the ORAA offers significant gains in overall system throughput and CC spectral efficiency to the benefit of MNOs. Moreover, the results show improvement in QoS of UEs, measured by UE throughput especially cell-edge UEs.

Chapter 5

Resource Allocation Algorithms with Spectrum Aggregation for OFDM-based Networks

As explained in Section 2.3, the high spectrum efficiency and low computational complexity for the generation and detection of OFDM, together with its flexibility and adaptivity, probably make it the strongest candidate technology for NGMN. Furthermore, to provide wide bandwidth - which is necessary to meet the QoS requirements of growing number of wireless devices - aggregating fragmented segments of spectrum is required.

In this chapter, the RA problem with SA in OFDM-based networks is studied. RA with SA can be formulated as a complex mixed integer optimisation problem under the practical constraints of transmission power and the limited number of CCs available for each user (SA constraint). A two-step solution is proposed: Step1: CC allocation is performed to satisfy users' SA constraints and remove the intractable integer constraints of the optimisation problem, Step2: power and the SC allocation algorithm assign resources among users sub-optimally. Two efficient

methods based on the two-step solution with reasonably low complexity referred to as TSRAA and ERAA are proposed. The performance of TSRAA and ERAA are compared with the highly complex COA introduced as an optimal solution. Simulation results verify that TSRAA provides a near optimum solution and exploits the multi-carrier diversity of wireless systems. Furthermore, numerical results show that ERAA achieves satisfying performance with very low complexity.

This chapter is organised as follows: in Section 5.1, RA with SA functionality is described and an optimisation problem is formulated. The proposed algorithms, i.e. TSRAA, ERAA and COA are explained in Section 5.2 and the complexity analysis of the proposed algorithms are presented in Section 5.3. Simulation results are discussed in Section 5.4, followed by conclusions in Section 5.5.

5.1 System Model and Problem Formulation

An OFDM-based cell with an AP, consisting of $\mathcal{N}$ users as $\boldsymbol{\alpha} = \{\alpha_1, \alpha_2, \cdots, \alpha_{\mathcal{N}}\}$ is considered. Each user $\alpha_n \in \boldsymbol{\alpha}$ may have different SA capability and is modelled as μ_n where μ_n represents the maximum number of CCs that $\alpha_n \in \boldsymbol{\alpha}$ can support. All users in a given scheduling time slot (TTI), compete for $\mathcal{M}$ non-overlapping orthogonal CCs as $\boldsymbol{\beta} = \{\beta_1, \beta_2, \cdots, \beta_{\mathcal{M}}\}$ where each $\beta_m \in \boldsymbol{\beta}$ has a different number of SCs (maximum $\mathcal{P}$) and can be written as $\boldsymbol{\gamma} = \{\gamma_m | \gamma_m \in \mathbb{N}\}_{1\times\mathcal{M}}$ where γ_m shows the number of SCs in a given β_m. Bandwidth of each β_m can be calculated as $\gamma_m \cdot \Delta f$ for $1 \leq m \leq \mathcal{M}$ and Δf denotes SC frequency spacing; for simplicity, $\Delta f = 1$ is assumed. A binary matrix $\mathbf{A}$ is defined as $\mathbf{A} = \{a_{m,\rho,n} | a_{m,\rho,n} \in \{0,1\}\}_{\mathcal{M}\times\mathcal{P}\times\mathcal{N}}$, representing a SC allocation map where $a_{m,\rho,n} = 1$ if and only if ρ^{th} SC located in m^{th} CC is allocated to n^{th} user uniquely and $a_{m,\rho,n} = 0$ otherwise. The SC allocation matrix $\mathbf{A}$ must satisfy the interference constraint as defined in Eq.

(5.1) i.e. two or more users cannot utilise the same SC simultaneously.

$$\sum_{n=1}^{\mathcal{N}} a_{m,\rho,n} \leq 1 \quad \text{for} \quad 1 \leq \rho \leq \mathcal{P} \quad \text{and} \quad 1 \leq m \leq \mathcal{M} \tag{5.1}$$

Similarly, a CC allocation matrix can be defined as a binary $\mathcal{M} \times \mathcal{N}$ matrix as follows:

$$\mathbf{E} = \{e_{m,n} | e_{m,n} \in \{0,1\}\}_{\mathcal{M}\times\mathcal{N}} \tag{5.2}$$

where $e_{m,n}$ represents whether or not the β_m is assigned to α_n, i.e.

$$e_{m,n} = \begin{cases} 0 & \iff \sum_{\rho=1}^{\mathcal{P}} a_{m,\rho,n} = 0 \\ 1 & \iff \sum_{\rho=1}^{\mathcal{P}} a_{m,\rho,n} \geq 1 \end{cases} \tag{5.3}$$

To represent the allocated power to each α_n for a given SC, during TTI, a power allocation matrix is defined as follows:

$$\mathbf{P} = \{p_{m,\rho,n} | p_{m,\rho,n} \geq 0\}_{\mathcal{M}\times\mathcal{P}\times\mathcal{N}} \tag{5.4}$$

where $p_{m,\rho,n}$ represents the allocated power for α_n in ρ^{th} SC located in β_m during a TTI. A channel quality matrix $\mathbf{H}$ is defined as a $\mathcal{M} \times \mathcal{P} \times \mathcal{N}$ matrix as:

$$\mathbf{H} = \{h_{m,\rho,n} | h_{m,\rho,n} \geq 0\}_{\mathcal{M}\times\mathcal{P}\times\mathcal{N}} \tag{5.5}$$

where $h_{m,\rho,n}$ is the channel quality of ρ^{th} SC located in β_m at the user α_n location. A SC channel gain matrix, $\mathbf{G}$ can be defined as:

$$\mathbf{G} = \left\{ g_{m,\rho,n} | g_{m,\rho,n} = \frac{h_{m,\rho,n}}{N_0 \cdot \Delta f} \right\}_{\mathcal{M}\times\mathcal{P}\times\mathcal{N}} \tag{5.6}$$

where N_0 is the noise spectral density and assumed to be constant for all SCs. The AP can adapt its transmission power for each user in a TTI to maximise the aggregated sum-rate of the network. It is assumed that the fading characteristics

for each SC are constant over TTI but vary from SC-to-SC. Further, it is assumed that the AP has knowledge about the SA capability of all users.

The aggregated sum-rate of the network (R) based on Shannon-Hartley's theorem can be formulated as:

$$R = \sum_{n=1}^{\mathcal{N}} V_n = \sum_{n=1}^{\mathcal{N}} \sum_{m=1}^{\mathcal{M}} r_{m,n} = \sum_{n=1}^{\mathcal{N}} \sum_{\rho=1}^{\mathcal{P}} \sum_{m=1}^{\mathcal{M}} e_{m,n} \cdot a_{m,\rho,n} \cdot \log_2 \left(1 + p_{m,\rho,n} \cdot g_{m,\rho,n}\right) \tag{5.7}$$

where V_n is the aggregated data-rate of α_n and $r_{m,n}$ is the data rate of α_n over β_m. In this chapter, SC and power allocation are formulated as a constrained optimisation problem with the objective of maximising the aggregated sum-rate R defined in Eq. (5.7). Hence, the optimisation problem can be formulated as:

$$\max_{a,\ p} \sum_{n=1}^{\mathcal{N}} \sum_{\rho=1}^{\mathcal{P}} \sum_{m=1}^{\mathcal{M}} e_{m,n} \cdot a_{m,\rho,n} \cdot \log_2 \left(1 + p_{m,\rho,n} \cdot g_{m,\rho,n}\right) \tag{5.8}$$

subject to,

$$e_{m,n} \in \{0, 1\} \tag{5.9}$$

$$\sum_{m=1}^{\mathcal{M}} e_{m,n} \leq \mu_n \tag{5.10}$$

$$a_{m,\rho,n} \in \{0, 1\} \tag{5.11}$$

$$\sum_{n=1}^{\mathcal{N}} a_{m,\rho,n} \leq 1 \tag{5.12}$$

$$p_{m,\rho,n} \geq 0 \tag{5.13}$$

$$\sum_{n=1}^{\mathcal{N}} \sum_{m=1}^{\mathcal{M}} p_{m,\rho,n} \leq P_T \tag{5.14}$$

$\forall\ 1 \leq m \leq \mathcal{M}$, $1 \leq \rho \leq \mathcal{P}$, and $1 \leq n \leq \mathcal{N}$. For the optimisation problem (Eq. (5.8)-(5.14)), the constraint in (5.10) guarantees SA restriction for each user in the network. Eq. (5.13) and Eq. (5.14) are power constraints of the AP; P_T is

the power budget of the AP. Due to the presence of binary variables, the resulting problem is mixed integer optimisation problem and the solution is prohibitively computationally complex [112],[123].

5.2 Proposed Solutions

5.2.1 Two-Step Resource Allocation Algorithm

The optimisation problem (Eq. (5.8)-(5.14)) is a complex mixed integer optimisation problem and computationally expensive. In this chapter, a novel approach is proposed to convert the given problem into a two-step optimisation problem and obtain a sub-optimal solution i.e. the first step is for carrier selection and the second step is for assigning powers and SCs.

5.2.1.1 Carrier Selection

In this step, the initial assignment of CCs to each user is determined. Initially, it is assumed that all users can aggregate an unlimited number of CCs, i.e. $e_{m,n} = 1$ for $1 \leq n \leq \mathcal{N}$ and $1 \leq m \leq \mathcal{M}$. By assuming $a_{m,\rho,n}$ as a continuous variable which can take any value between 0 to 1, the optimisation problem (Eq. (5.8)-(5.14)) can be rewritten as:

$$\max_{a,\ p} \sum_{n=1}^{\mathcal{N}} \sum_{\rho=1}^{\mathcal{P}} \sum_{m=1}^{\mathcal{M}} e_{m,n} \cdot a_{m,\rho,n} \cdot \log_2 \left(1 + p_{m,\rho,n} \cdot g_{m,\rho,n}\right) \tag{5.15}$$

subject to,

$$a_{m,\rho,n} \geq 0 \tag{5.16}$$

$$\sum_{n=1}^{\mathcal{N}} a_{m,\rho,n} \leq 1 \tag{5.17}$$

$$p_{m,\rho,n} \geq 0 \tag{5.18}$$

$$\sum_{n=1}^{\mathcal{N}} \sum_{m=1}^{\mathcal{M}} p_{m,\rho,n} \leq P_T \tag{5.19}$$

This problem is a modified version of the classic waterfilling algorithm and optimal SC allocation is determined by assigning each SC to the user with the best SC channel gain given by $g_{m,\rho,n}$. Moreover, the optimal power distribution and SC allocation conform to the waterfilling solution [106], as follows:

$$p_{m,\rho,n} = e_{m,n} \cdot \left(K - \frac{1}{g_{m,\rho,n}} \right)^{+} \tag{5.20}$$

$$a_{m,\rho,n} = \begin{cases} 0 & \iff \quad p_{m,\rho,n} = 0 \\ 1 & \iff \quad p_{m,\rho,n} \ > \ 0 \end{cases} \tag{5.21}$$

where

$$K = \frac{P_T + \sum_{n=1}^{\mathcal{N}} \sum_{\rho=1}^{\mathcal{P}} \sum_{m=1}^{\mathcal{M}} \frac{e_{m,n} \cdot a_{m,\rho,n}}{g_{m,\rho,n}}}{\sum_{n=1}^{\mathcal{N}} \sum_{\rho=1}^{\mathcal{P}} \sum_{m=1}^{\mathcal{M}} e_{m,n} \cdot a_{m,\rho,n}} \tag{5.22}$$

and $(x)^+$ stands for $\max(x, 0)$. After obtaining $p_{m,\rho,n}$ and $a_{m,\rho,n}$, data rate $(r'_{m,n})$ can be estimated for each user on different CCs as follows:

$$r'_{m,n} = \sum_{\rho=1}^{\mathcal{P}} a_{m,\rho,n} \cdot \log_2 \left(1 + p_{m,\rho,n} \cdot g_{m,\rho,n}\right) \tag{5.23}$$

For each user α_n, $r'_{m,n}$ is sorted in descending order and μ_n CCs are selected with the highest $r'_{m,n}$. Based on the selected CCs, the corresponding $e_{m,n}$ of each user are set to one and the rest are set to zero. Once carrier selection for each user is complete, the SCs and powers are assigned within selected carriers to each user according to the second step. The TSRAA's first step can be summarised as follows:

1: **Initialise $\mathbf{A} = \mathbf{0}$, $\mathbf{P} = \mathbf{0}$** and **$\mathbf{E} = \mathbf{1}$**.

2: **Find A** and **P** using the waterfilling solution (Eq. (5.20)-(5.22)).

3: **Calculate** $r'_{m,n}$ for $1 \leq m \leq \mathcal{M}$ and $1 \leq n \leq \mathcal{N}$ (Eq. (5.23)).

4: **Sort** $r'_{m,n}$ for each user α_n, in descending order.

5: **Select** μ_n CCs with the highest rate ($r'_{m,n}$), for each user α_n.

6: **Set** $e_{m,n}$ to 1 based on an index of selected CCs for each user α_n.

7: **Pass** obtained **E** to second step (SC and power allocation).

5.2.1.2 Sub-carrier and power allocation

In this step, SCs and powers within selected CCs are allocated optimally to each user based on obtained **E**. It is similar to the previous step, the only difference being that all CCs are not available to each user, i.e. some elements of **E** are set to zero in the carrier selection step. Again the solution is a classic waterfilling algorithm (Eq. (5.20)-(5.22)). TSRAA's second step can be summarised as follows:

1: **Initialise** $\mathbf{A} = \mathbf{0}$, $\mathbf{P} = \mathbf{0}$ and get obtained **E** from the carrier selection step.

2: **Find A** and **P** using the waterfilling solution (Eq. (5.20)-(5.22)).

3: **Report** final results **E**, **A** and **P** to users in the network.

5.2.2 Efficient Resource Allocation Algorithm

In this section another RA algorithm, referred to as ERAA, is proposed. ERAA is computationally more efficient than TSRAA and gives a satisfying performance. Similar to TSRAA, ERAA follows a two-step approach. ERAA not only considers SC channel quality but also approximately equalises the load on different carriers in the network. Load balancing is a useful feature and may help avoid situations in which multiple users compete for the SCs in a single carrier while the SCs in other carriers are not utilised.

In ERAA, the CCs are initially assigned to each user based on the average effective carrier gain $\overline{\mathbf{G}}$ instead of each individual SC's gain; $\overline{\mathbf{G}}$ can be defined as $\mathcal{M} \times \mathcal{N}$ matrix as follows:

$$\overline{\mathbf{G}} = \left\{ \overline{g}_{m,n} | \overline{g}_{m,n} = \frac{\sum_{\rho=1}^{\mathcal{P}} g_{m,\rho,n}}{\gamma_m} \right\}_{\mathcal{M}\times\mathcal{N}} \tag{5.24}$$

This process reduces the complexity of TSRAA remarkably without any appreciable loss in network performance. The carrier-selection step involves multiple levels and in each level, β_m is assigned to user α_n with the highest estimated data rate $r''_{m,n}$ (Eq. (5.26)) among users in the network under the constraint of a maximum number aggregated CCs. For this purpose, the following assumptions are made:

1. The total power budget is distributed equally among users per aggregated carrier, i.e.

$$P' = \frac{P_T}{\sum_{n=1}^{\mathcal{N}} \mu_n} \tag{5.25}$$

   where P' is assigned power for each user in each aggregated CC.

2. When β_m is shared between C_m users, it is assumed that its bandwidth is divided equally between C_m users. This assures load balancing among different carriers, i.e.

$$r''_{m,n} = \frac{\gamma_m}{C_m} \cdot \log_2 \left(1 + \frac{C_m \cdot P' \cdot \overline{g}_{m,n}}{\gamma_m} \right) \tag{5.26}$$

Initially, $C_m = 1$ for $1 \leq m \leq \mathcal{M}$ is assumed. By assigning β_m to a user, C_m is incremented by one. In each level, the user with the highest estimated rate ($r''_{m,n}$) on a particular CC is selected. This algorithm continues until all users in the network reach their SA restriction limit. After obtaining $\mathbf{E}$, powers and SCs are allocated as in the second step of TSRAA. To clarify, ERAA's carrier-selection step can be summarised as follows:

1: **Initialise** $\mathbf{E} = \mathbf{0}$ and $C_m = 1$ for $1 \leq m \leq \mathcal{M}$.

2: **Calculate** $\overline{\mathbf{G}}$ and P' (Eq. (5.24) and Eq. (5.25)).

3: **repeat**

4: **Calculate** $r''_{m,n}$ for $1 \leq m \leq \mathcal{M}$ and $1 \leq n \leq \mathcal{N}$ (Eq. (5.26)).

5: **Find** the pair of α_n and β_m with the highest $r''_{m,n}$ provided that $\sum_{m=1}^{\mathcal{M}} e_{m,n} < \mu_n$ and $e_{m,n} = 0$.

6: **Set** $e_{m,n}$ to 1 and update $\mathbf{E}$.

7: **Increment** C_m to 1.

8: **until** there is no more α_n that satisfies $e_{m,n} \leq \mu_n$ for $1 \leq m \leq \mathcal{M}$.

5.2.3 Combinatorial Algorithm

As mentioned in Section 5.2.1, RA with SA for OFDM-based networks is a mixed integer optimisation problem and NP-hard. There is no work in literature to date to solve the problem optimally. Thus, to evaluate the performance and complexity of TSRAA and ERAA, both are compared with a COA introduced here. A COA is built based on the fact that waterfilling is the optimum solution when optimal carrier allocation is pre-known; therefore,to find the best possible carrier allocations, all possible carrier allocations are examined in terms of the network's throughput. In the COA, carrier allocation for the user with the smallest contribution is removed. This process continues until there are no more users who have aggregated more than their SA capability. To clarify, COA can be summarised as follows:

1: **repeat**

2: **Initialise** $\mathbf{A} = \mathbf{0}$, $\mathbf{P} = \mathbf{0}$ and $\mathbf{E} = \mathbf{1}$.

3: **Calculate** $r'_{m,n}$ for $1 \leq m \leq \mathcal{M}$ and $1 \leq n \leq \mathcal{N}$ (Eq. (5.23)).

4: **Find** the pair of α_n and β_m with the lowest $r'_{m,n}$ provided that $\sum_{m=1}^{\mathcal{M}} e_{m,n} > \mu_n$ and $e_{m,n} = 1$.

5: **Set** $e_{m,n}$ to 0 and update $\mathbf{E}$.

6: **until** there is no more α_n that satisfies $\sum_{m=1}^{\mathcal{M}} e_{m,n} > \mu_n$.

5.3 Computational Complexity Analysis

In this thesis, the proposed approach in [124] is employed to solve water filling problem based on geometric view. The proposed Geometric Water-Filling (GWF) approach eliminates the procedure to solve the non-linear system for the water level, and provides explicit solutions and helpful insights to the problem and the solution [124]. Herein, total number of operations is applied as a measure of the complexity level [125].

The proposed GWF algorithm occupies less computational resource than traditional water filling. It is seen that it needs $\mathcal{C}$ (total number of channels) loops at most to find best channel in each loop and it needs 4 arithmetic operations and 2 logical operations to complete each loop. Thus, the worst-case computational complexity of the proposed solution is $8\mathcal{C}+3$ (from the operations of $6\mathcal{C}+3+2\mathcal{C}$) fundamental arithmetical and logical operations under the $2(\mathcal{C}+1)$ memory units to store required data. In Table 5.1, the worst-case computational complexity of the all three algorithms are provided:

Moreover, due to the fact that the waterfilling algorithm is the most computationally intensive part of TSRAA, ERAA and COA, the complexity analysis is based on the required number of its executions (the complexity of other operations are omitted in the analysis). For TSRAA and ERAA regardless of $\mathcal{M}$, $\mathcal{N}$ and μ_n, the waterfilling algorithm needs to be run only twice and once, respectively. However, for COA, the waterfilling algorithm needs to be run roughly $\mathcal{C}_{\text{COA}}$ times (Eq. (5.27)); each waterfilling algorithm is for distributing $\sum_{m=1}^{\mathcal{M}} \gamma_m$ SCs among $\mathcal{N}$

TABLE 5.1: Worst-case computational complexity using GWF approach.

Solutions	**Arithmetical Operations**	**Logical Operations**
COA	$\sum_{n=1}^{\mathcal{N}}(\mathcal{M}-\mu_n)(8\sum_{m=1}^{\mathcal{M}}\gamma_m+3)$	$2\sum_{n=1}^{\mathcal{N}}(\mathcal{M}-\mu_n)(\sum_{m=1}^{\mathcal{M}}\gamma_m+1)$
TSRAA	$16\sum_{m=1}^{\mathcal{M}}\gamma_m+6$	$4\sum_{m=1}^{\mathcal{M}}\gamma_m+4$
ERAA	$8\sum_{m=1}^{\mathcal{M}}\gamma_m+3$	$2\sum_{m=1}^{\mathcal{M}}\gamma_m+2$

users. Eq. (5.27) shows that COA's complexity grows linearly with $\mathcal{M}$ and $\mathcal{N}$.

$$\mathcal{C}_{\text{COA}} \approx \sum_{n=1}^{\mathcal{N}}(\mathcal{M}-\mu_n) \tag{5.27}$$

It can be seen that ERAA is the most efficient algorithm in terms of complexity; TSRAA is more complex than ERAA with a rate of two; in addition, both algorithms' complexities are independent from $\mathcal{M}$ and $\mathcal{N}$. Figure 5.1 depicts the computational complexity of all three algorithms for the different values of $\mathcal{N}$. For simplicity, $\mathcal{M}=7$ and $\mu_n=3$ for $1\leq n\leq\mathcal{N}$ are assumed. The waterfilling algorithm is well studied in literature and there are many techniques available to reduce its complexity, for instances readers can refer to [126],[127].

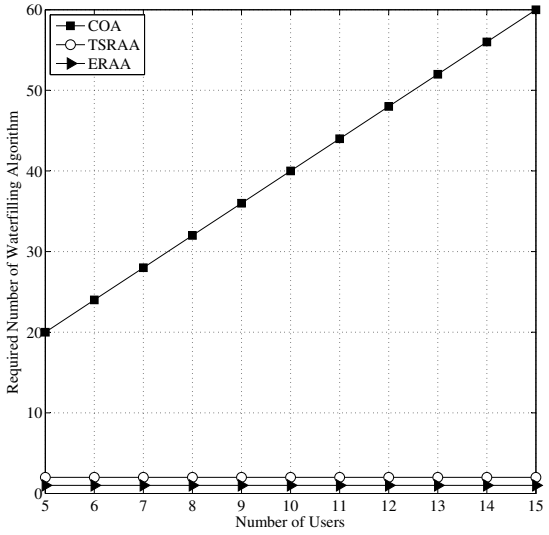

FIGURE 5.1: Complexity comparison of different algorithms based on the required number of executions of the waterfilling algorithm ($\mathcal{M}=7$ and $\mu_n=3$).

TABLE 5.2: Simulation parameters.

Parameter	**Value**
$\mathcal{M}$	8
P_T	10mdB
$\mu_n \in$	$\{1, 2, 3, 4, 5\}$
$\gamma_m \in$	$\{2, 3, 4\}$

5.4 Simulation Results and Discussion

To assess the performance of the proposed algorithms, the performance of TSRAA and ERAA are compared with the optimal solution of COA. The performance of algorithms is measured and compared in terms of single-cell throughput, users throughput and throughput (load) of each CC. The key simulation parameters are listed in Table 5.2.

As the computational complexity of the COA is high, $\mathcal{M} = 8$ and the maximum number of four SCs per CC are assumed. Figure 5.2 shows single-cell throughput versus number of users. As shown in Figure 5.2, throughput improves by increasing the number of users from 1 to 20 in all three algorithms; however, the optimal solution – COA - utilises all available SCs more quickly than the other two methods. The performance gap between TSRAA and COA is small and becomes even smaller as $\mathcal{N}$ increases, which is the case for realistic settings. In addition, ERAA gives a reasonably good performance.

Further, throughput of different users when there are only 10 users and 8 CCs in the network is shown in Figure 5.3. User indexes are ordered based on their SA capability (user index is formatted as $\alpha_n(\mu_n)$). For instance, in the case of A(1) user A can utilise only 1 CC, but J(5) means user J can aggregate up to 5 different CCs. In this case, all three algorithms similarly offer users with the higher SA capability and better SC quality better throughput than other users in the network.

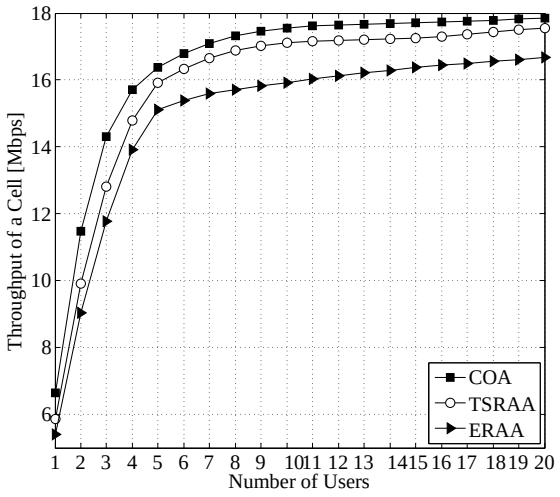

FIGURE 5.2: Single-cell throughput versus number of users.

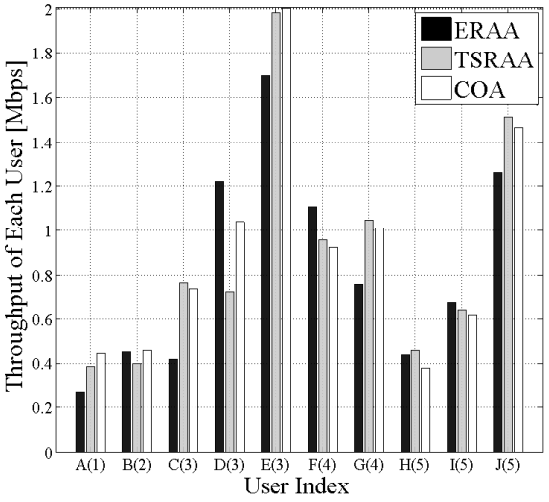

FIGURE 5.3: Per user throughput versus user index which is ordered based on users' SA capability $\mathcal{M} = 8$.

In Figure 5.4, traffic loads of CCs are presented. CCs are ordered based on the number of their SCs (CCs are formatted as $\beta_m(\gamma_m)$). For instance, in the case of 1(2) CC 1 has 2 SCs, but 8(4) means CC 8 has 4 SCs. The high level of load indicates that the CC is one of the main contributors for delivering data to the cell, which itself is dependent on the number of its SCs and the experienced channel quality of overall CC for different users. For example, CC 8(4)'s load is higher than other CCs in the network. implying better channel quality and a higher number of SCs. As COA shows optimum results with regard to load balancing, it can be used

as a reference for the purpose of comparison. The COA and TSRAA demonstrate almost the same level of performance in the aspect of load distribution - the former slightly higher than the latter most of the time - but ERAA is lower than that of both methods. Therefore, TSRAA gives superior load balancing when compared to ERAA, but is inferior to COA to a lesser extent.

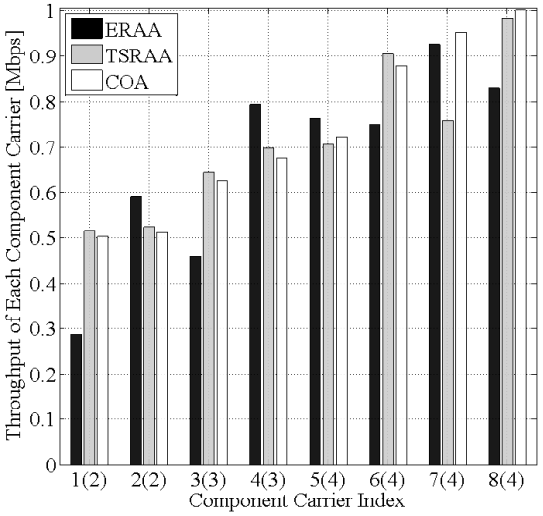

FIGURE 5.4: Per CC throughput (load) versus CC index which is ordered based on CCs' number of SCs.

5.5 Conclusions

In this chapter, a RA problem for OFDM-based networks with SA is formulated as an optimisation problem. With the practical constraints of limited transmission power and a finite number of CCs available for each user, the optimisation problem becomes a complex mixed integer problem with a mathematically intractable solution. Two novel RA algorithms are proposed to solve the optimisation problem sub-optimally. Both proposed algorithms, TSRAA and ERAA, are based on a two-step approach: carrier selection, power and SC allocation. Using simulations, the performance of the proposed algorithms is evaluated in terms of single-cell throughput, per user throughput and per carrier load. As the simulation results

illustrate, TSRAA not only balances the carrier load well, but also achieves near optimum throughput with low complexity. ERAA reduces complexity even further, but this comes at the cost of a slightly reduced throughput gain.

Chapter 6

Conclusions and Future Work

NGMN's radio access is anticipated to be evolved and developed from existing LTE-A networks, as well as building upon new RATs. In addition, SA plays an important role in NGMN, and is expected to be used in different scenarios including, 1) Enabling NGMN's new RAT to operate on a lower frequency band ($\leq$ 6 GHz) for a smooth migration from 4G to NGMN. 2) Improving spectrum utilisation via transmitting on unlicensed spectrum. 3) M2M communication. It is believed that LTE-A and CR together with SA would lead to the realisation of NGMN.

In this thesis, RRM function with SA in CR, LTE-A and OFDM-based networks is studied. The core RRM strategy presented in this thesis is to take advantage of multi-user diversity in both time and frequency dimensions across different CCs (multi-carrier diversity) and schedule transmissions on to radio resources with better channel conditions. In addition, due to the fact that the above-mentioned function is highly dynamic and new decisions have to be made in each TTI, it is vital to have low complexity algorithms as well. Therefore, the design of high performance and efficient RRM strategies becomes crucial.

6.1 Conclusions

The thesis aims to provide novel RRM algorithms for NGMN with SA. Based on the work in the thesis, the following conclusions are drawn:

1. In Chapter 3, an aggregation-based spectrum assignment method using genetic algorithm is proposed. The rewarded sum of bandwidth is maximised as an optimisation criterion to realise efficient assignment of available whitespaces. Further, the realistic constraints of CCI and MAS for the optimisation problem are considered. The performance of the proposed algorithm is validated by running a number of computer simulations and the efficiency of the proposed approach is evaluated by comparing the RCA and MSA algorithms, available in SOTA. The proposed solution decreases number of rejected users from 40 users to 20 users and improves the spectrum utilisation three times.

2. In Chapter 4, the RB allocation problem with consideration of UEs' SA capability as well as MCS assignment in LTE-A networks is addressed. The problem is formulated under the backlogged traffic model as an ILP problem and proves that the ILP can be solved as a LP problem optimally. The optimum and efficient solution for RRM using PF scheduling is proposed. The proposed RRM solution considers MCS assignment, RB scheduling (for both PCC and SCCs) and SCC selection jointly. The advantage of the proposed solution comes from allowing UEs to exploit multiple CCs to select higher MCSs and take advantage of SA. The proposed solution increases throughput of cell from 14 Mbps to 17 Mbps for center-centre deployment.

3. In Chapter 5, the RA problem for SA-enabled OFDM-based networks is formulated as an optimisation problem. With the practical constraints of limited transmission power and a finite number of CCs available for each

user, the optimisation problem becomes a complex mixed integer optimisation problem with a mathematically intractable solution. Two novel RA algorithms are proposed to solve the optimisation problem sub-optimally. Both proposed algorithms, TSRAA and ERAA, are based on two-step approach: carrier selection, power and SC allocation. Using simulations, the performance of the proposed algorithms is evaluated in terms of single-cell throughput, per user throughput and per carrier load. As the simulation results illustrate, TSRAA not only makes balances the carrier load well, but also achieves near optimum throughput with low complexity. In addition, ERAA reduces complexity even further, but at the cost of slightly reduced throughput gain.

6.2 Assumptions and Technical Limitations

This thesis treats the area of RRM in NGMN, with focus on DL direction. This study investigates the problem of single-cell RRM with centralised RA without cooperation among users. Because of assumptions which are taken, there are some limitations as follows:

Single-cell RRM: In this work, it is assumed that cells are deployed in such a way that there is no inter-cell interference among them. This approach cannot be used for frequency reuse of one scenarios. In contrast to this single-cell RRM, multi-cell RRM takes a broader view and optimises radio resource allocation across a group, or cluster, of cells while cells use same frequency.

DL direction: In this thesis, RRM in DL is considered and assumed that all decisions are made centrally; however UL direction is not discussed. Most of presented techniques and insights can be adapted to the UL.

Perfect CSI: Resources on next scheduling time slot are allocated based on users measurements in previous CSI reports. Therefore the predictability of the channel conditions has high importance from the overall system point of view; large and uncorrelated interference variation or high mobility of users from one time slot to the other makes the network optimisation difficult. In this study, it is assumed that channel feedback varies slowly in each scheduling time slot and is available on a radio resource size granularity over all CCs.

QoS Requirements of Different Traffics: Proposed techniques do not consider the buffer size of users as well as QoS class identifier of packets - which is a method to ensure bearer traffic is allocated appropriate QoS. Therefore, the introduced approaches treat different types of bearer traffic as one, i.e. neglects different delivery requirements of packets.

Power Allocation: In DL transmission, base station distributes its power on the radio resources according to the corresponding channel quality. For optimal power allocation, the waterfilling power allocation might be used, whereby higher power is allocated to channels whose fading and interference are in favorable conditions [106]. However, Yu *et al.* [107] proved that for the Rayleigh fading channel in adaptive modulation framework - more general than the OFDM based setting - the spectral efficiency loss due to constant-power waterfilling is negligible. Hence, in this work for simplicity purposes, it is assumed that DL power is distributed uniformly over the radio resources, i.e. no DL power control is employed.

Backlogged Traffic Model: To assess the network performance backlogged traffic model (known as full-buffer model) is used where queue length of every user is much longer than the amount of data that can be scheduled during each TTI [24].

Neglecting Control Channels: For the sake of simplicity, control channels overhead and time-dynamic models of feedback channels are excluded in the formulated problems.

Neglecting MIMO Configuration: In this thesis, DL transmission of LTE-FDD without MIMO functionality is considered.

6.3 Future Work

Although, in this thesis, novel RRM methods for NGMN are proposed, tremendous research efforts are still required in the future, serving the following three purposes:

1. To consider RRM for UL while considering UE's battery lifetime. An energy-efficient RRM for the UL in LTE-A with SA through maximising the energy efficiency under the per-user QoS requirements and per-UE power constraints is necessary. In particular, SCC activation/deactivation procedures (in both DL and UL) to save UE's battery will be focused upon.

2. As mentioned in Chapter 1 and Chapter 2, there is a growing gap between the increasing data rate of users and the growth rate of the current mobile communication systems. One of the promising ways to solve the contention between traffic demand and the actual system capacity growth is to exploit more available spectrum resources. CRNs aim to provide abundant new spectrum opportunities by exploiting unlicensed spectrum opportunistically. In future work, RRM solutions to expand LTE spectrum with CR technology (LTE-CR) using SA will be investigated. The impact of PUs activity on available CCs will be considered.

The future work serving the first and second purposes requires combining both CRN and LTE-A networks, as a continuation of the analysis in Chapter 3 and Chapter 4.

Appendix A

Proof: Constraint Matrix C is Totally Unimodular

In this section, it is proven that the constraint matrix C (defined in Eq. (4.32)) is TUM. Without loss of generality, it is assumed that $\mathcal{P} = 4$, $\mathcal{N} = 3$, $\mathcal{M} = 2$ and $\mathcal{K} = 3$. According to Eq. (4.32), 1's, -1's and 0's pattern of C can be illustrated on Figure A.1. Regardless of the mentioned values of ($\mathcal{P}$, $\mathcal{N}$, $\mathcal{M}$ and $\mathcal{K}$), the pattern is valid for any arbitrary integer values. In the following figures, black squares represent 1's, blank squares 0's and red squares represent -1's.

If a matrix O is TUM, then the matrix $O^{'}$ obtained from O by any one of the following operations is still TUM, i.e. TUM is preserved under the following operations:

Rule1: Multiplying a row or column by -1 [110],[128].

Rule2: Performing Gauss-Jordan pivots on any non-zero entry of a matrix [129].

Rule3: Deleting/adding repeated rows or columns [110],[128].

Rule4: Deleting/adding rows or columns containing only 0's except one 1 [110],[128].

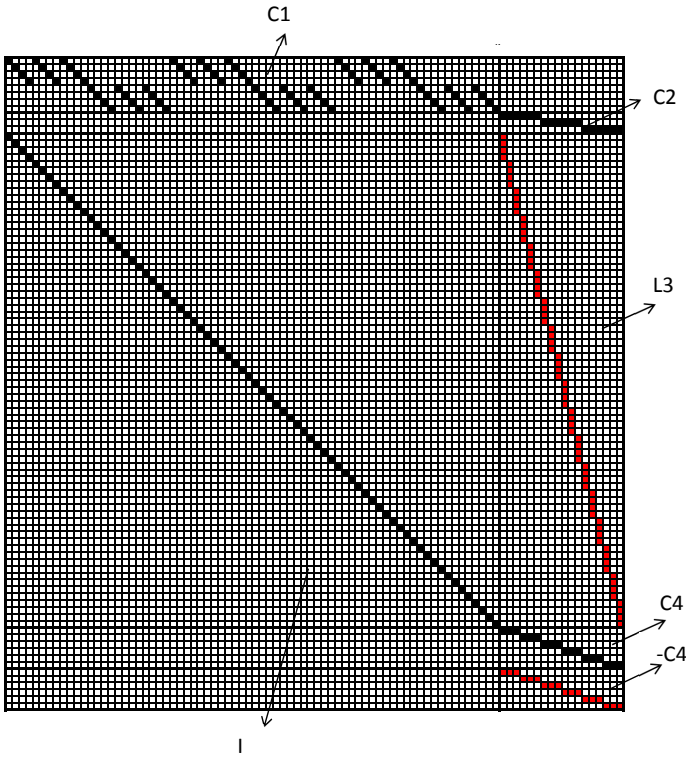

FIGURE A.1: Original coefficient matrix C.

Backward proof procedure is taken to prove that C is TUM. Initially, it is assumed that C is TUM:

Step1: Multiplying a set of rows of $(-C_4)$ with -1 and removing repeated rows (Rule1 and Rule3). The result is shown in Figure A.2.

Step2: Pivoting over all 1's elements of I (Rule2), the resulting matrix of Step1 in Figure A.2. can be converted to one in Figure A.3.

Step3: Because all columns on the left side of the resulting matrix in Figure A.3 contain only one 1 element, the left side of Figure A.3 can be removed (Rule4). The result is shown in Figure A.4(a).

Step4: Deleting repeated rows of L_3 (Rule4). The result is shown in Figure A.4(b).

Step5: Multiplying a set of rows with -1 (Rule1). The result is shown in Figure A.4(c).

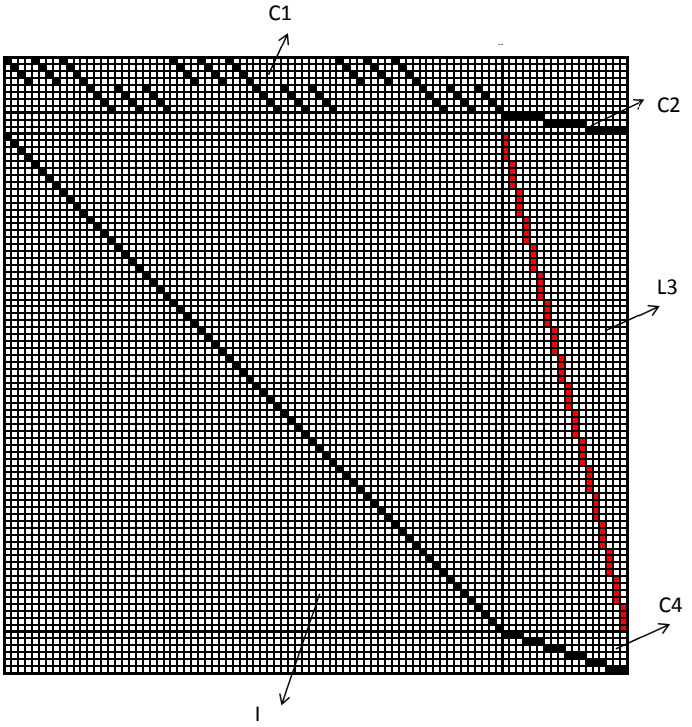

FIGURE A.2: Result of Step1.

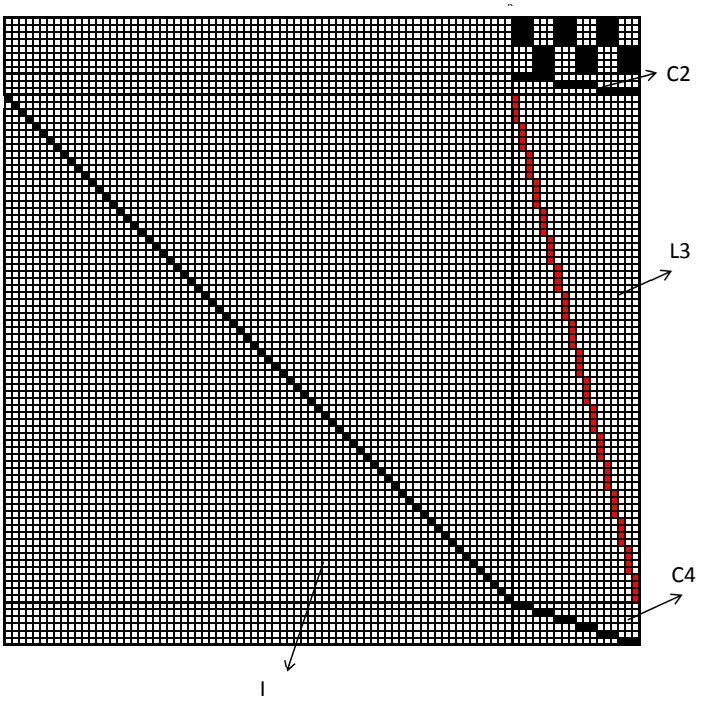

FIGURE A.3: Result of Step2.

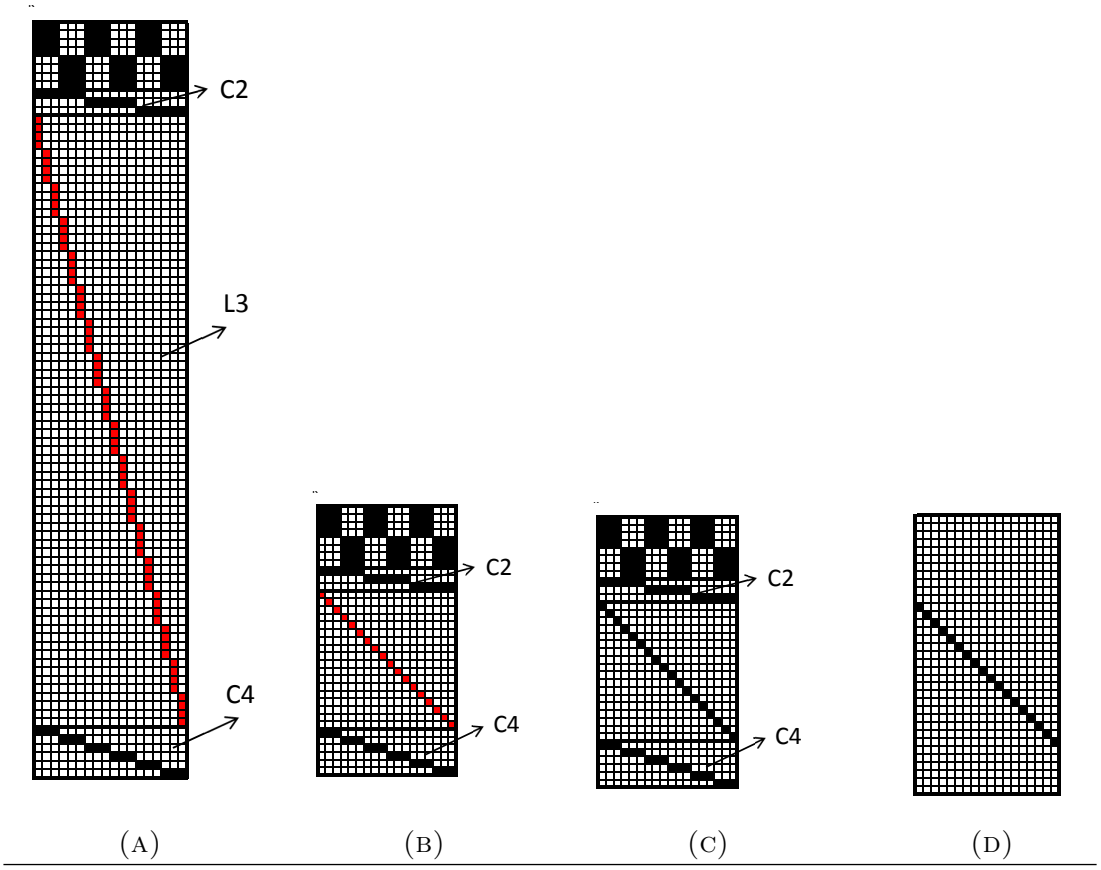

FIGURE A.4: (A): Result of Step3. (B): Result of Step4. (C): Result of Step5.

Step6: Pivoting over all 1's elements of the middle matrix (Rule2), the resulting matrix in Figure A.4(c) can be converted to an identity matrix - Figure A.4(d) - which is TUM [110].

All of the mentioned steps also preserve unimodularity in backward (from Step6 to Step1). Therefore, it can be concluded that C is TUM.

Bibliography

[1] Cisco visual networking index: Global mobile data traffic forecast 2014–2019. (Date last accessed 2016-07-18). [Online]. Available: http://goo.gl/S6lvIg

[2] P. Z. Wolfgang Bock, Dominic Field and K. Rogers. The growth of the global mobile internet economy. (Date last accessed 2016-07-18). [Online]. Available: https://goo.gl/2t14X4

[3] Report says 75 percent of world's population have mobile phones. (Date last accessed 2016-07-18). [Online]. Available: http://goo.gl/VfydhO

[4] S. P. Erik Dahlman and J. Sköld, *4G LTE/LTE-Advanced for Mobile Broadband*. Academic Press, 2011.

[5] J. Xiao, R. Hu, Y. Qian, L. Gong, and B. Wang, "Expanding lte network spectrum with cognitive radios: From concept to implementation," *Wireless Communications, IEEE*, vol. 20, no. 2, pp. 12–19, April 2013.

[6] C. Shannon, "Communication in the presence of noise," *Proceedings of the IRE*, vol. 37, no. 1, pp. 10–21, Jan 1949.

[7] Fedral communications commission spectrum policy task force. (Date last accessed 2016-07-18). [Online]. Available: https://goo.gl/ZXmbSB

[8] H. Lee, S. Vahid, and K. Moessner, "A survey of radio resource management for spectrum aggregation in lte-advanced," *Communications Surveys Tutorials, IEEE*, vol. 16, no. 2, pp. 745–760, Second 2014.

[9] "Background on IMT-Advanced," ITU-R, Tech. Rep., May. 2008, (Date last accessed 2016-07-18). [Online]. Available: http://www.3gpp.org.

[10] QinetiQ. A study of the provision of aggregation of frequency to provide wider bandwidth services. (Date last accessed 2016-07-18). [Online]. Available: http://goo.gl/K9skoj

[11] F. C. Di Benedetto, *Cognitive Radio and Networking for Heterogeneous Wireless Networks*. Springer, 2015.

[12] L. Garcia, K. Pedersen, and P. Mogensen, "Autonomous component carrier selection: interference management in local area environments for lte-advanced," *Communications Magazine, IEEE*, vol. 47, no. 9, pp. 110–116, September 2009.

[13] Qualcomm. Extending benefits of lte advanced to unlicensed spectrum. (Date last accessed 2016-07-18). [Online]. Available: https://goo.gl/wHz4UF

[14] G. Yuan, X. Zhang, W. Wang, and Y. Yang, "Carrier aggregation for lte-advanced mobile communication systems," *Communications Magazine, IEEE*, vol. 48, no. 2, pp. 88–93, February 2010.

[15] C. Park, L. Sundstrom, A. Wallen, and A. Khayrallah, "Carrier aggregation for lte-advanced: design challenges of terminals," *Communications Magazine, IEEE*, vol. 51, no. 12, pp. 76–84, December 2013.

[16] 4GAmericas. Lte carrier aggregation technology development and deployment worldwide. (Date last accessed 2016-07-18). [Online]. Available: http://goo.gl/VY5Gfu

[17] P. Bhat, S. Nagata, L. Campoy, I. Berberana, T. Derham, G. Liu, X. Shen, P. Zong, and J. Yang, "Lte-advanced: an operator perspective," *Communications Magazine, IEEE*, vol. 50, no. 2, pp. 104–114, February 2012.

[18] Samsung electronics launches the world's first lte advanced tri-band carrier aggregation smartphone. (Date last accessed 2016-07-18). [Online]. Available: http://goo.gl/WNZXnz

[19] "Feasibility study for Further Advancements for E-UTRA (LTE-Advanced)," 3GPP Technical Report 36.912, Tech. Rep., Mar. 2010, (Date last accessed 2016-07-18). [Online]. Available: http://www.3gpp.org.

[20] F. Huang, W. Wang, H. Luo, G. Yu, and Z. Zhang, "Prediction-based spectrum aggregation with hardware limitation in cognitive radio networks," in *Vehicular Technology Conference (VTC 2010-Spring), 2010 IEEE 71st*, 2010, pp. 1–5.

[21] J. Huang, V. Subramanian, R. Agrawal, and R. Berry, "Downlink scheduling and resource allocation for ofdm systems," *Wireless Communications, IEEE Transactions on*, vol. 8, no. 1, pp. 288–296, Jan 2009.

[22] W. Ho and Y.-C. Liang, "Optimal resource allocation for multiuser mimo-ofdm systems with user rate constraints," *Vehicular Technology, IEEE Transactions on*, vol. 58, no. 3, pp. 1190–1203, March 2009.

[23] S. Rostami, K. Arshad, and P. Rapajic, "Resource allocation algorithms for OFDM based wireless systems," in *2015 IEEE 26th Annual International Symposium on Personal, Indoor and Mobile Radio Communications - (PIMRC)*, Hong Kong, P.R. China, Aug. 2015, pp. 1268–1273.

[24] H. S. Liao, P. Y. Chen, and W. T. Chen, "An efficient downlink radio resource allocation with carrier aggregation in lte-advanced networks," *IEEE Transactions on Mobile Computing*, vol. 13, no. 10, pp. 2229–2239, Oct 2014.

[25] S. Rostami, K. Arshad, and P. Rapajic, "A joint resource allocation and link adaptation algorithm with carrier aggregation for 5g lte-advanced network,"

in *Telecommunications (ICT), 2015 22ed International Conference on*, April 2015.

[26] Z. Huang, Y. Ji, and B. Zhao, "An efficient resource allocation algorithm with carrier aggregation in lte advanced systems," in *Wireless Communications Signal Processing (WCSP), 2012 International Conference on*, Oct 2012, pp. 1–6.

[27] J. Ikuno, M. Wrulich, and M. Rupp, "System level simulation of lte networks," in *Vehicular Technology Conference (VTC 2010-Spring), 2010 IEEE 71st*, May 2010, pp. 1–5.

[28] M. S. D. B. Rawat and S. Shetty, *Dynamic Spectrum Access for Wireless Networks*. Springer, 2015.

[29] Ofcom spectrum management strategy. (Date last accessed 2016-07-18). [Online]. Available: http://goo.gl/JecW21

[30] B. Wang and K. Liu, "Advances in cognitive radio networks: A survey," *Selected Topics in Signal Processing, IEEE Journal of*, vol. 5, no. 1, pp. 5–23, Feb 2011.

[31] J. Bingham, "Multicarrier modulation for data transmission: an idea whose time has come," *Communications Magazine, IEEE*, vol. 28, no. 5, pp. 5–14, May 1990.

[32] S. Hara and R. Prasad, "Overview of multicarrier cdma," *Communications Magazine, IEEE*, vol. 35, no. 12, pp. 126–133, Dec 1997.

[33] C. Y. Wong, R. Cheng, K. Lataief, and R. Murch, "Multiuser ofdm with adaptive subcarrier, bit, and power allocation," *Selected Areas in Communications, IEEE Journal on*, vol. 17, no. 10, pp. 1747–1758, Oct 1999.

[34] J. Mitola and J. Maguire, G.Q., "Cognitive radio: making software radios more personal," *Personal Communications, IEEE*, vol. 6, no. 4, pp. 13–18, Aug 1999.

[35] I. Akyildiz, W.-Y. Lee, M. C. Vuran, and S. Mohanty, "A survey on spectrum management in cognitive radio networks," *Communications Magazine, IEEE*, vol. 46, no. 4, pp. 40–48, April 2008.

[36] S. Rostami, K. Arshad, and K. Moessner, "Order-statistic based spectrum sensing for cognitive radio," *Communications Letters, IEEE*, vol. 16, no. 5, pp. 592–595, 2012.

[37] I. F. Akyildiz, W.-Y. Lee, M. C. Vuran, and S. Mohanty, "Next generation/dynamic spectrum access/cognitive radio wireless networks: A survey," *Computer Networks*, vol. 50, no. 13, pp. 2127 – 2159, 2006.

[38] A. Ghasemi and E. Sousa, "Collaborative spectrum sensing for opportunistic access in fading environments," in *New Frontiers in Dynamic Spectrum Access Networks, 2005. DySPAN 2005. 2005 First IEEE International Symposium on*, Nov 2005, pp. 131–136.

[39] T. Yucek and H. Arslan, "A survey of spectrum sensing algorithms for cognitive radio applications," *Communications Surveys Tutorials, IEEE*, vol. 11, no. 1, pp. 116–130, First 2009.

[40] H. Tang, "Some physical layer issues of wide-band cognitive radio systems," in *New Frontiers in Dynamic Spectrum Access Networks, 2005. DySPAN 2005. 2005 First IEEE International Symposium on*, Nov 2005, pp. 151–159.

[41] D. Ariananda, M. Lakshmanan, and H. Nikookar, "A survey on spectrum sensing techniques for cognitive radio," in *Cognitive Radio and Advanced*

Spectrum Management, 2009. CogART 2009. Second International Workshop on, May 2009, pp. 74–79.

[42] M. Masonta, M. Mzyece, and N. Ntlatlapa, "Spectrum decision in cognitive radio networks: A survey," *Communications Surveys Tutorials, IEEE*, vol. 15, no. 3, pp. 1088–1107, Third 2013.

[43] H. Li and R. Qiu, "A graphical framework for spectrum modeling and decision making in cognitive radio networks," in *Global Telecommunications Conference (GLOBECOM 2010), 2010 IEEE*, Dec 2010, pp. 1–6.

[44] W.-Y. Lee and I. Akyldiz, "A spectrum decision framework for cognitive radio networks," *Mobile Computing, IEEE Transactions on*, vol. 10, no. 2, pp. 161–174, Feb 2011.

[45] J. Peha, "Approaches to spectrum sharing," *Communications Magazine, IEEE*, vol. 43, no. 2, pp. 10–12, Feb 2005.

[46] Q. Zhao and A. Swami, "A survey of dynamic spectrum access: Signal processing and networking perspectives," in *Acoustics, Speech and Signal Processing, 2007. ICASSP 2007. IEEE International Conference on*, vol. 4, April 2007, pp. IV–1349–IV–1352.

[47] L.-C. Wang and C.-W. Wang, "Spectrum management techniques with qos provisioning in cognitive radio networks," in *Wireless Pervasive Computing (ISWPC), 2010 5th IEEE International Symposium on*, May 2010, pp. 116–121.

[48] I. Christian, S. Moh, I. Chung, and J. Lee, "Spectrum mobility in cognitive radio networks," *Communications Magazine, IEEE*, vol. 50, no. 6, pp. 114–121, June 2012.

[49] C. Wijting *et al.*, "Key Technologies for IMT-Advanced Mobile Communication Systems," *Wireless Communications, IEEE*, vol. 16, no. 3, pp. 76–85, June 2009.

[50] "Further Advancements for E-UTRA Physical Layer Aspects," 3GPP Technical Report 36.814, Tech. Rep., Mar. 2010, (Date last accessed 2016-07-18). [Online]. Available: http://www.3gpp.org.

[51] P. Mogensen *et al.*, "Lte-advanced: The path towards gigabit/s in wireless mobile communications," in *Wireless Communication, Vehicular Technology, Information Theory and Aerospace Electronic Systems Technology, 2009. Wireless VITAE 2009. 1st International Conference on*, May 2009, pp. 147–151.

[52] S. Parkvall, E. Dahlman, A. Furuskar, Y. Jading, M. Olsson, S. Wanstedt, and K. Zangi, "Lte-advanced - evolving lte towards imt-advanced," in *Vehicular Technology Conference, 2008. VTC 2008-Fall. IEEE 68th*, Sept 2008, pp. 1–5.

[53] B. M. B. K.R. Rao, Zoran S. Bojkovic, *Wireless Multimedia Communication Systems: Design, Analysis, and Implementation,*. CRC Press, 2014.

[54] S. Rostami, K. Arshad, and P. Rapajic, "Aggregation-based spectrum assignment in cognitive radio networks," in *Advanced Computing and Communication Systems (ICACCS), 2013 International Conference on*, Dec 2013, pp. 1–6.

[55] Q. Li, G. Li, W. Lee, M. il Lee, D. Mazzarese, B. Clerckx, and Z. Li, "Mimo techniques in wimax and lte: a feature overview," *Communications Magazine, IEEE*, vol. 48, no. 5, pp. 86–92, May 2010.

[56] A. Damnjanovic, J. Montojo, Y. Wei, T. Ji, T. Luo, M. Vajapeyam, T. Yoo, O. Song, and D. Malladi, "A survey on 3gpp heterogeneous networks," *Wireless Communications, IEEE*, vol. 18, no. 3, pp. 10–21, June 2011.

[57] A. Ghosh, N. Mangalvedhe, R. Ratasuk, B. Mondal, M. Cudak, E. Visotsky, T. Thomas, J. Andrews, P. Xia, H. Jo, H. Dhillon, and T. Novlan, "Heterogeneous cellular networks: From theory to practice," *Communications Magazine, IEEE*, vol. 50, no. 6, pp. 54–64, June 2012.

[58] D. H. Holma and D. A. Toskala, *LTE for UMTS - OFDMA and SC-FDMA Based Radio Access*. Wiley Publishing, 2009.

[59] K. Pedersen, F. Frederiksen, C. Rosa, H. Nguyen, L. Garcia, and Y. Wang, "Carrier aggregation for lte-advanced: functionality and performance aspects," *Communications Magazine, IEEE*, vol. 49, no. 6, pp. 89–95, June 2011.

[60] M. Iwamura, K. Etemad, M.-H. Fong, R. Nory, and R. Love, "Carrier aggregation framework in 3gpp lte-advanced [wimax/lte update]," *Communications Magazine, IEEE*, vol. 48, no. 8, pp. 60–67, August 2010.

[61] S. Ahmadi, *A Practical Systems Approach to Understanding 3GPP LTE Releases 10 and 11 Radio Access Technologies*. Academic Press, 2014.

[62] "Lte; evolved universal terrestrial radio access (E-UTRA); base station radio transmission and reception (3gpp ts 36.104 version 10.2.0 release 10)," ETSI TS 136.104, Tech. Rep., Nov. 2011, (Date last accessed 2016-07-18). [Online]. Available: http://goo.gl/INzgxv

[63] "Evolved universal terrestrial radio access (E-UTRA); user equipment radio transmission and reception," 3GPP TS 36.101, Tech. Rep., APR. 2015, (Date last accessed 2016-07-18). [Online]. Available: http://www.3gpp.org.

[64] "User equipment (ue) radio access capabilities (release 12)," 3GPP TS 36.306, Tech. Rep., MAY. 2014, (Date last accessed 2016-07-18). [Online]. Available: http://www.3gpp.org.

[65] P. Goldstein. (2015) Verizon, at&t, ericsson expect pre-standard 5g deployments to feed into official standards.

[66] W. Roh, J.-Y. Seol, J. Park, B. Lee, J. Lee, Y. Kim, J. Cho, K. Cheun, and F. Aryanfar, "Millimeter-wave beamforming as an enabling technology for 5g cellular communications: theoretical feasibility and prototype results," *Communications Magazine, IEEE*, vol. 52, no. 2, pp. 106–113, February 2014.

[67] T. Parker. Sk telecom rolls out lte advanced with carrier aggregation. (Date last accessed 2016-07-18). [Online]. Available: http://goo.gl/z3CGxI

[68] EE debuts 300mbps lte-a network using huawei's carrier aggregation router. (Date last accessed 2016-07-18). [Online]. Available: http://goo.gl/Ia4lbs

[69] Huawei. Huawei and optus launch world-first td-lte advanced carrier aggregation network. (Date last accessed 2016-07-18). [Online]. Available: http://goo.gl/kBe03W

[70] A1, NSN demo lte-advanced carrier aggregation. (Date last accessed 2016-07-18). [Online]. Available: http://goo.gl/LSPRQg

[71] P. Goldstein. At&t lights up lte advanced carrier aggregation in chicago, other markets. (Date last accessed 2016-07-18). [Online]. Available: http://goo.gl/NZNPJd

[72] BradMolen. Lg g pro 2 review: new year, new note contender. (Date last accessed 2016-07-18). [Online]. Available: http://goo.gl/AP3MJR

[73] A. F. Htc one (m8) is the first u.s. smartphone to support carrier aggregation. (Date last accessed 2016-07-18). [Online]. Available: http://goo.gl/9jFFtI

[74] P. Goldstein. Apple unveils larger iphone 6, 6 plus, adds support for VoLTE. (Date last accessed 2016-07-18). [Online]. Available: http://goo.gl/T4fygz

[75] M. Degrasse. Qualcomm, huawei, china mobile verify three-component carrier aggregation. (Date last accessed 2016-07-18). [Online]. Available: http://goo.gl/IqIzsa

[76] M. Sternad, T. Svensson, T. Ottosson, A. Ahlen, A. Svensson, and A. Brunstrom, "Towards systems beyond 3g based on adaptive ofdma transmission," *Proceedings of the IEEE*, vol. 95, no. 12, pp. 2432–2455, Dec 2007.

[77] K. Pedersen, T. Kolding, F. Frederiksen, I. Kovacs, D. Laselva, and P. Mogensen, "An overview of downlink radio resource management for utran long-term evolution," *Communications Magazine, IEEE*, vol. 47, no. 7, pp. 86–93, July 2009.

[78] F. tang Chen and G. lin Tao, "A novel mcs selection criterion for supporting amc in lte system," in *Computer Application and System Modeling (ICCASM), 2010 International Conference on*, vol. 6, Oct 2010, pp. V6–598–V6–603.

[79] N. Guan, Y. Zhou, L. Tian, G. Sun, and J. Shi, "Qos guaranteed resource block allocation algorithm for lte systems," in *Wireless and Mobile Computing, Networking and Communications (WiMob), 2011 IEEE 7th International Conference on*, Oct 2011, pp. 307–312.

[80] "Lte; evolved universal terrestrial radio access (e-utra);physical layer procedures,," 3GPP TS 36.213 version 10.1.0 Release 10, Tech. Rep., APR. 2010, (Date last accessed 2016-07-18). [Online]. Available: http://www.3gpp.org.

[81] K. Sundaresan and S. Rangarajan, "Energy efficient carrier aggregation algorithms for next generation cellular networks," in *Network Protocols (ICNP), 2013 21st IEEE International Conference on*, Oct 2013, pp. 1–10.

[82] H. Wang, C. Rosa, and K. Pedersen, "Uplink component carrier selection for lte-advanced systems with carrier aggregation," in *Communications (ICC), 2011 IEEE International Conference on*, June 2011, pp. 1–5.

[83] F. Capozzi, G. Piro, L. Grieco, G. Boggia, and P. Camarda, "Downlink packet scheduling in lte cellular networks: Key design issues and a survey," *Communications Surveys Tutorials, IEEE*, vol. 15, no. 2, pp. 678–700, Second 2013.

[84] Y. Wang, K. Pedersen, T. Sorensen, and P. Mogensen, "Carrier load balancing and packet scheduling for multi-carrier systems," *Wireless Communications, IEEE Transactions on*, vol. 9, no. 5, pp. 1780–1789, May 2010.

[85] 5g radio access. (Date last accessed 2016-07-18). [Online]. Available: http://goo.gl/aYIf3P

[86] B. Farhang-Boroujeny, "Ofdm versus filter bank multicarrier," *Signal Processing Magazine, IEEE*, vol. 28, no. 3, pp. 92–112, May 2011.

[87] F. Schaich, "Filterbank based multi carrier transmission (fbmc)- evolving ofdm: Fbmc in the context of wimax," in *Wireless Conference (EW), 2010 European*, April 2010, pp. 1051–1058.

[88] B. Priyanto, H. Codina, S. Rene, T. B. Sorensen, and P. Mogensen, "Initial performance evaluation of dft-spread ofdm based sc-fdma for utra lte uplink," in *Vehicular Technology Conference, 2007. VTC2007-Spring. IEEE 65th*, April 2007, pp. 3175–3179.

[89] D. Chen, Q. Zhang, and W. Jia, "Aggregation aware spectrum assignment in cognitive ad-hoc networks," in *Cognitive Radio Oriented Wireless Networks*

and Communications, 2008. CrownCom 2008. 3rd International Conference on, 2008, pp. 1–6.

[90] F. Ye, R. Yang, and Y. Li, "Genetic algorithm based spectrum assignment model in cognitive radio networks," in *Information Engineering and Computer Science (ICIECS), 2010 2nd International Conference on*, Dec 2010, pp. 1–4.

[91] F. Yang, M. Wang, and S. Wang, "Aggregated spectrum assignment algorithm based on chaotic system in cognitive radio," in *Computing, Measurement, Control and Sensor Network (CMCSN), 2012 International Conference on*, July 2012, pp. 343–347.

[92] H. Lee, S. Vahid, and K. Moessner, "Utility-based dynamic spectrum aggregation algorithm in cognitive radio networks," in *Vehicular Technology Conference (VTC Fall), 2012 IEEE*, Sept 2012, pp. 1–5.

[93] H. Salameh, M. Krunz, and D. Manzi, "Spectrum bonding and aggregation with guard-band awareness in cognitive radio networks," *Mobile Computing, IEEE Transactions on*, vol. 13, no. 3, pp. 569–581, March 2014.

[94] L. Giupponi, R. Agusti, J. Perez-Romero, and O. Sallent, "Inter-operator agreements based on qos metrics for improved revenue and spectrum efficiency," *Electronics Letters*, vol. 44, no. 4, pp. 303–304, February 2008.

[95] H. Tian, S. Gao, J. Zhu, and L. Chen, "Improved Component Carrier Selection Method for Non-Continuous Carrier Aggregation in LTE-Advanced Systems," in *Vehicular Technology Conference (VTC Fall), 2011 IEEE*, Sept 2011, pp. 1–5.

[96] F. Wu, Y. Mao, S. Leng, and X. Huang, "A carrier aggregation based resource allocation scheme for pervasive wireless networks," in *Dependable,*

Autonomic and Secure Computing (DASC), 2011 IEEE Ninth International Conference on, Dec 2011, pp. 196–201.

[97] X. Cheng, G. Gupta, and P. Mohapatra, "Joint carrier aggregation and packet scheduling in lte-advanced networks," in *Sensor, Mesh and Ad Hoc Communications and Networks (SECON), 2013 10th Annual IEEE Communications Society Conference on*, June 2013, pp. 469–477.

[98] J. Niu, T. Su, G. Li, D. Lee, and Y. Fu, "Joint transmission mode selection and scheduling in lte downlink mimo systems," *Wireless Communications Letters, IEEE*, vol. 3, no. 2, pp. 173–176, April 2014.

[99] K. Arshad, M. Imran, and K. Moessner, "Collaborative spectrum sensing optimisation algorithms for cognitive radio networks," *International Journal of Digital Multimedia Broadcasting*, vol. 2010, no. 1, pp. 1–20, 2010.

[100] M. Wylie-Green, "Dynamic spectrum sensing by multiband ofdm radio for interference mitigation," in *New Frontiers in Dynamic Spectrum Access Networks, 2005. DySPAN 2005. 2005 First IEEE International Symposium on*, Nov 2005, pp. 619–625.

[101] J. Poston and W. Horne, "Discontiguous OFDM considerations for dynamic spectrum access in idle TV channels," in *New Frontiers in Dynamic Spectrum Access Networks, 2005. DySPAN 2005. 2005 First IEEE International Symposium on*, 2005, pp. 607–610.

[102] Z. Zhao, Z. Peng, S. Zheng, and J. Shang, "Cognitive radio spectrum allocation using evolutionary algorithms," *Wireless Communications, IEEE Transactions on*, vol. 8, no. 9, pp. 4421–4425, 2009.

[103] Y. Li, L. Zhao, C. Wang, A. Daneshmand, and Q. Hu, "Aggregation-based spectrum allocation algorithm in cognitive radio networks," in *Network Operations and Management Symposium (NOMS), 2012 IEEE*, 2012, pp. 506–509.

[104] A. H. Wright and Y. Zhao, "Markov chain models of genetic algorithms," in *In Proceedings of the Genetic and Evolutionary Computation (GECCO) conference*. Morgan Kaufmann, 1999, pp. 734–741.

[105] D. R. Stark and J. C. Spall, "Computable rate of convergence in evolutionary computation," in *Information Fusion, 2002. Proceedings of the Fifth International Conference on*, vol. 1, July 2002, pp. 88–93 vol.1.

[106] L. Hoo, B. Halder, J. Tellado, and J. Cioffi, "Multiuser transmit optimization for multicarrier broadcast channels: asymptotic fdma capacity region and algorithms," *Communications, IEEE Transactions on*, vol. 52, no. 6, pp. 922–930, June 2004.

[107] W. Yu and J. Cioffi, "Constant-power waterfilling: performance bound and low-complexity implementation," *Communications, IEEE Transactions on*, vol. 54, no. 1, pp. 23–28, Jan 2006.

[108] Y. Wang, K. Pedersen, T. Sorensen, and P. Mogensen, "Carrier load balancing and packet scheduling for multi-carrier systems," *Wireless Communications, IEEE Transactions on*, vol. 9, no. 5, pp. 1780–1789, May 2010.

[109] L. B. Jiang and S.-C. Liew, "Proportional fairness in wireless lans and ad hoc networks," in *Wireless Communications and Networking Conference, 2005 IEEE*, vol. 3, March 2005, pp. 1551–1556 Vol. 3.

[110] A. Schrijver, *Theory of Linear and Integer Programming*. John Wiley & Sons, Chichester, 1986.

[111] E. T. Hubertus Th. Jongen, Klaus Meer, *Optimization Theory.* Springer, 2004.

[112] S. Boyd and L. Vandenberghe, *Convex Optimization.* New York, NY, USA: Cambridge University Press, 2004.

[113] B. H. Korte and J. Vygen, *Combinatorial optimization : theory and algorithms.* Berlin, Heidelberg, Paris: Springer, 2000. [Online]. Available: http://goo.gl/MxdEh0

[114] A. Hoffman and J. Kruskal, "Integral boundary points of convex polyhedra in linear inequalities and related systems (h. kuhn and a. tucker, eds.)," *Annals of Maths. Study*, vol. 38, pp. 223–246, 1956.

[115] J. Matousek and B. Gärtner, *Understanding and Using Linear Programming*, ser. Universitext. Springer Berlin Heidelberg, 2006, (Date last accessed 2016-07-18). [Online]. Available: https://goo.gl/pdQgjP

[116] J. C. Nash, "The (dantzig) simplex method for linear programming," in *Computing in Science and Engg.* IEEE Educational Activities Department, 2000, vol. 2, no. 1, pp. 29–31.

[117] M. H. WRIGHT, "The interior-point revolution in optimization:history, recent developments, and lasting consequences," *AMERICAN MATHEMATICAL SOCIETY*, vol. 42, no. 1, p. 39–56, Sep 2004.

[118] N. Karmarkar, "A new polynomial-time algorithm for linear programming," in *Proceedings of the Sixteenth Annual ACM Symposium on Theory of Computing*, ser. STOC '84. New York, NY, USA: ACM, 1984, pp. 302–311, (Date last accessed 2016-07-18). [Online]. Available: http://goo.gl/59MZzq

[119] J. Gondzio, "Interior point methods 25 years later," *European Journal of Operational Research*, p. 2012.

[120] S. Sra, S. Nowozin, and S. Wright, *Optimization for Machine Learning*, ser. Neural information processing series. MIT Press, 2012, (Date last accessed 2016-07-18). [Online]. Available: https://goo.gl/MxFSJL

[121] R. Robere, "Interior point methods and linear programming," *University of Toronto*, 2012.

[122] R. K. Jain, D.-M. W. Chiu, and W. R. Hawe, "A quantitative measure of fairness and discrimination for resource allocation in shared computer systems," Digital Equipment Corporation, Tech. Rep., 1984. [Online]. Available: http://goo.gl/eSC1A9

[123] D. P. Bertsekas, *NonLinear Programming*. Belmont, MA, USA: Athena Scientific, 1999.

[124] P. He, L. Zhao, S. Zhou, and Z. Niu, "Water-filling: A geometric approach and its application to solve generalized radio resource allocation problems," *IEEE Transactions on Wireless Communications*, vol. 12, no. 7, pp. 3637–3647, July 2013.

[125] C. H. Papadimitriou and K. Steiglitz, *Combinatorial Optimization: Algorithms and Complexity*. Upper Saddle River, NJ, USA: Prentice-Hall, Inc., 1982.

[126] G. Munz, S. Pfletschinger, and J. Speidel, "An efficient waterfilling algorithm for multiple access ofdm," in *Global Telecommunications Conference, 2002. GLOBECOM '02. IEEE*, vol. 1, Nov 2002, pp. 681–685 vol.1.

[127] D. Palomar and J. Fonollosa, "Practical algorithms for a family of waterfilling solutions," *Signal Processing, IEEE Transactions on*, vol. 53, no. 2, pp. 686–695, Feb 2005.

[128] K. Truemper, "A decomposition theory for matroids. v. testing of matrix total unimodularity," *Journal of Combinatorial Theory, Series B*, vol. 49, no. 2, pp. 241 – 281, 1990. [Online]. Available: http://goo.gl/rE9D5M

[129] J. Lee, *A First Course in Combinatorial Optimization.* Cambridge Texts in Applied Mathematics, 2004.